NASA TECHNICAL NOTE

NASA TN D-8429

LASER DOPPLER DUST DEVIL MEASUREMENTS

James W. Bilbro, Harold B. Jeffreys,
John W. Kaufman, and Edwin A. Weaver

George C. Marshall Space Flight Center
Marshall Space Flight Center, Ala. 35812

NATIONAL AERONAUTICS AND SPACE ADMINISTRATION • WASHINGTON, D. C. • FEBRUARY 1977

1 REPORT NO.	2. GOVERNMENT ACCESSION NO.
NASA TN D-8429	

4 TITLE AND SUBTITLE

Laser Doppler Dust Devil Measurements

5. REPORT DATE
February 1977

6. PERFORMING ORGANIZATION CODE

7. AUTHOR(S) James W. Bilbro, Harold B. Jeffreys, John W. Kaufman, and Edwin A. Weaver

8. PERFORMING ORGANIZATION REPORT # M-211

9. PERFORMING ORGANIZATION NAME AND ADDRESS

George C. Marshall Space Flight Center
Marshall Space Flight Center, Alabama 35812

10. WORK UNIT NO.

11. CONTRACT OR GRANT NO.

13. TYPE OF REPORT & PERIOD COVERED

Technical Note

12. SPONSORING AGENCY NAME AND ADDRESS

National Aeronautics and Space Administration
Washington, D.C. 20546

14. SPONSORING AGENCY CODE

15. SUPPLEMENTARY NOTES

Prepared by Electronics and Control Laboratory, Science and Engineering

16. ABSTRACT

A Scanning Laser Doppler Velocimeter (SLDV) system was employed at a test site on the Gila River Indian Reservation south of Phoenix, Arizona, for the purpose of detecting, tracking, and measuring the velocity flow field of naturally occurring tornado-like flows (dust devils) in the atmosphere. Approximately 80 dust devils were observed with the system during the test period from August 10 through August 16, 1975. This report provides a review and general description of the dust devil phenomenon and outlines the test program, measurement system, and data processing techniques used to collect information on the dust devil flow field. The general meteorological conditions occurring during the test program are also described, and the information collected on two selected dust devils are discussed in some detail to show the type of information which can be obtained with a SLDV system. The results from these measurements agree well with those of other investigators and illustrate the potential for the SLDV in future endeavors; consequently, recommendations are given for a comprehensive test program using a variety of sensors for obtaining a more complete description of the dust devil phenomenon.

17. KEY WORDS	18. DISTRIBUTION STATEMENT
Laser Doppler Dust Devil Velocity Profiles	Cat 47

19. SECURITY CLASSIF. (of this report)	20. SECURITY CLASSIF. (of this page)	21. NO. OF PAGES	22. PRICE
Unclassified	Unclassified	90	$5.00

* For sale by the National Technical Information Service, Springfield, Virginia 22161

ACKNOWLEDGMENTS

The authors wish to express their appreciation to several people for their invaluable contribution to the program: Mr. R. M. Huffaker, formerly of NASA/MSFC, for his part in the instigation of this program; the personnel of Lockheed, who performed the data collection, including Messrs. Charles Craven, Edward Gorzynski, Robert Howle, and Michael Krause; the personnel of Raytheon, who performed the data analysis, including Dr. Charles Sonnenschein, Mr. Charles DiMarzio, Mr. Douglas Toomey, and Ms. Dorothy Clippinger; and the personnel of the University of Arkansas, who were involved in processing of the data for three dimensional display, including Dr. Ron Skieth, Dr. Bill Ashmore, and Mr. Arato Kimura. Appreciation is also expressed to our MSFC colleagues, Messrs. Daryl Craig, Ron George, and Pete Marrero, for their support during this program.

A special thanks is due Dr. Sherwood Idso of the United States Soil Conservation Service who provided a tremendous service throughout the test program by selecting and serving as local coordinator for the test site and by participating in the collection of the data. Dr. Idso's past experience in dust devil research was an important contribution in conducting this test program.

The authors are extremely grateful to the Tribal Council of the Gila River Indian Reservation for allowing these tests to be conducted.

TABLE OF CONTENTS

LIST OF ILLUSTRATIONS

LIST OF ILLUSTRATIONS (Concluded)

LIST OF TABLES

LASER DOPPLER DUST DEVIL MEASUREMENTS

I. INTRODUCTION

Those members of the meteorological community concerned with tornados and related flow fields have long recognized that detailed velocity information on the dust devil flow field would be a significant contribution to their studies. Because of the interest of the National Oceanic and Atmospheric Administration (NOAA) in these studies and the potential benefit to many people in the United States, the Technology Utilization Office of NASA sponsored a program to remotely measure the dust devil velocity flow field using a Scanning Laser Doppler Velocimeter (SLDV) system developed by Marshall Space Flight Center (MSFC). This system, originally developed for research on wing-tip vortices, was modified to provide a horizontal scan plane and was set up at a test site on the Gila River Indian Reservation south of Phoenix, Arizona. Approximately 80 dust devils were observed with the SLDV during the test period from August 10 through August 26, 1975. These dust devils were observed and measured daily between approximately 11 a.m. and 3 p.m. when the ambient temperature was approximately 38°C and the soil surface temperature was in excess of approximately 63°C. The dust devils were observed in varying wind conditions from 0 to approximately 5 m/s during the test period. Cloudy conditions existed for several days and one thunderstorm occurred in the test area during the test period. The occurrence of dust devils on cloudy days and on the days following the thunderstorm was reduced to zero until the soil had dried and reached or exceeded what appeared to be the critical 63°C ground surface temperature.

Several of the dust devil data records were processed and analyzed at the Raytheon Company in Sudbury, Massachusetts, with additional analyses occurring at the University of Arkansas, Fayetteville, Arkansas. The results of the initial analyses indicate that the SLDV is capable of detecting, tracking, and measuring the velocity profiles of dust devils in varying wind conditions. In addition, the system can determine relative values of backscatter due to the increased number of dust particles in the area of the dust devil. During the test program, a frequency translator was successfully employed in the SLDV for the first time. This device permits the determination of velocity direction

along the line of sight and is seen as a valuable addition to the system in studying complex naturally occurring and/or man-made tornado-like flows.

Section II of this report provides a general description of the dust devil phenomenon together with a summary of previous measurements. The description of the SLDV system is given in Section III, with the outline of the test program and a description of the data processing techniques being given in Sections IV and V. A discussion of the prevailing meteorological conditions together with the analysis of two selected dust devil runs is provided in Section VI. A summary of results and recommendations for additional testing is presented in Section VII.

II. DUST DEVIL PHENOMENON

Large-scale masses of converging air always rotate cyclonically (counterclockwise) in the northern hemisphere. Large-diameter dust devils, on the order of a couple of kilometers or more, also rotate in the cyclonic direction normally, although anticyclonic circulation is not uncommon. Small-diameter dust devils (a few meters) may rotate in either direction without preference. In 1939 D. Brunt mathematically expressed the conservation of angular momentum of large cyclonic circulating systems on the basis of expanding vortex principles in small-scale circular motion [1]. As a basic concept, quiet air rotates with the surface of the Earth and has an absolute angular momentum defined as cyclonic. Cyclonic spin in large-scale converging systems is caused by the rotation of the Earth. The mass of air converging inward rotates more rapidly than the Earth's surface because of its excessive angular momentum. Diverging air, rotating slower than the Earth's angular velocity, appears as though it is rotating in the opposite direction (anticyclonically) and introduces clockwise circulation of air with respect to a fixed point of observation. These basic principles, in addition to the fact that winds are modified from idealized vortex by translatory motion of the system and by friction, introduce the complexities in understanding large- and small-scale air motion.

It has been observed that true convective dust devils are more numerous on calm days, or under conditions of "quiet air" which is rotating with the surface of the Earth. Factors in favor of dust devil development are: open terrain with

level or gentle slope characteristics, limited or no vegetation, sunny days with intense solar radiation for ground and near-ground air heating, extreme lapse rate of air temperature near the ground, and low moisture content of the ground and air. Observations of dust devils in the Tularosa Basin, New Mexico, and in Arizona, Utah, and Nevada confirm that such conditions commonly exist during the development of dust devils. Also, dust devils generally form in certain locations in desert regions. In the Tularosa Valley, it is common to see dust devils form in a north-south line approximately 10 to 15 km west of the foothills of the Sacramento Mountains. Their general surface path is south to north, parallel with the mountain range. Brooks [1] observed approximately 500 fully developed dust devils near Tucson, Arizona (1952 to 1957), and found that they usually moved slowly toward the northeast.

The Compendium Of Meteorology [2] cites the following information concerning the dust devil:

a. Dust devils are 1/100 to 1/10 as large as tornados.

b. A dust devil has no pendant cloud, but a whirling column of dust or sand in which the size of the particles increases with the distance from the center.

c. Dust devils occur more frequently on hot days over dry terrain, and they occur during situations of strong surface convection.

d. Rotation direction is accidental.

e. The horizontal rotation and upflow within a dust devil usually exceed 10 m/s.

f. Their average height is approximately 180 m.

g. The time of duration is determined by the relationship: 300 m in height equals 1 h.

h. In special incidences they have been known to turn into tornados (as have water spouts).

A. Dust Devil Literature Review

In 1968 Ryan and Carroll [3] performed a series of dust devil field studies in the Mojave Desert (80 km northeast of Los Angeles). During these experiments, 80 dust devils were penetrated with special sensor systems and 1119 dust devils were observed at close range. Measurements with these sensor systems included the following:

1. Air temperature to a height above the point at which the lapse rate ceased to be superadiabatic

2. Wind velocity and duration

3. Atmospheric vorticity

4. Velocity inside dust devils

5. Dust devil characteristics:

   a. Time of occurrence

   b. Location

   c. Duration

   d. Frequency

   e. General structure

   f. Direction of rotation

6. Aircraft measurements of temperature at heights of 77, 150, 300, 920, and 1540 m

7. Pole temperatures at 0.3, 1, 2, 4, 7, and 14 m above ground

8. Ground temperature.

As a result of these tests, Ryan and Carroll were able to relate the following.

1. Lapse rates from surface to 0.3 m or less were measured to be as much as 9000 times the dry adiabatic.

2. Lapse rates between 0.3 and 10 m were normally 20 to 40 times the dry adiabatic.

3. Above 10 m the lapse rates were moderately superadiabatic.

4. Vertical wind velocity in dust devils seemed to depend on the thickness and temperature lapse rate of the moderately superadiabatic layer and the calculated Monin-Obukhov scale height.

5. The maximum rotational wind velocity was dependent on W_{max} and dust devil diameter.

In addition to these results they postulated that dust devils could be divided theoretically into three distinct vertical regions above the surface. The first of these regions comprises the lower boundary layer which is characterized by turbulent inflow that is visible as a diffusive, shallow dust cloud near the ground. At the base the friction layer dust is entrained into the core of the dust devil. The second region resembles a thin, sharply defined cylindrical or slightly conical rotating dust column having a very large height-to-diameter ratio. This volume is surrounded by a rotating airflow that exhibits little or no mixing with the main cylindrical dust column. The third region begins where the top of the dust column becomes turbulent, with dust diffusing radially with height like a detraining plume of effluent. This region appears to be the dust devil decay region. Along the core axis of the three regions, there is a relatively low-velocity downdraft with radial outflow, at least near the ground; and, in a sense, the dust devil can be considered to be a two-cell vortex. This theory was later expanded by Ryan as the result of additional testing.

According to Ryan and Carroll, Kno has derived solutions for atmospheric vortices and states that the wind velocities in dust devils could be expressed in the following form:

$$W_{max} \propto \left(\frac{g}{\theta}\frac{\partial\theta}{\partial z}\right)^{1/2} z$$

$$V_{max} \propto (W_{max}/z\gamma)^{1/2}\,\xi_{\nu}$$

where

W_{max} = maximum vertical wind velocity

V_{max} = maximum tangential wind velocity

g = gravitational acceleration

θ = potential temperature

z = height

γ = kinematic viscosity

ξ_{ν} = environmental vorticity.

These expressions, as yet, are not too conclusive because of assumptions and lack of verification from field data.

In addition to their own work, Ryan and Carroll stated that Flowers (1936), Ives (1947), and Williams (1948) found the following information concerning dust devils in earlier research:

1. Dust devils are generated only when the near-surface atmosphere is superadiabatic to considerable height.

2. Dust devils occur most frequently under moderate to light wind conditions.

3. Dust devils reach heights up to 1 km and diameters of 100 m or so.

4. Dust devils can generally attain longitudinal wind velocities as great as 13.8 m/s, although Ives reports velocities up to 50 m/s.

J. A. Ryan [4] continued the research of dust devil field data taken in the Mojave Desert in 1968 [3]. In his work Ryan emphasized the search for correlations between various atmospheric properties and dust devil characteristics. In this case he divided the lower atmosphere into four distinct thermal layers:

Layer 1 — The extremely superadiabatic layer from the surface to approximately 0.3 m where the lapse rate (γ_1) is approximately 60°C/m

Layer 2 — A strongly superadiabatic layer from approximately 0.3 to 10 m where γ_2 is approximately 0.25°C/m

Layer 3 — A thick, typical range of 100 m to 1 km with moderately superadiabatic conditions where γ_3 is approximately 1.2×10^{-2}°C/m

Layer 4 — The overlying dry to subadiabatic layer.

The dust devil wind velocities were found to be dependent on the degree of instability in the γ_3 layer. This finding served to clarify the relationship between the precise rate of ambient temperature and the dynamical characteristics of mature dust devils. However, it indicated only that temperature structure should be involved in dust devil initiation. Ryan further states that the atmospheric properties contributing to dust devil maintenance may be different from those responsible for initiation, as can be seen from the earlier work of Ryan and Carroll [3] which revealed that, although local atmospheric vertical vorticity played a role in dust devil initiation (providing initial rotation), the dust devil inflow-upflow appeared to be responsible for rotation maintenance.

The frequency of dust devil occurrence was further investigated by Ryan. For dust devil occurrence for diameters >1.0 m, the only correlation that could be found was with the lapse rates of the γ_2 layer. It was seen that dust devil frequency increased markedly with increasing lapse rates in this near surface layer. As for dust devil diameter, Ryan states that it is also evident that increasingly larger dust devils appear as γ_2 increases and that the mean diameter likewise increases.

Ryan mentions that Neubauer suggested that dust devil frequency depends on $\Delta T_o/T_o$, increasing as this ratio increases, where T_o is the mean ground surface temperature over a diurnal cycle and ΔT_o is the difference between the ground surface temperature at a given time and the diurnal mean temperature. This infers that surface temperature, rather than the degree of atmospheric instability, is the governing factor. Through special approximations of $\Delta T/T_o$ for the study of dust devil frequency, duration, etc., Ryan found no correlation and, therefore, states that $\Delta T_o/T_o$ is not a pertinent physical parameter.

Ryan concludes that the only factors apparently involved in the initiation of dust devils are γ_2 temperature lapse conditions and local horizontal shear with associated turbulence. Shear (vertical vorticity) provides the required initial rotary motion, whereas turbulence triggers the upward movement of the unstable air.

The interesting feature of the dust devil is that the air encompassed in these small systems exhibits such orderly behavior. The disorganized physics of unstable air over a hot desert region in the forenoon and afternoon appears to suggest complete chaos such that no organized circulation could possibly exist. D. E. Fitzjarrald [5] looked at vorticity associated with a limited number of dust devils in a field program conducted in the same general area investigated by Carroll and Ryan — the El Mirage Dry Lake in the Mojave Desert of Southern California. Reference 5 describes the instrumentation used in Fitzjarrald's field study. Fitzjarrald's work is summarized briefly as follows:

1. The study was based on the premise that there exists a large scale of motion which provides the necessary vorticity to sustain the rapidly rotating dust devil.

2. No correlation was seen between the sense of vorticity meter and dust devil rotation (the vorticity meter is described as a paddle wheel 1 m in diameter with four 27.5 cm blades, mounted with the axis of rotation oriented vertically, which measures upward-downward motion only). (Carroll and Ryan later found this statement to be invalid, and Fitzjarrald, in agreement, recommended an improved method to more properly measure larger-scale vorticity.)

3. In Fitzjarrald's study of 11 dust devils for air temperature and $\underline{v}$ and $\underline{w}$ winds inside the bases of the vortices (measurements at 2.0 m above ground), the only significant points were: (1) tangential wind speeds reached values of 8 to 12 m/s, (2) some $\underline{w}$ measurements showed limited vertical air motion, and (3) a slight increase in core temperature was evident for four of nine dust devil core temperatures recorded.

Fortner and Ihara [6] make some brief comments concerning dust devils that occur near Tokyo, Japan. They state that the meteorological conditions most favorable for the formation and maintenance of dust whirls, or dust devils, are:

1. Relatively level terrain with loose surface material

2. Intense surface heating, with temperature lapse rates near the surface greatly exceeding the dry adiabatic

3. Winds near the surface below certain critical speeds.

Many researchers of dust devils discuss the extreme temperature lapse rate conditions at ground level. This seems to be a primary condition for dust devil development; however, various other governing atmospheric conditions must prevail to support and maintain this vortex phenomenon. While it is agreed that excessive lapse rates at ground level strongly indicate that dust devils will occur, it is more important to be able to identify those atmospheric properties that introduce superadiabatic lapse conditions at ground level. It is interesting to note that, according to Fortner and Ihara, the dust whirls that occur north of Tokyo (Kanto Plains) do not occur over an arid region or over a plateau, and there is no indication that the near surface temperature lapse rate greatly exceeds the dry adiabatic. They observed the development of a number of dust whirls up to a mile in diameter. Their conclusion was that the thickness of the unstable layer and the strength of the wind field in this layer were undoubtedly the prime factors in producing the dust whirls.

Sinclair [7] presents a composite of statistics on some 456 dust devils observed by various researchers. These dust devils were categorized according to diameter near the base, height, and rotational direction. The statistics show that small dust devils having a diameter less than 1.5 m to approximately 10 m and a maximum height of approximately 6 m rotate cyclonically more frequently (i.e., 3:1). Dust devils with diameters greater than approximately 50 m and heights of 300 m and greater also have a slight tendency to rotate cyclonically. For the intermediate sized dust devils, cyclonic and anticyclonic rotations appear equally likely at least in the area of Tucson, Arizona.

Sinclair also cites additional information on dust devil characteristics from two independent sites (areas of high dust devil occurrence), each approximately 259 km^2 in area. One site engulfed the city of Tucson; the other was in the AVRA Valley centered approximately 32 km west of Tucson. The investigation took place during the summers of 1960 through 1962 and yielded the following information:

1. Dust devil initial location of development: in dry river beds that lie in the lee of small hills.

2. Lifetime: from a few seconds (most frequent) to approximately 20 min. A few have been observed to last more than 2 h. Dust devil duration increases with size.

3. Maximum activity: 1300 to 1400 Local Standard Time (LST); that is, the time of maximum soil surface temperature.

4. Number of occurrences: approximately 50 to 60 per day, with an increasing number from June to July. Days with significant cumulus cloud coverage show a suppression of dust devil development.

5. Time of day of occurrence: from approximately 1000 to 1700 LST.

6. Surface temperature lapse rate: extremely superadiabatic

7. Surface winds: The greatest dust devil activity occurred when winds were less than 5 m/s. Dust devil activity is suppressed under conditions of high surface wind speeds.

8. Direction of travel: Dust devils in the Tucson and AVRA Valley areas generally travel from west to east.

9. Rotation (cyclonic-anticyclonic): no real preference proven.

Sinclair's report on this investigation contains details far beyond what is stated herein. However, further recording of the characteristics of dust devils is certainly encouraged, particularly how dust devil occurrences are related to other types of thermals, such as the dry thermal plume. In conclusion, Sinclair states that additional information is needed to ascertain the role of distinct dry thermal elements, the size of dust devils, and the heat and momentum budget of the desert atmosphere.

Lamberth [8] made measurements of 21 dust devils with the use of stationary sensors at the White Sands Missile Range, New Mexico, between May 15 and September 15, 1959. Measurements of atmospheric pressure, wind velocity, and temperature were obtained. The dust devils occurred between 1030 and 1400 LST with the most frequent dust devil passages at the observation site being at approximately 1400 LST. The following generalities were observed about the 21 dust devils:

1. Peak occurrence: approximately 1400 LST

2. Direction of travel: from SW to NE

3. Height range: 3 to 60 m

4. Diameter: 1 to 30 m

5. Rotation direction: no preference

6. Maximum wind speed increase: approximately 12 m/s

7. Pressure decrease: 40 to 220 N/m^2 (0.4 to 2.2 mb) with an average of 90 N/m^2 (0.9 mb)

8. Temperature range (measured at 1.3 m height): 27.7° to 37.7°C, average of 33.3°C

9. Lapse rate temperature (1.3 m level versus 14.7 m level above ground): -18.5° to -23.6°C, mean lapse rate of -15.8°C

10. Cloud condition: mostly clear or some scattered clouds.

Lamberth concludes by stating that it is best to measure dust devil data with mobile sensor/recorder systems because, even in areas where the number of occurrences of such vortices is high, the probability that an adequate number will pass over a "fixed observation location" is extremely low. Also, all sensors/systems to sense meteorological criteria related to the dynamics of dust devils should be faithfully responsive so that 0.1 s measurements can be taken.

Some interesting comments and conclusions were made by J. C. Kaimal and J. G. Businger [9] in a paper which describes the characteristics of a convective plume and a dust devil from measurements made at a stationary instrumented site in Kansas. The convective plume and the dust devil occurred approximately 20 min apart in the early afternoon of July 22, 1967.

According to Kaimal and Businger, convective plumes are usually identified by their sawtooth appearance in temperature recordings obtained during passage at a stationary sensor. They exhibit vertical continuity and tilt in the downwind direction, and wind velocity tracers show that they are reasonably free of erratic fluctuations within the boundaries defined by the temperature trace. Such plumes are more clearly defined in the morning when the winds are light and the unstable boundary layer is developing; however, the dust devil is far less frequent. The dust devil selected for discussion in Reference 9 showed the downdraft very clearly. The paper by Kaimal and Businger should be reviewed for information on site instrumentation and many other specific details. Some of the significant points are summarized here:

The Plume

1. The most striking feature of the plume is the sharp drop in temperature at the upwind edge.

2. The microfronts of the plume can be less than 1 cm thick.

3. The maintenance of such a front associated with a plume in the turbulent environment seems to require very active stretching along the front and strong convection perpendicular to the front.

4. The $\underline{w}$ wind component shows a marked increase going from the lower (5.66 m sensor height) to the upper level (22.6 m sensor height), which is consistent with the stretching (see preceding item 3).

5. The $\underline{w}$ component was predominantly positive (upward flow) within the plume in question and negative outside its bounds. This was most characteristic in the recorded 22.6 m $\underline{w}$ wind sensor measurement.

6. The $\underline{w}$ wind component remains low within much of the plume but has a sudden increase just ahead of the front.

7. The $\underline{v}$ wind component for the plume in question was relatively inactive.

8. A marked temperature increase occurred at the 5.66 m and 22.6 m sensing height during passage of the plume in question, which is in good correlation with the $\underline{w}$ wind component trends.

9. This convective plume showed that approximately 2.5 times the amount of air passing (horizontal cross section of plume) at 22.6 m than at the 5.66 m height. This suggests significant entrainment.

The Dust Devil

1. The dust devil that passed the site in near proximity in time (20 min previous) of the convective plume showed a strong updraft around the vortex and a downdraft within the core (common to the dust devil).

2. The volume of air surrounding the dust devil is quite turbulent; therefore, the boundaries of the dust devil are not as clearly defined as the plume.

3. The $\underline{w}$ wind component data of the dust devil in question showed nearly identical magnitudes at the 5.66 and 22.6 m levels, indicating little vertical stretching between the levels. (This statement is questioned since the horizontal cross section of the dust devil at the two levels should be more closely examined.)

4. The temperature trace of the horizontal cross section of the dust devil is not as sawtoothed as the convective plume.

5. The $\underline{w}$ wind component data increased suddenly at both levels (i.e., 5.66 and 22.6 m) just prior to the arrival of the dust devil.

6. The $\underline{v}$ component showed that the dust devil was a cyclonic event. Reversal of this component during the dust devil passage was clearly evident from the recorded data.

Kaimal and Businger discuss these plume and dust devil data in great detail and provide an inferred theoretical relationship.

In summary, the major differences between the convective plume and dust devil observed by Kaimal and Businger were as follows:

1. The plume, unlike the dust devil, is basically a nonrotating system.

2. The plume appeared to be transported at some mean velocity near the ground; the dust devil moves with a mean flow nearer its upper height.

3. Vertical stretching of the plume seemed quite obvious; the dust devil data lacked such an indication.

This work is an excellent source of information comparing a convective plume to a dust devil. Needless to say, much more work must be undertaken to add more detail to the interesting work accomplished by Kaimal and Businger.

Rudolf Geiger [10] states some interesting facts concerning dust devils. Geiger cites a dust devil that was observed to last for 7 h in Utah. Its height was approximately 800 m over an extended travel path of 60 km. (As mentioned earlier, dust devils can extend to heights of 1000 m in many arid zones of the Earth.) Geiger reports some cases of damage to hot bed windows and other minor disturbances to people and property. Again, Geiger, like other investigators, relates the occurrence of dust devils to the superheated condition of the ground and near-ground air. It is not uncommon to witness dust devil disturbance during conditions of thunderstorm development.

W. M. Porch [11] discusses suspension and resuspension of desert dust. Porch states that the increase in afternoon wind and associated suspension of desert dust seems to be a regular feature of the desert area under normal meteorological conditions. Using light-scattering detection instruments (the nephelometer) with fast response capability, he was able to detect short-term changes in aerosol content due to blown dust. His nephelometer data show that aerosol suspension under these circumstances occurs as short-term (≤ 2.0 min), concentrated puffs of dust. The frequency of these puffs appears to be dependent on wind speed and turbulence. Little or no dust devil materials (dust, sand, etc.) were actually measured by nephelometer principles; however, Porch shows aerosol-light scatter data as measured by aircraft from field data of 1972. He found a steady increase rather than a steady decrease in aerosol content with height. This suggests that it may have been possible for dust devil activity to distribute these aerosols even to heights of 5 km. Porch expresses interesting speculations concerning this manner of resuspension of material, such as contaminants, which could cause health hazards.

Sherwood B. Idso [12, 13] gives new information about the possible causative mechanism of the dust vortices. These articles should be reviewed in detail; however, a few points of interest are as follows:

1. The atmospheric vortex that is most difficult to classify is the type that forms near dust storm frontal boundaries. R. S. Ingram, as referenced by Idso [12], describes these vortices as eddy tornados and associates their formation to that of eddies that form downstream of prominent rocks in a fast-flowing stream of water. Ingram finds the most likely area for their occurrence to be between 0.8 and 4.8 km downwind of a significant topographic disturbance (small mountain system or hill) having a path length of 0.4 to 1.6 km. Idso also has seen eddy tornados develop and diminish in a short period of time.

2. Idso discussed "vortex twinning" in which loops of horizontal vortex tube may be drawn up out of the local boundary layer and break at the top to form pairs of oppositely rotating vortices. He states that when such vortex tubes encounter a small mountain or hill, they may be more apt to be drawn up in loops than when they roll across the flat desert terrain. The parent roll vortices may be either of a mild fair-weather type which could produce dust devil pairs, or they may be of a more violent nature located in density current heads which may produce twin tornados. The fact that paired vortices occur in the lee of isolated mountains gives considerable credence to the hypothesis that vortex twinning may be responsible for their generation.

3. Vortex pairs spin in opposite directions, and multiple vortices may form which share the same sense of rotation.

4. Pairs of water spouts have been observed frequently. Twin formations were seen to funnel from the base of an unstable cloud layer over the north central Gulf of Mexico in June 1971; after approximately 3 to 4 min in forming, the funnels slowly merged and shortly disappeared. The observation point was too far away to determine whether the two funnels were spinning in opposite directions. The cloud bases were estimated at approximately 2135 m, whereas the two funnels extended downward approximately 300 m from the cloud base. Several other funnels developed over a period of approximately 30 min of this partial-funnel development event.

Idso [13] also states that Julian D. Hayden, who directed much of the archaeological work at Ventana Cave (on the Papago Indian Reservation, south of Phoenix, Arizona), told him about small dust devils that traveled through the Ventana Cave. Hayden's communication with Idso was as follows:

> When we started work, tiny whirls of dust would start up in the rear of the cave, increase in size as they approached the mouth of the cave, and by the time they reached the top of the talus, they were powerful enough to take our wheelbarrows and planking with them. We could watch them for miles in their progress across the desert to the east, rising to several hundred feet in height.

In addition Idso [14] notes that on various occasions observers have witnessed dust devils traversing lakes and other small bodies of water. The dust devils develop over land and then travel onto water with enough force to last for several minutes. At the base, over water, these vortices raise a circular ridge of moisture a few inches from the water surface. On one occasion an observer reported that water particles were lifted with such persistence that the entire height extent of the dust devil was composed of mist.

G. D. Freier [15] reports on the electric field associated with a large dust devil that developed in the Sahara Desert at Kidal, French West Africa, on September 29, 1960. The electric field measurements were made during an eclipse of the Sun at 1330 LST in the afternoon. Air temperature at the time was recorded at 41.1°C (location of temperature measurement with respect to the ground is not stated). Freier states that the fully developed dust devil was approximately 200 m high and approximately 8 m in diameter, and the closest approach to the dust devil with his electric field mill was approximately 30 m. The electric field mill record showed a positive electric charge (volts/meter) in the near vicinity of the dust devil which implied positive charge about the Earth. Electric field studies near and within dust devils are cited in other similar work; however, additional investigation on this matter is needed.

An investigation of the electric field of dust devils was carried out by W. D. Crozier near Socorro, New Mexico [16]. The site was a semidesert mesa named Jornada del Muerto located approximately 30 km southeast of Socorro. The primary method of investigation was field mill recording of the potential gradient. The recording of the physical characteristics of dust devils was also attempted, but limited satisfactory results were obtained because of occasional equipment limitations or failure.

During one phase of the investigation (in August 1964), an electric moment[1] of 3.3 Cm was measured for a rather large dust devil that passed approximately 730 m from the instrument site. The charge density was on the order of 1×10^6 e/cm^3 (e = elementary change).

A second field study took place in June and July of 1966. Of 53 dust devils studied, only 17 were used (some data were based on fewer than 17) to obtain the following summarized results:

1. Range of distance of dust devils from field electric instrument site: 100 to 1090 m, average distance was 485 m.

2. Measured potential gradient[2] (volts/meter): range 50 to 1580 V/m, average 224 V/m.

3. Electric moment (coulomb meter): range 0.009 to 55.0, average 5.51.

4. Height of dust devils based on 10 out of the 17 cases considered: range 22 to 230 m, average 84 m.

5. Diameter based on 10 out of the 17 cases considered (same dust devils as preceding item 5): range 11 to 62 m, average 27.3 m.

6. Charge density (e/cm^3) based on 8 out of the 17 cases considered: range 0.06×10^6 to 9.0×10^6, average 3.7×10^6.

---

1. From Crozier [16], the electric moment is understood to be the product of the electric charge and the distance between charge and image.

2. Potential gradient is always negative, indicating negative charge in the dust devil.

Generally, Crozier relates the following:

1. Considerable dynamic changes can be observed to take place during the life cycle of any one dust devil.

2. The potential gradient of some dust devils was too small to measure; others exceeded the maximum range of the sensor/system being used to measure the potential (i.e., 3 kV/m).

3. Photographic data of some dust devils yielded useless results because the vortices outgrew the field of view.

4. In some quite large dust devils, the dust column narrowed significantly at the base (10 m); in others the base diameter was several tens of meters.

5. The dust densities at great heights usually were comparatively small, and it seems reasonable to believe that most of the electric charge resides at the lower levels.

6. Winds at the time of dust devil occurrence were almost always highly variable in direction and speed.

7. The translational motion of the dust devil is largely derived from the general wind field in which it is immersed.

8. According to Crozier, C. D. Stow concluded in 1969 that dust devils rarely occur when wind speed exceeds 4 m/s, but Crozier has some doubt about this conclusion

9. Electron charge density of dust devils appears generally to be approximately 10^6 e/cm^3.

B. Reported Dust Devil Damage

The following observations, from the official weather records [13] of Phoenix, Arizona, have been made concerning dust devils and damage:

Thursday 29 May 1902

A violent whirlwind of very narrow path passed through the city from the southwest at 3:15 p.m. It demolished a livery stable, throwing outward the walls on the northeast corner, and carrying the whole roof some distance from the stable, while various debris were found carried several hundred feet away. Several sheds and minor buildings suffered as it passed on towards the northeast. Fresh westerly wind from 6 p.m. to time of 8 p.m. observation. Clear during day.

Friday 30 May 1902

Clear. No phenomena. A whirlwind of destructive violence unroofed the store of H. A. Diehl, near corner of Washington and Center streets at 2 p.m.

It is interesting to note, first of all, that these two violent whirlwinds occurred on consecutive days. Secondly, their strengths would seem to indicate that they were more than just common dust devils.

Dust devil (dust whirl) damage, although usually minor and not reported, caused concern to many people. A dust whirl of high intensity caused considerable damage to a house roof in Nicosia, Cyprus, at 1315 GMT, July 31, 1969, as reported by J. B. McGinnigle [17]. Approximately 400 roof tiles, each weighing 2 kg, were torn from a roof and scattered in an easterly dispersed pattern from the point of damage. The dust whirl path was from WSW to ENE. Damage occurred on the east slope of the roof on which the roof orientation (main ridge) was SW-NE. Open windows in the house allowed a strong draft in which light items, such as papers, were actually blown out the open windows on the east side. Such items were found lodged at the walls of surrounding houses several meters distant. Chairs and other heavier, non-anchored objects were toppled and displaced in an easterly direction from their point of rest. At the onset of the dust whirl very strong and sudden wind was experienced for approximately 10 s during which time windows, shutters, and other loose items were blown about violently. Heavy dust settled through cracks and at other obvious locations as a result of debris from the vortex. An estimate of the dust whirl travel rate was 10 m/s rotating cyclonically. The estimated vertical height was 100 m, and the diameter of the circulating top appeared to be approximately 50 m.

The nearest meteorological observing station is at Nicosia Airport approximately 2 km southwest of the site of the dust devil damage. The following observations were made at the airport just after the roof damage incident:

Time:	1337 GMT
Wind Direction:	280°
Wind Speed:	7.5 m/s
Air Temperature:	35.5°C
Dew Point:	14.6°C
Relative Humidity:	29 percent.

(An anemogram shows onset of sea-breeze at 1310 to 1315 GMT at the airport.) Little pressure change was recorded at the airport any time near that of the occurrence of the dust whirl. No clouds, except small amounts of cumulus (base 2135 m) over the Troodos Mountain range, were reported. A much earlier pilot balloon ascent (0800 GMT) made on a nonroutine basis, at the Nicosia Airport, showed that the low-level winds were very low in speed (1 to 3 m/s) from the northwesterly direction. This information adds little value in trying to understand the dust devil event that occurred more than 5 h later. However, assuming light low-level winds (1 to 4 km), intense heating at the surface, persistent westerly winds near the surface at 4 to 7 m/s, etc., would be expected to enhance the development of a dust devil with such damaging effects. McGinnigle states that dust devils are common in summer in the central plains area of Cyprus. They generally appear to be approximately 30 to 60 m in vertical development and generally occur with the onset of the sea-breeze (late morning to early afternoon development). He further states that the dust devils usually move with the wind speed and direction at the top of the circulating vortex. McGinnigle's report is one of very few that discuss property damage associated with dust devils. Needless to say, the damage from such events throughout the world runs into the millions of dollars per year.

It should be mentioned that Barcilon and Drazin [18], Maxworthy [19], and others have done extensive work on dust devil research, water spout studies, atmospheric vortex modeling, etc., but further discussion of other significant and extensive reports is beyond the scope of this review.

C. Idealized Dust Devil Model

The evolution, sustentation, and deterioration of dust devils, as with other atmospheric vortices, are still somewhat of a mystery. The general atmospheric conditions and regions of the Earth in which dust devils occur are known, but the actual development of any one such vortex event has not yet been determined. One of the authors of this report has conducted some extensive studies of lower atmospheric wind (i.e., mean profile phenomena, turbulence, shears, etc.) and has also made some subjective investigations of dust devil activity, particularly in the Southwestern United States and in Northern Africa. From these studies and this review, an attempt is made to extend some personal concepts on how dust devils develop. The main theme herein is based on the propagation of wind gusts downward to the surface during conditions when the ground is hot and the adjacent air at the ground is extremely unstable due to intense solar heating.

Position 1. Figure 1 aids in the discussion of the development and life cycle of an idealized dust devil. At position 1, a significant volume of relative warm, dry air begins to descend. This volume of air propagates downward to the surface, as is commonly observed and measured at meteorological tower sites having instruments capable of measuring such air motion. The volume of air at position 1 is semiunstable (i.e., not superadiabatic, but the temperature decrease with height is beyond adiabatic, as is frequently measured at locations where dust devils occur).

Position 2. As the air descends, it gains additional energy in the form of heat due to hydrostatic compression of the initially unstable volume of air as well as the action of descending and mixing with extremely unstable air next to the ground.

Position 3. With the excessive heat gain to the descending air, when the parcel of air is forced to move to position 3, it experiences maximum instability over the depicted trajectory shown by Figure 1. The microstructure of the extremely unstable air near the surface at position 3 forces the originally descending air particle to briefly turn outward horizontally and then suddenly upward with an excessively imposed cyclonic motion (or anticyclonically depending upon the microclimatic state of the thermodynamic nature of the soil and near-surface air in regard to heat, density, and localized circulatory structure). The circulatory microstructure, as identified by the notations α, β, and γ, forces the horizontal motion of near-surface air to turn cyclonically.[3]

3. In contradiction to authoritative concepts on dust devil spin direction, and especially to the fact that it is expected to be cyclonic due to Earth rotational principles, it is suggested that dust devils, whirlwinds, etc., spin according to and solely due to the small-scale circulatory phenomena of the immediate environment (air, soil, vegetation, etc.) in which they develop.

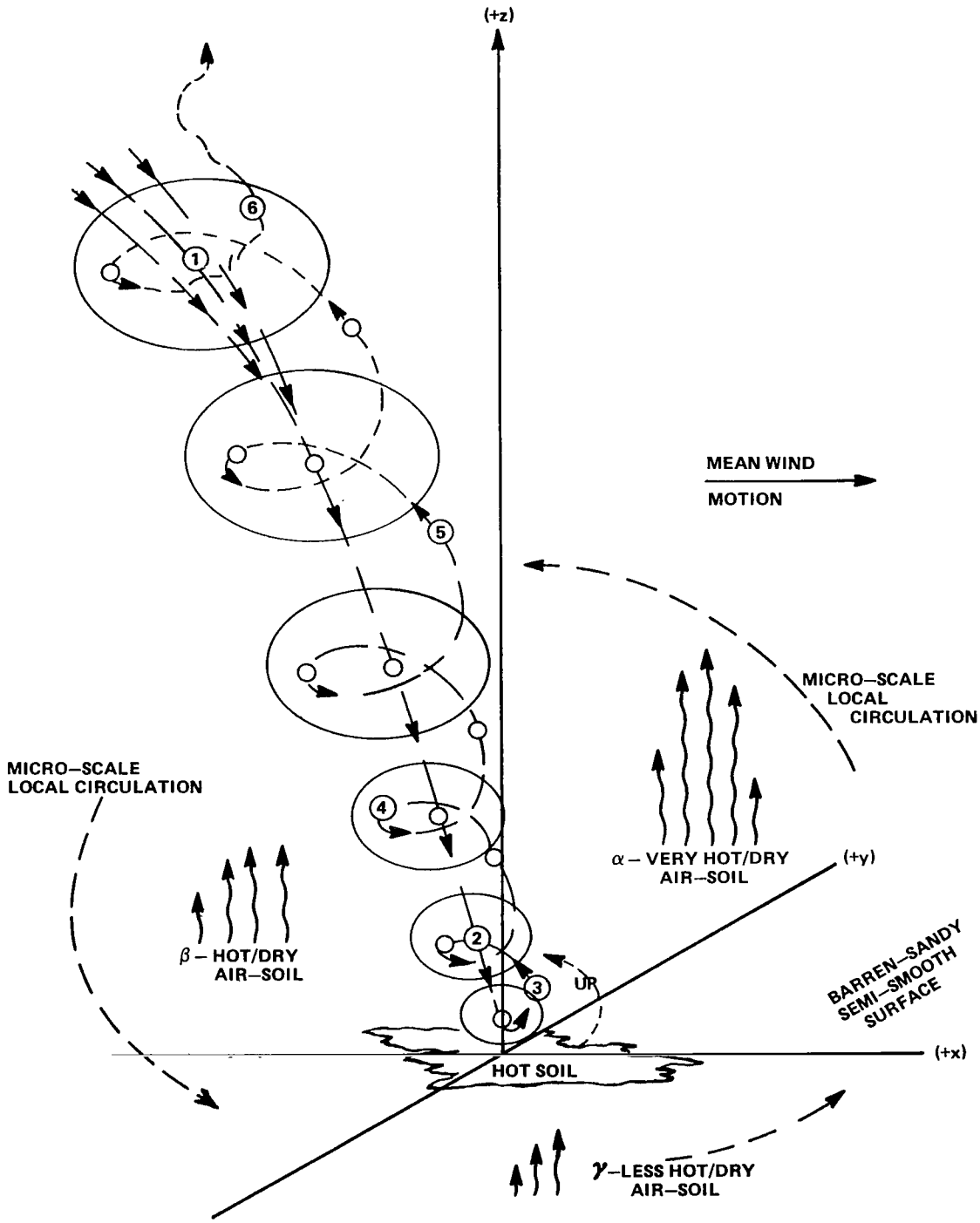

Figure 1. Idealized model of a dust devil.

Position 4. As shown by the idealized illustration, the diameter of the outer vortex of the system will tend to increase as the particle of air ascends in its cyclonic path. This increase is the result of such factors as entrainment of air, the decrease in the air density-pressure field with height, and stretching characteristics due to $\underline{u}$ and $\underline{v}$ variations up the horizontal winds. The latter point is better realized when dust devils are observed. It is not uncommon for the base of a dust devil to follow a very distinct and direct path as it traverses the ground, whereas the uppermost portion of the visible dust column may be seen to meander pronouncedly.

Position 5. At the mid-height position of the idealized dust devil, distinct transitions take place. Below this point, the dust devil is more systematically composed. The inner core is generally well organized with the outer vortex circulation, at least up to the time at which the dust devil begins to deteriorate. Above position 5, it is not unlikely to find meandering taking place; diffused vortex behavior is common; and, once the dust devil begins to degenerate, all orderly behavior of the system ceases above the mid-height position.

Position 6. The most erratic behavior (i.e., nonconformity to orderly vortex principles) of any dust devil is at the very top. Lack of well-organized vortex circulation is obvious as evidenced by the irregular behavior of wind at the uppermost height of any dust devil. Local upper level air motions disturb the upper portion of the idealized dust devil and distort and diffuse the system. Observations have shown that a dust devil can decay completely at the top only to repeatedly regenerate into a well-organized vortex ascending to greater and greater heights.

Once the idealized dust devil experiences external forces due to environmental winds, etc., or moves over a surface area dissimilar to that depicted by the idealized microclimatic conditions (surface heat structure, surface roughness, extraneous turbulent mixing, etc.) that sustain such as vortex, the dust devil then deteriorates and mixes with environmental turbulent air and loses its well-organized vortex identity.

This proposed idealized model treats air composing each such dust devil as a viscous substance. The density varies not only in the vertical but also in the horizontal x and y directions. A particle of air that follows the vertical downward path will, therefore, experience a hydrostatic pressure increase during its descent. Once the particle is impelled to rotate in the outer ring (vortex) and spiral upward, the particle would ascend along a "bent-thread-on-screw" trajectory over a path in which the density decrease would assume the

identical change with height that it underwent on initial descent. The bent-thread-on-screw path may be described as follows. First, assume a screw is placed in the vertical mode with the screw tip touching a horizontal solid plate. Second, consider that the screw is bent from a true vertical axis (in the negative x-direction as illustrated by Figure 1). Subsequently, if the screw is assumed to be of the dimension of a dust devil, then the density change in the horizontal (y-axis), through the plane (x-axis) of the curve of "screw-axis-bend," would be greater with distance from the core of the dust devil in the positive y-direction than in the negative y-direction. Thus, with regard to the idealized model, the density of the air from the center of vortex of the dust devil decreases more with distance in the positive y-direction than in the negative y-direction. This only suggests that less dense (warm) air is ascending upward more rapidly in the positive y-direction than in the opposite (negative) y-direction. This is supported by the fact that the very hot/dry air, as illustrated, is in the positive y-direction. The physics of this assumed dust devil model is simply based on the bent-thread-on-screw geometry in which the solid metal center of the screw is the dust devil core and the inclined tilted thread is simply the vortex of the dust devil. The authors believe this concept is logical. Based upon observations of dust devils in which objects the size of sage brush can be seen to be displaced (spiralling) upward on the incline of the bent-thread-on-screw configuration, such a postulation of dust devil geometry cannot be far from wrong.

III. SYSTEM DESCRIPTION

Operation of an SLDV [20] may be understood with the aid of Figure 2. A laser beam is transmitted through an interferometer which diverts a small amount of energy to the detector for use as a reference beam. The remainder of the energy passes through a telescope to a target consisting of naturally suspended aerosols in the atmosphere. Some of the transmitted energy is back-scattered by the target particles and enters the detector by the path shown in Figure 2. This returning energy has been shifted in frequency by an amount proportional to the component of particle velocity parallel to the direction of propagation according to the Doppler principle as shown in Figure 3.

The two beams incident on the detector have two different frequencies as shown in Figure 4: a large reference beam at the optical frequency f_o, and the smaller signal beam at the new frequency $f_o + f_d$ where f_d is the Doppler shift frequency. When these beams are added, the resulting beam contains a contribution at the difference of these frequencies.

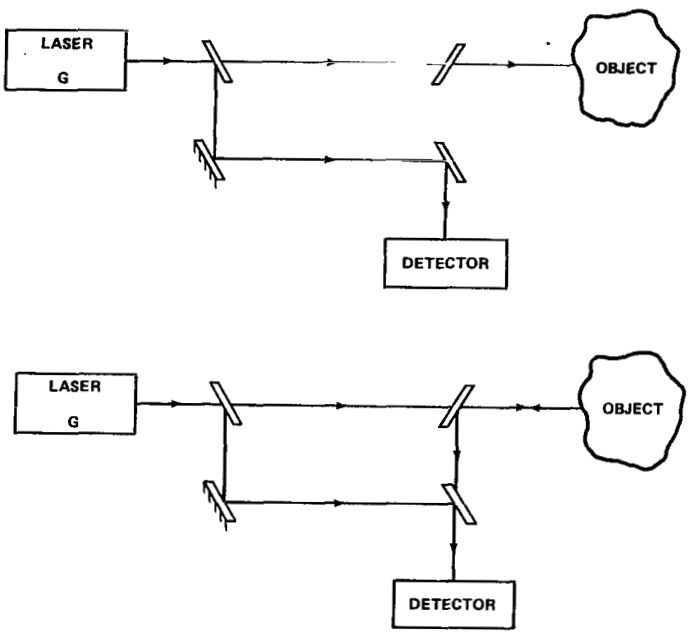

Figure 2. Laser beam path.

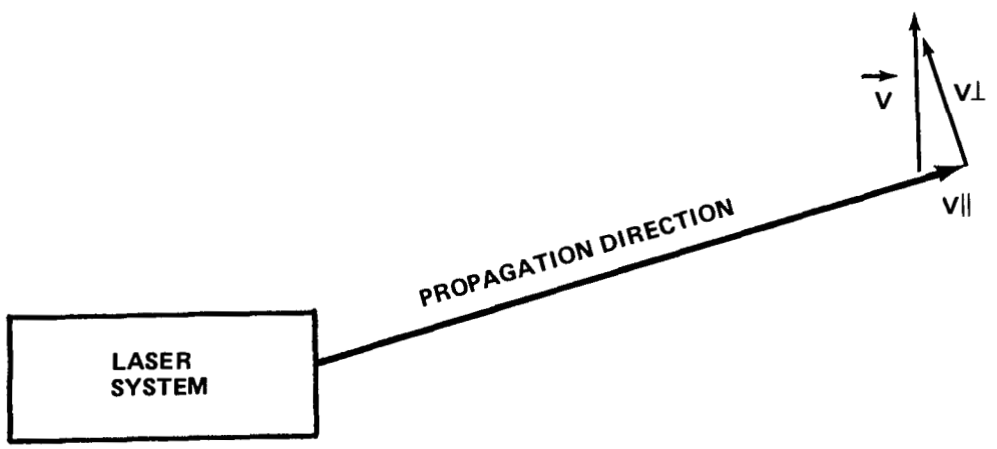

Figure 3. Laser Doppler velocity measurement.

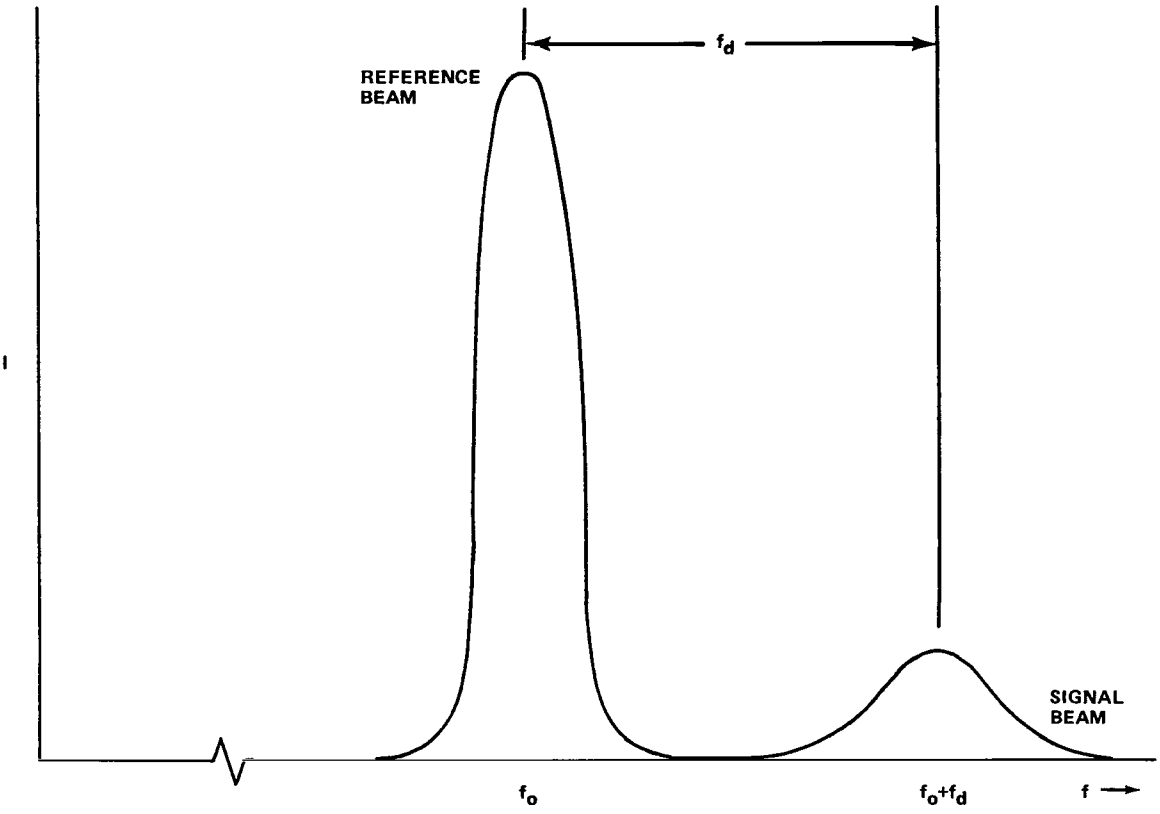

Figure 4. Illustration of optical heterodyning.

A spectral analysis of the output of the detector yields the Doppler spectrum of the target, where the frequency can be related to the target velocity by the relationship 100 kHz approximately equals 0.59 m/s.

The power at each frequency is a measure of the product of the backscatter coefficient of the target particles which are moving at that frequency and the system response at that range and frequency. The system response is designed to be independent of frequency over a large range.

A composite picture of the SLDV is shown in Figure 5. The system is mounted in an instrument van which is rigidly supported on a platform on the ground. The optical system is in the rear of the van with processing electronics, display, and tape recorder in the middle, and computer in the front. The upper right corner of the figure shows a sample output. The x and y coordinates are shown as functions of time on separate graphs. Additional outputs are available including y as a function of x, tabular data, and diagnostic outputs. Furthermore, tape recordings are made of the complete spectrum every integration time for more detailed analysis.

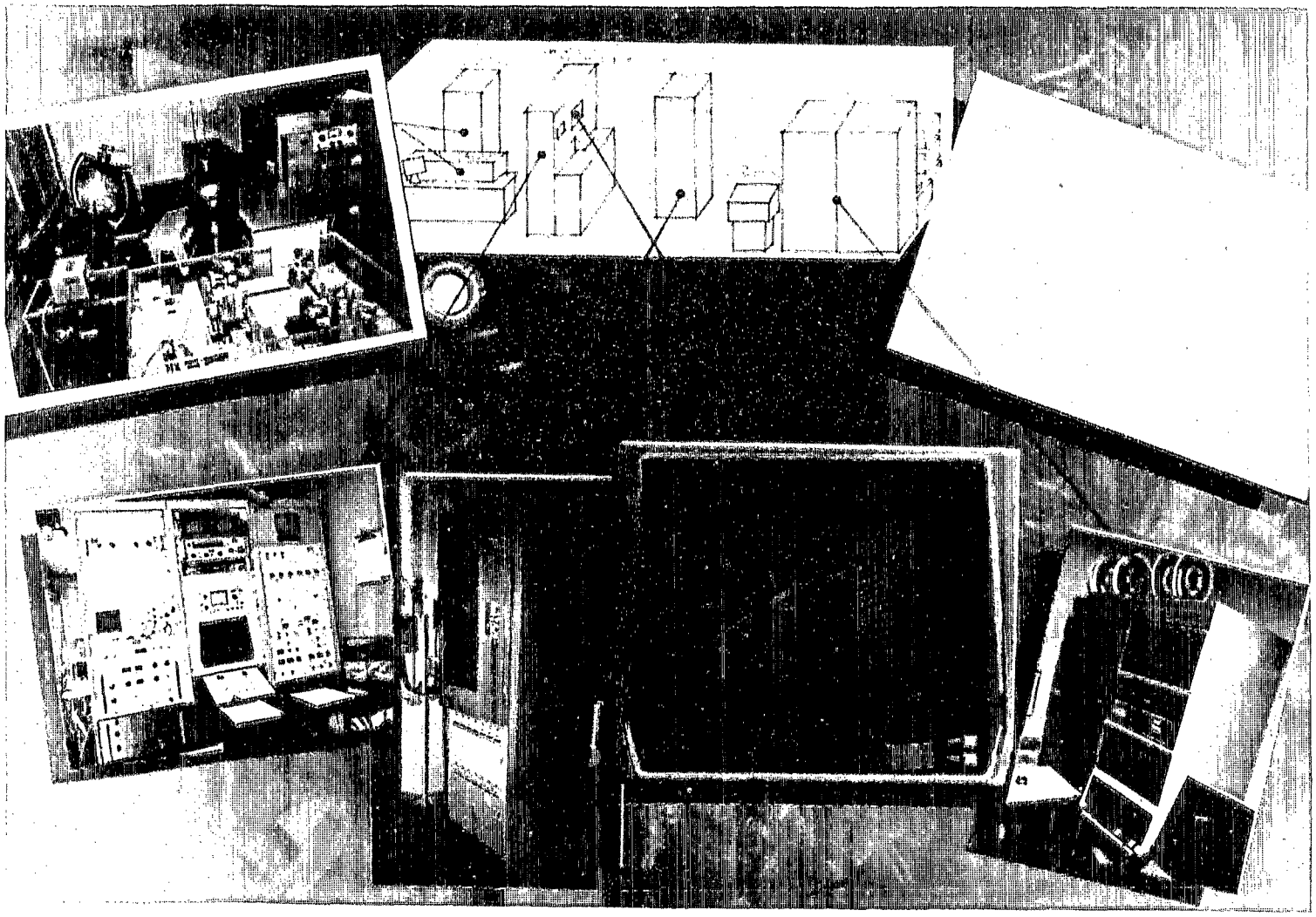

Figure 5. SLDV system composite.

A block diagram of the SLDV is shown in Figure 6. The system uses a stable CO_2 laser beam expanded and focused by a 30.48 cm telescope. Laser radiation is separated by the interferometer into a reference or local oscillator (LO) beam of a few milliwatts and a transmitted beam of more than 10 W. Optionally, a frequency translator is used to offset the LO frequency. The transmitted beam is passed through a telescope and scanning mirror to the target, reflected back through the telescope, and superimposed on the LO in the interferometer. The combined signal is incident on an Hg:Cd:Te detector cooled to liquid nitrogen temperature (77 K). Range resolution is obtained by the focusing of the optical system. The range of focus was varied by movement of the telescope secondary, and the azimuth angle was varied by means of a movable mirror reflecting the transmitted beam. By executing a fast range scan and a slow angle scan, the system scanned a horizontal plane. A spectral analysis of the heterodyne signal indicated the velocity of air at each focal volume. The processor thresholded the data, determined significant parameters of the spectrum, and output them to the computer. The raw data, giving a complete description of the spectrum, was recorded in pulse code modulation (PCM) format on a high speed tape for later, more detailed analysis. The data presented in this report are from the analysis of the high speed tapes.

IV. TEST PROGRAM DESCRIPTION

A. Test Site

Dust devil data collection with the SLDV system occurred on the Gila River Indian Reservation south of Phoenix, Arizona. Two test sites were used during the test program; however, due to equipment and logistics problems, the most meaningful data were collected during the end of the test period at the second test site. This test site is shown in Figure 7. The SLDV system was located in the semitrailer van, with equipment storage and support service being located in the smaller mobile van unit. The vans were positioned such that the SLDV was able to scan over an open field as shown in Figure 8. This field was in the process of being leveled for irrigation and the soil was extremely dry and powdery. While the soil conditions were very good for the entrainment of sand in the dust devil, the Earth mover involved in the leveling process created dust clouds which at times hampered the data analysis process. The cloud generated by the Earth mover, together with two dust devils in the background, is shown in Figure 9. The analysis of Run 9, Day 238 (covered in Section V) clearly shows the impact of the dust cloud on the dust devil data processing.

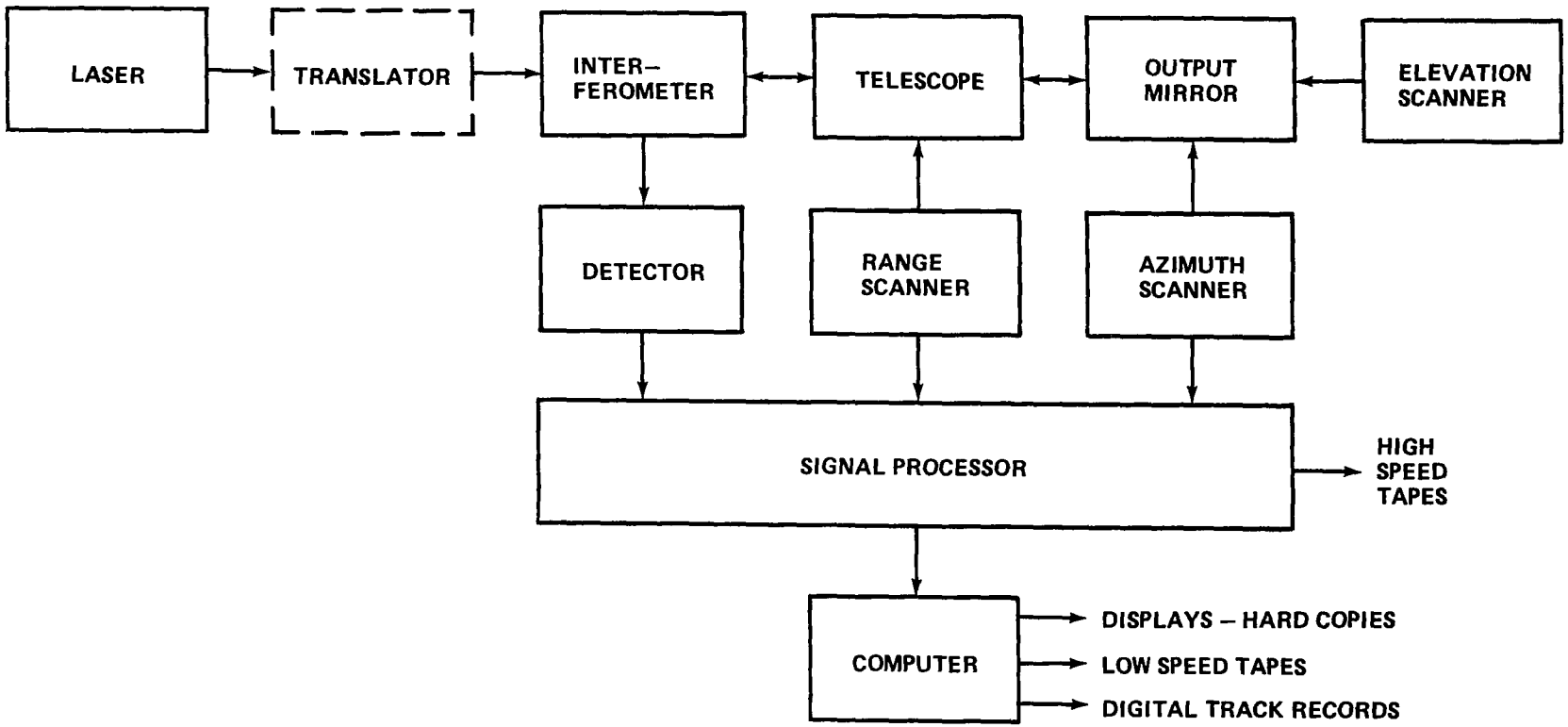

Figure 6. SLDV block diagram.

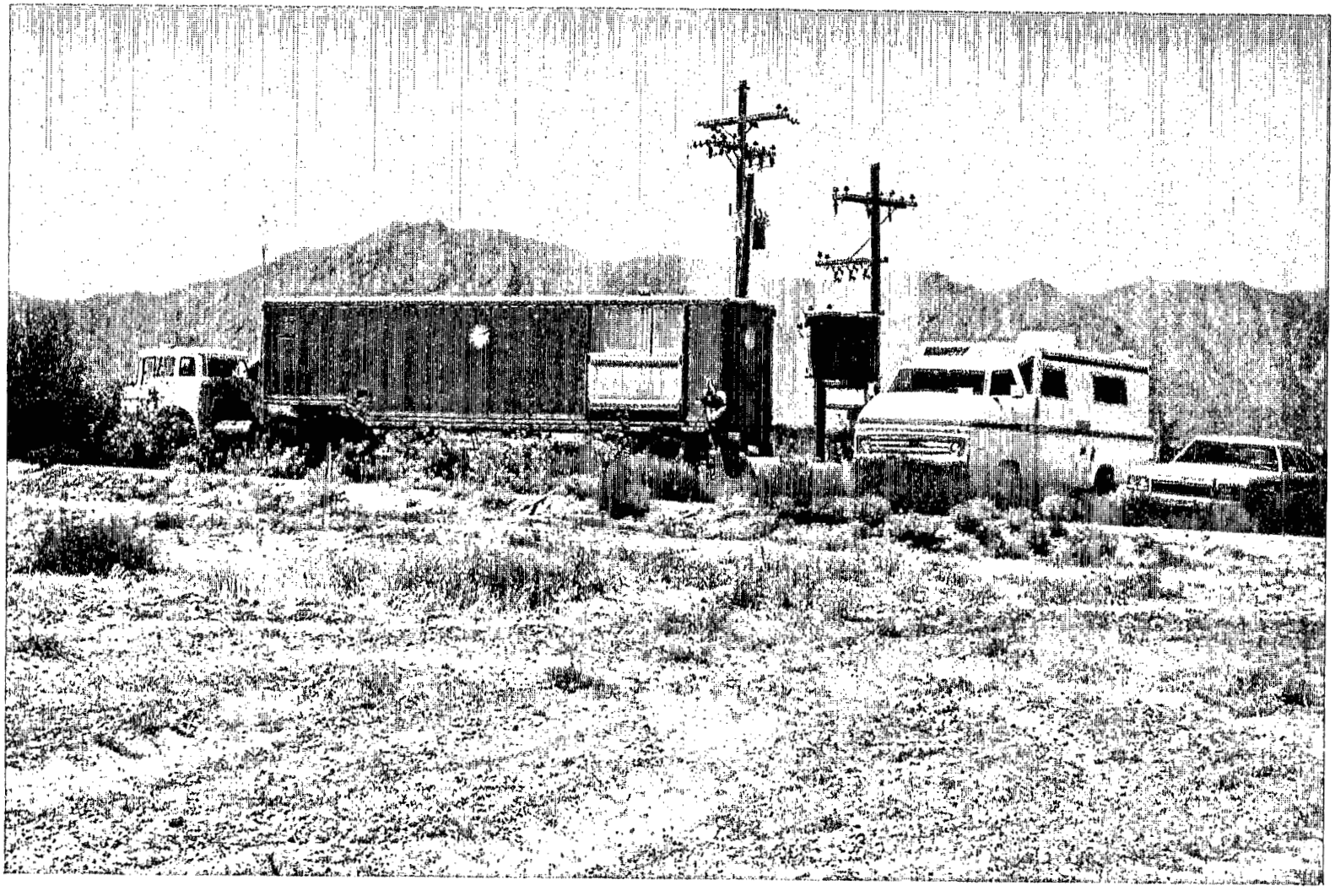

Figure 7. Dust devil test site.

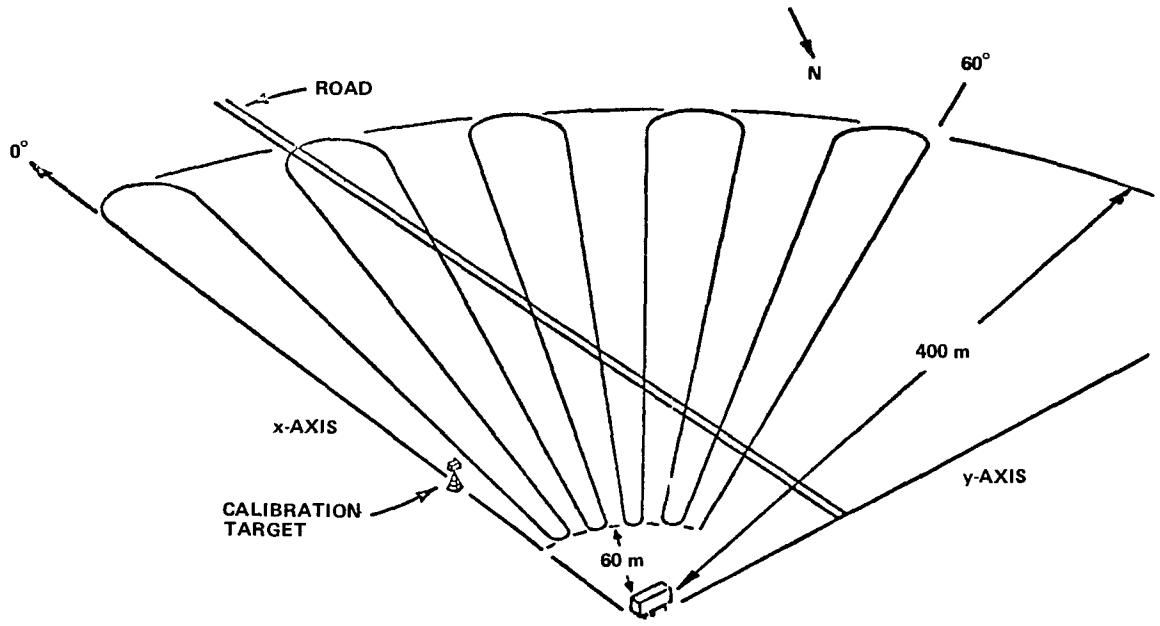

Figure 8. SLDV scan pattern.

The majority of dust devils occurring during the test program did not have sufficient strength to entrain a large amount of dust. While this did not affect the SLDV system, it did hamper the efforts to provide photographic information. Because of this, dust was artificially induced into the dust devil by kicking the sand at the base as shown in Figure 10. Once the sand was loosened, it was immediately picked up by the dust devil. This method allowed photographic records to be made, but because of the high backscatter caused by the sand the return signal from the dust devil very nearly exceeded the dynamic range of the SLDV system causing problems in determining the S/N ratio involved with the dust devil.

B. Test Procedure

The procedures used during this test program were for the purpose of obtaining the following information:

1. The velocity profile across the dust devil as a function of time, at a constant altitude

2. The velocity profile as a function of time for several altitudes

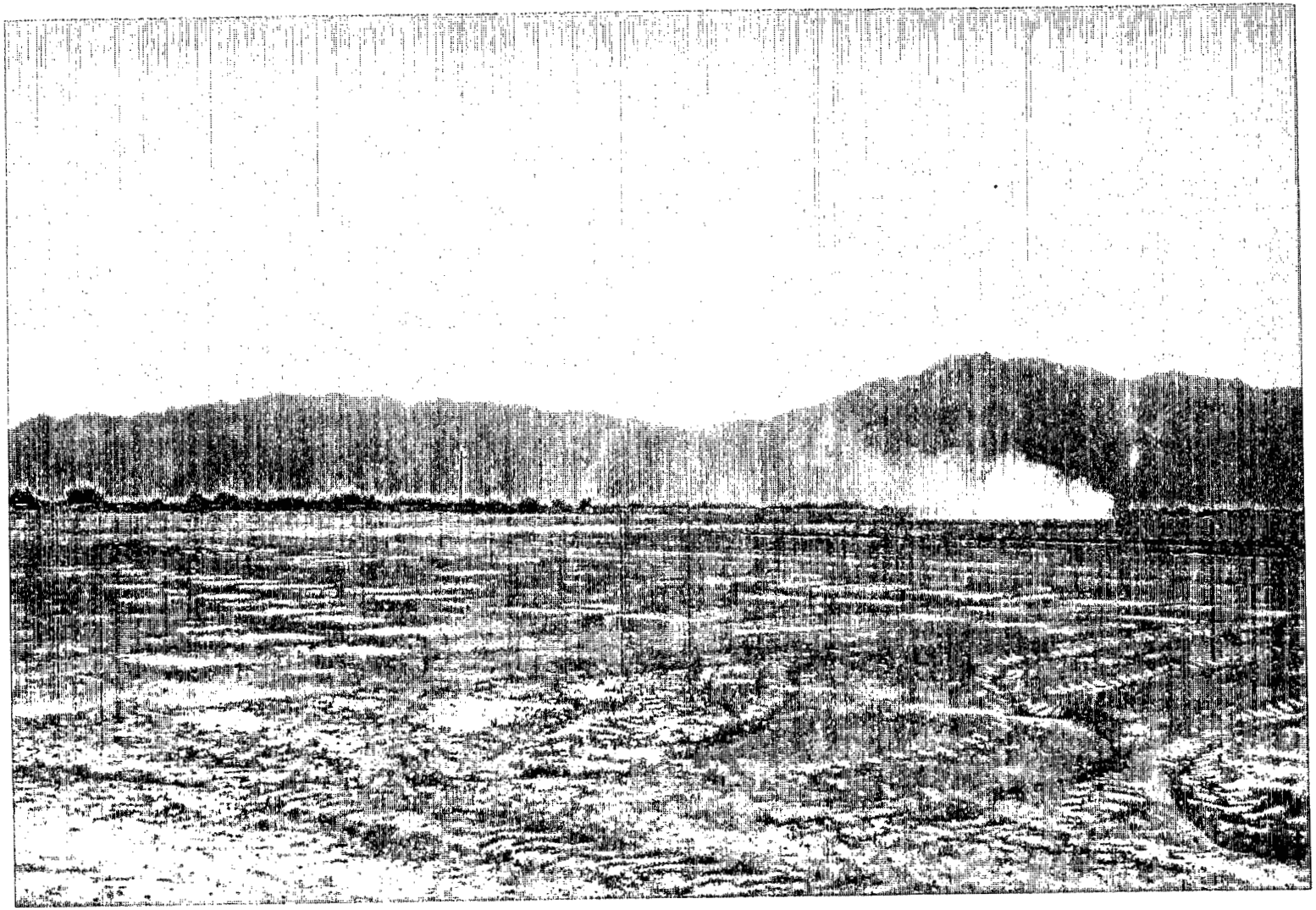

Figure 9. Dust cloud caused by Earth mover.

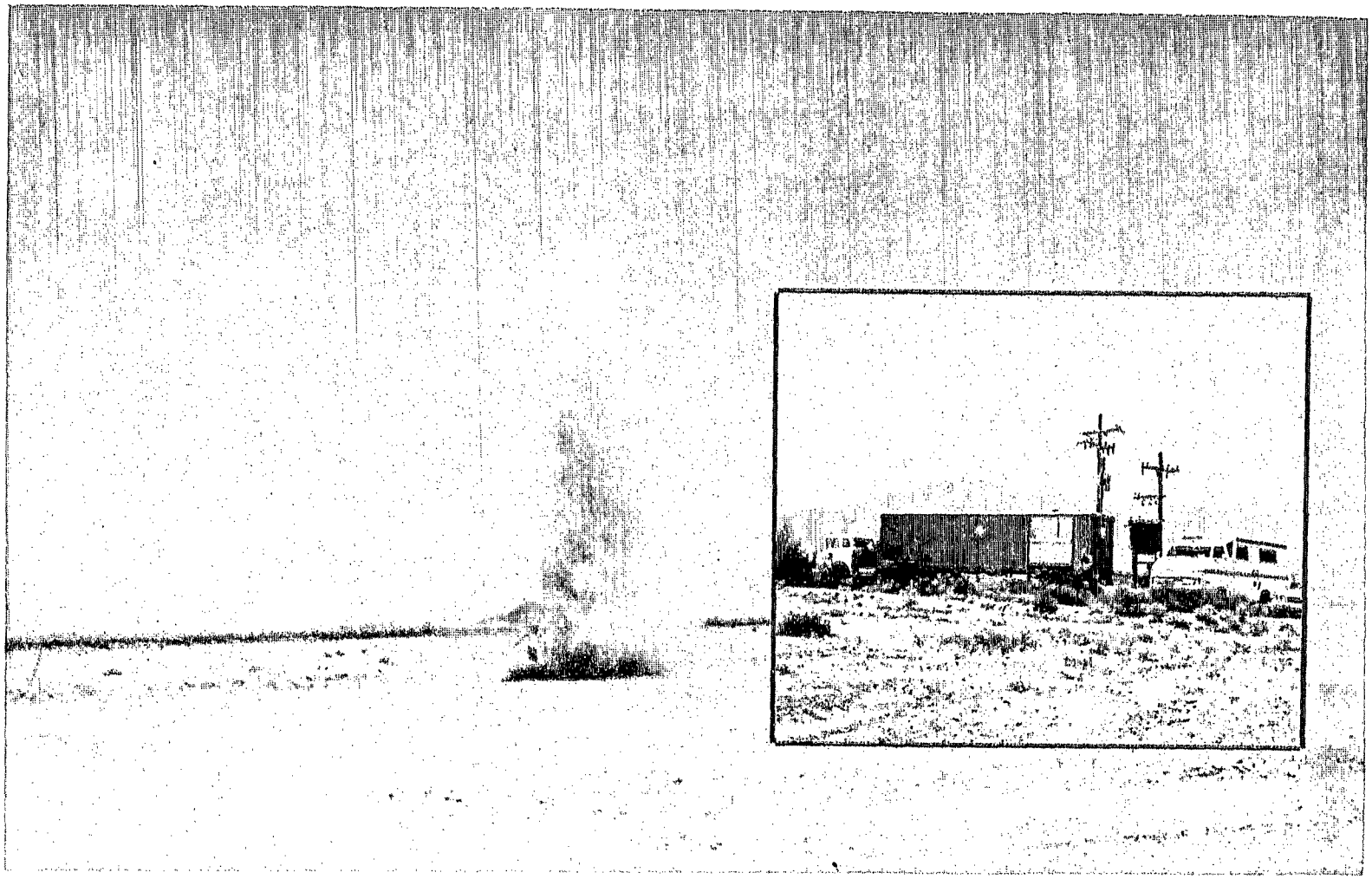

Figure 10. Dust devil.

3. The velocity information in the vicinity of the dust devils

4. The dust devil tracks

5. Photographic records of the dust devil

6. Translated data on dust devils

7. Data on the generation and decay of dust devils

8. The available meteorological information from the National Weather Service

9. Local meteorological information such as wind speed and direction, temperature, humidity, and barometric pressure.

10. On-site analysis of SLDV computer data

11. High speed data tape information for additional processing.

The majority of these data was successfully collected throughout the test program, the main exception being the information on local meteorological conditions. Equipment failures resulted in the loss of nearly all of these data.

The actual operation of the SLDV system was made extremely difficult by the extremely high temperatures inside the test van. Internal temperatures in excess of 73°C were reached regularly and caused excessive equipment failures. Because of this, all equipment was turned off until dust devils would begin to occur with some regularity, usually around 11 a.m. MST. At this point, the SLDV system was calibrated using the rotating sandpaper disk shown in Figure 8. This disk provided a Doppler target at a known range and of a known signal strength, allowing the determination of system performance and the calibration of the system range scan. Following this procedure, a scan plane was determined which would cover the area of dust devil generation, and the SLDV system set in operation. When a dust devil was detected, several scans were attempted through the dust devil at different altitudes. These data were recorded on high speed tape for post analysis. The on-site computer, signal processor, and spectrum analyzer were continuously monitored for dust devil activity.

V. DATA PROCESSING/ANALYSIS

A. Description of the Data

The high speed tape data contain all the relevant data collected by the SLDV system except the elevation angle. Specifically, for each integration time, the data contain a unique frame number identifying the data point, the coordinates of the scan, the time, and the amplitudes in each of the 104 frequency cells (approximately 100 kHz wide) after the spectrum analyzer. Additionally, each run contains a header with the run number, starting time, mode of operation of the spectrum analyzer, a number identifying the data as translated or untranslated, and the integration time in milliseconds.

The significant parameters of dust devil spectra may be determined by considering Figure 11. At a point on line of sight (1), the system is shown to be focused in front of the dust devil. The parallel velocity V is shown as a function of range. The system is focused to have maximum response at the point shown, and the spectrum may appear, as shown, with a small peak due to the ambient wind and a large peak due to the velocity of the dust devil. The highest velocity in the spectrum with an amplitude above the noise will be V_{pk} the highest velocity along the line of sight. On the opposite side of the dust devil, the flow is away from the system resulting in negative velocities, and the argument is reversed.

It has been determined from previous tests on vortices that the best parameter for location of vortex flow field cores is the maximum amplitude in the spectrum, excluding velocities where the ambient wind is significant. This fact has been verified in experimental and theoretical studies pertaining to the aircraft wake vortex data obtained with this system.

These facts suggest the following methods of processing as illustrated in Figure 12:

1. Amplitude threshold to remove the noise.

2. Define V_{HI} and V_{LO} as the highest and lowest velocities, respectively, in the threshold spectrum.

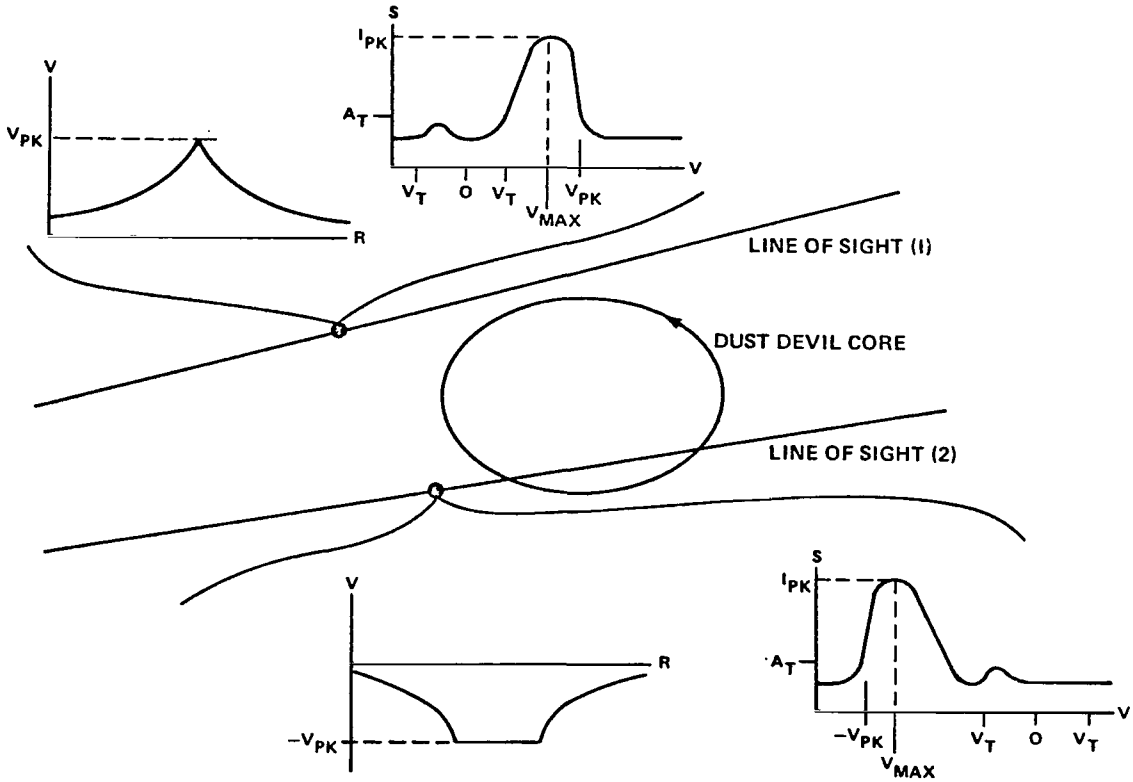

Figure 11. Significance of dust devil spectra.

3. Velocity threshold at positive and negative velocities independently to remove the wind signal.

4. Define the point I_{pk}, V_{max} as the highest amplitude in the spectrum with its associated velocity. Additionally, it is often useful to know:

a. The width of the spectrum, given by N, the number of frequency cells above threshold.

b. The sum of the amplitude in the whole spectrum, S.

c. The parameter V_{pk} defined as either V_{HI} or V_{LO}, whichever is further from zero velocity.

When the frequency translator is not used, the sense of the velocity can not be determined and the problem simplifies as shown in Figure 13.

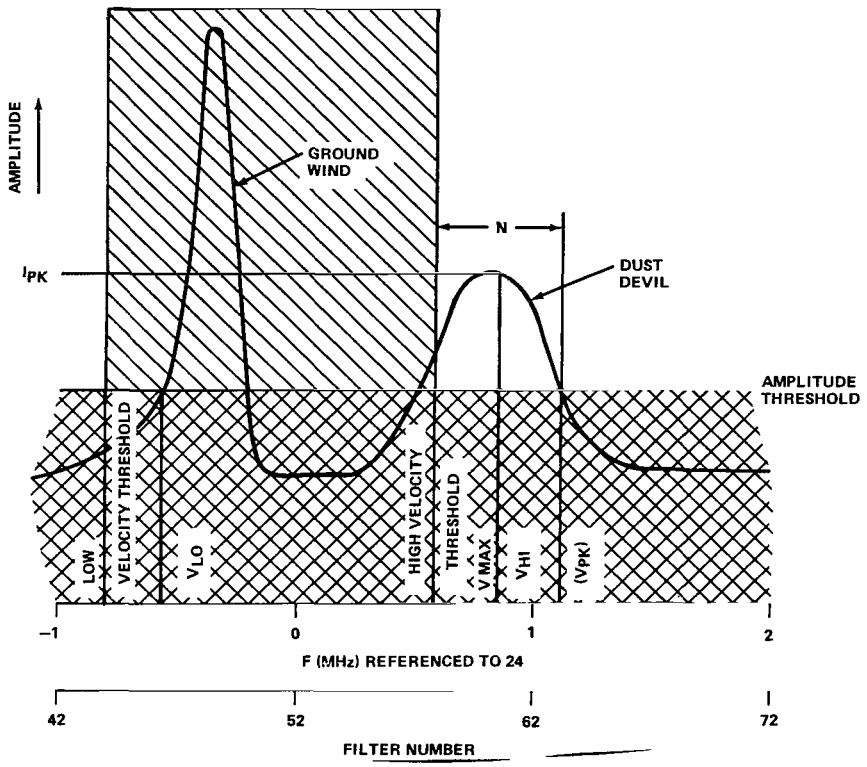

Figure 12. Dust devil signal spectrum (translated).

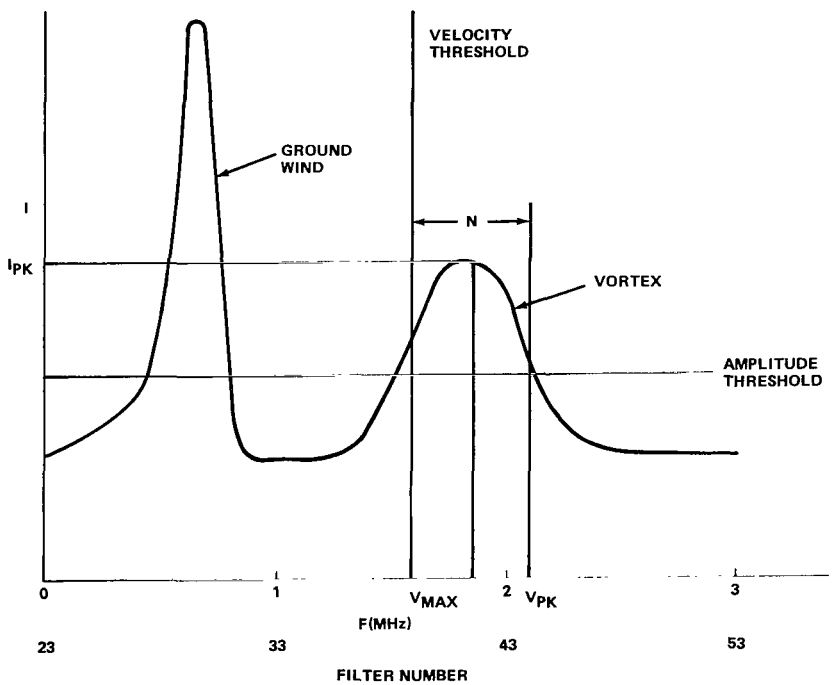

Figure 13. Dust devil signal spectrum (untranslated).

The parameters to be considered in the data presentation include:

I_{pk} used for center location

V_{HI}, V_{LO} used for velocity profiles (translated data)

V_{pk} used for velocity profiles (untranslated data)

S used for backscatter intensity profiles.

Sample signal spectra from Day 238, Run 2, of the dust devil measurement program are given in Figure 14. Figure 14a gives a typical spectrum for a single dust devil in the system's field of view. Figure 14b gives the spectrum for the system's output with observations of the atmospheric wind approximately 2 s later with the dust devil not in the system's field of view.

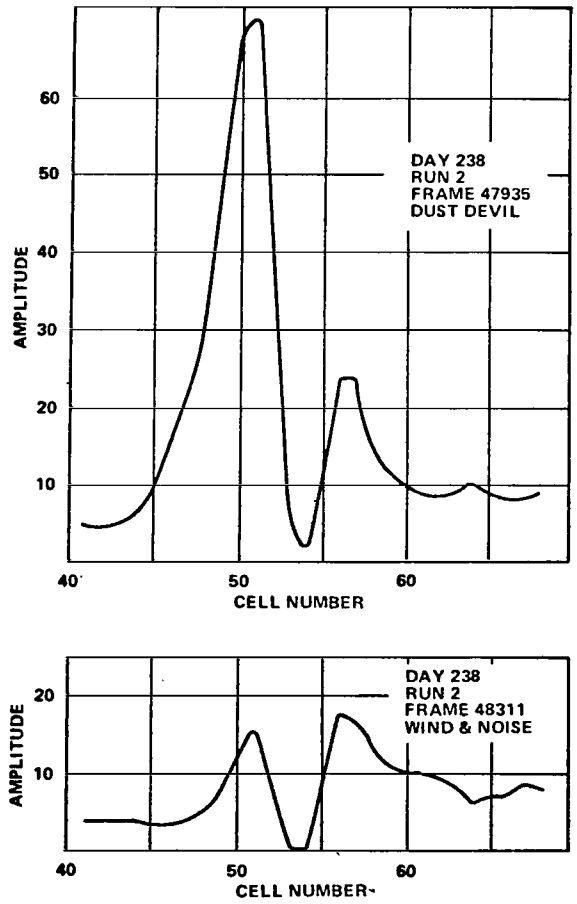

Figure 14. Typical spectra from a single dust devil and the atmospheric wind.

B. Data Processing Techniques

Most of the data processing is performed by a modification of a vortex location algorithm developed for analysis of aircraft vortices at John F. Kennedy International Airport. The algorithm is described in detail in Reference 20.

The vortex location algorithm accomplishes a number of different functions. First of all, it determines the starting and ending frames of each scan of the azimuth scanner. Next, it provides for thresholding and width (frequency) integration of the data. Points having high amplitudes are selected by a triplet algorithm and printed out for each scan. An iterated centroid calculation is performed on the data to obtain the locations of the vortices. At the end of a run, a summary output is presented which includes the x and y coordinates and time for the dust devil in each scan together with diagnostic data. Finally, output files are generated for further data analysis.

Location is accomplished by thresholding the spectra to remove wind and noise, locating the highest amplitude in the thresholded spectrum (I_{pk}), and selecting those data points for which I_{pk} is a relative maximum. Points may be deleted if their amplitude is sufficiently below the highest in the scan.

When this process is completed, the dust devil location is determined using an iterated centroid method. The location is determined by locating the highest I_{pk}, considering all of the points falling within a correlation circle of specified radius of this point, and calculating the centroid weighted with the amplitude above the threshold. A similar procedure is used to determine if a second dust devil is present using the highest I_{pk} outside of the correlation circle defined for the first one. Points occurring in both circles are considered to be associated with both dust devils for purposes of the centroids. If a majority of the points in either dust devil is in the overlap region, the point which initiated the location of the second is deleted and the iteration procedure is begun again. The x and y locations of each center are shown after each stage of the iteration.

The integrated signal plots show, for a complete scan, the integrated signal for each data point at the x and y coordinates of the point. To obtain the best possible dynamic range, each plot is normalized separately so that the highest signal in the scan is represented by the number 99. The normalization factor is shown at the top of each plot. Also shown is the total integrated signal for the scan. It should be recognized that the first and last scan on each reel of tape may be incomplete and, thus, include substantially fewer points than other scans in the same run.

The velocity plots show the cell numbers corresponding to V_{pk} and V_{max} for an entire scan as a function of angle, with the velocities plotted using the letters H and L, respectively. Cell 23 corresponds to zero velocity and each cell represents 0.54 m/s in velocity. Amplitude thresholds were chosen as low as possible with respect to the noise floor on that run.

The integrated signal and velocity plots are numbered with scan numbers which are sequential within each reel of tape. Additionally, each plot is labeled with the elevation angle and the elapsed time since the start of the run. The time is arbitrarily chosen at the starting time of the scan.

For many of the runs, the highest integrated signal and V_{pk} in each scan are plotted as functions of time. It should be recognized that in some cases the gain may have been changed during the run. Detailed examples of these plots are shown in Section VI.

In addition to the data processing techniques which were developed for vortex processing, an interactive display system was developed specifically for the examination of the dust devil data [21]. The first step in the interactive display system is to determine the variations in signal strength on a cell by cell basis for an entire dust devil run and to ascribe a certain percentage of the variations as being caused by atmospheric variations. Intensity fluctuations above this level should then be due solely to the variations in backscatter caused by the dust devil. A plot of the amount by which each velocity cell exceeded the 98 percent point is shown in Figure 15. It can be seen that cell no. 60 corresponding to approximately 4.7 m/s exhibited the strongest intensity fluctuation during the run. It is reasonable to assume that an x-y plot of this cell could give an indication of the location of the dust devil during the run. This plot is shown in Figure 16. Unfortunately, the hardcopy is not able to show the occurrence of these points with time as would be evident in watching the display. The next portion of the interactive display system allows the operator to obtain a plot of the detected velocity versus range and angle for each scan frame as is shown in Figure 17. It can be seen that the dust devil is located approximately in the center of the scan plane, with noise generated by the scanner system appearing at the minimum range points. A fourth plot (Fig. 18) that can be obtained is the plot of velocity versus range and intensity at a given angle of the scan. In this case, the range turnaround noise is again seen at the minimum range, with the dust devil at the extreme range. Because of the extreme flexibility in choosing the parameters to be displayed, the use of the interactive display system can provide an operator with a considerable amount of knowledge concerning the formation and transport of the dust devil phenomenon. Because of the immense quantity of data produced by this display system, it is primarily intended for use as a data evaluation and screening tool.

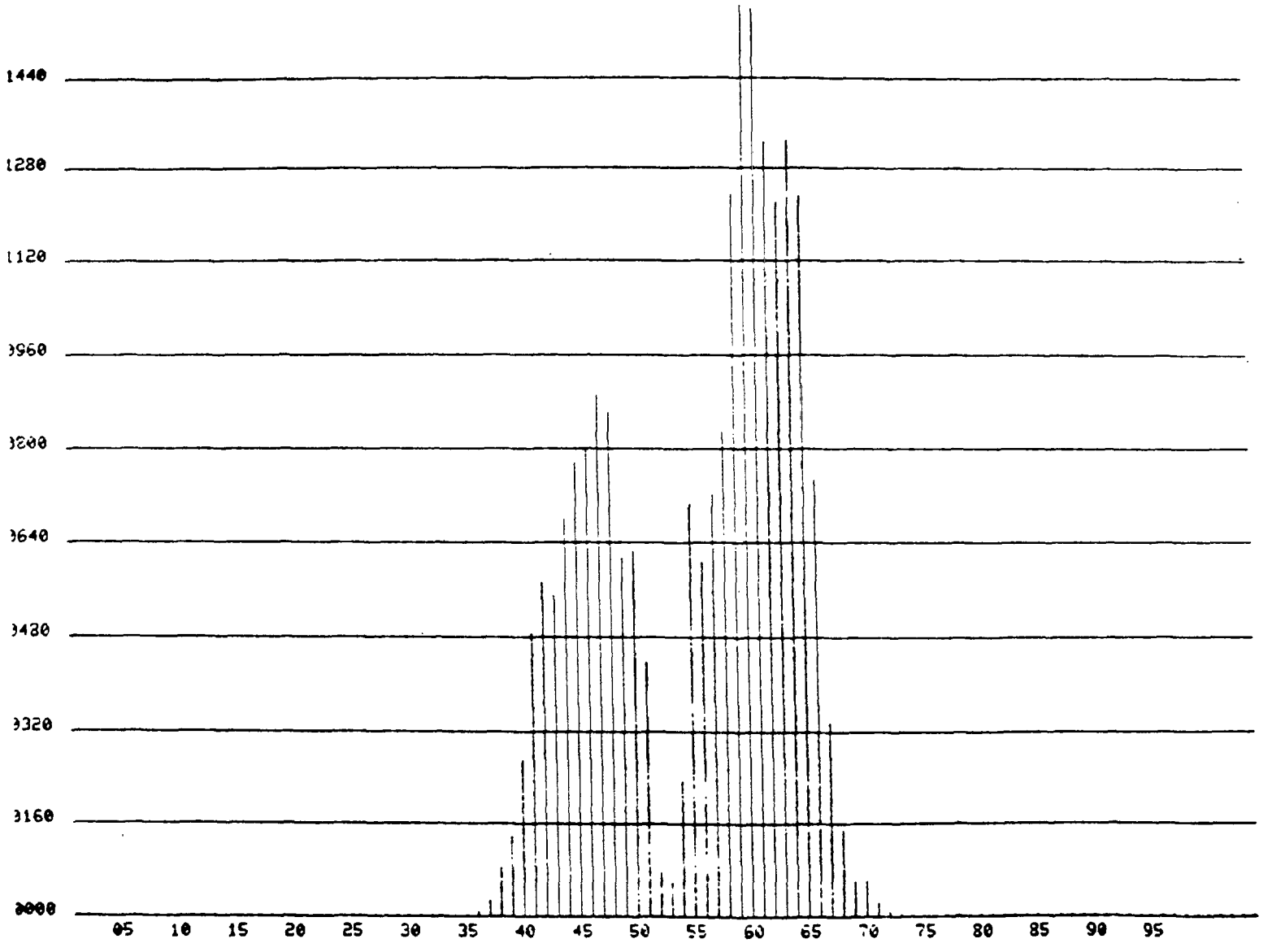

Figure 15. Variations in signal amplitude.

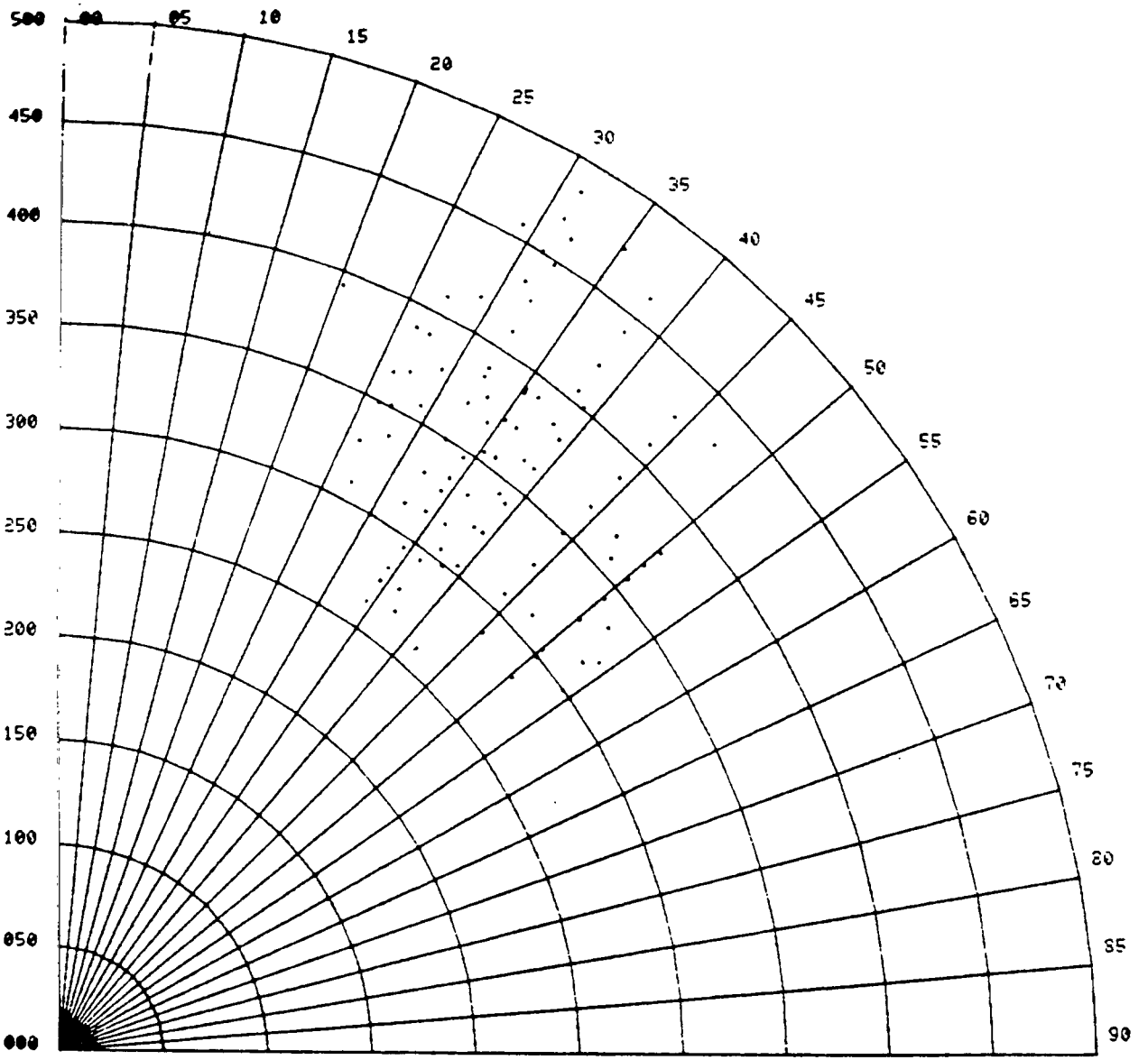

Figure 16. x-y plot of a given velocity cell.

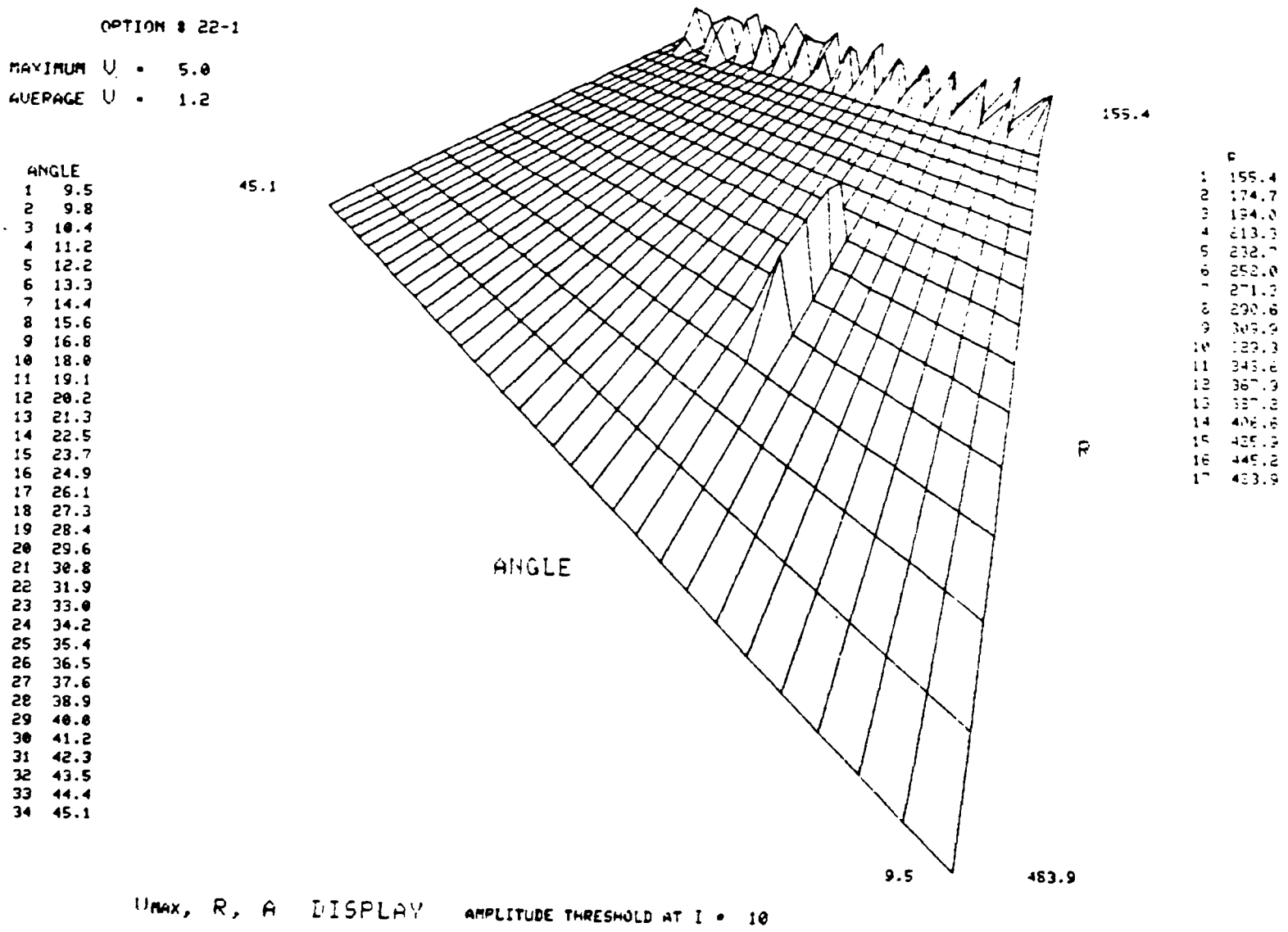

Figure 17. Velocity versus range and angle.

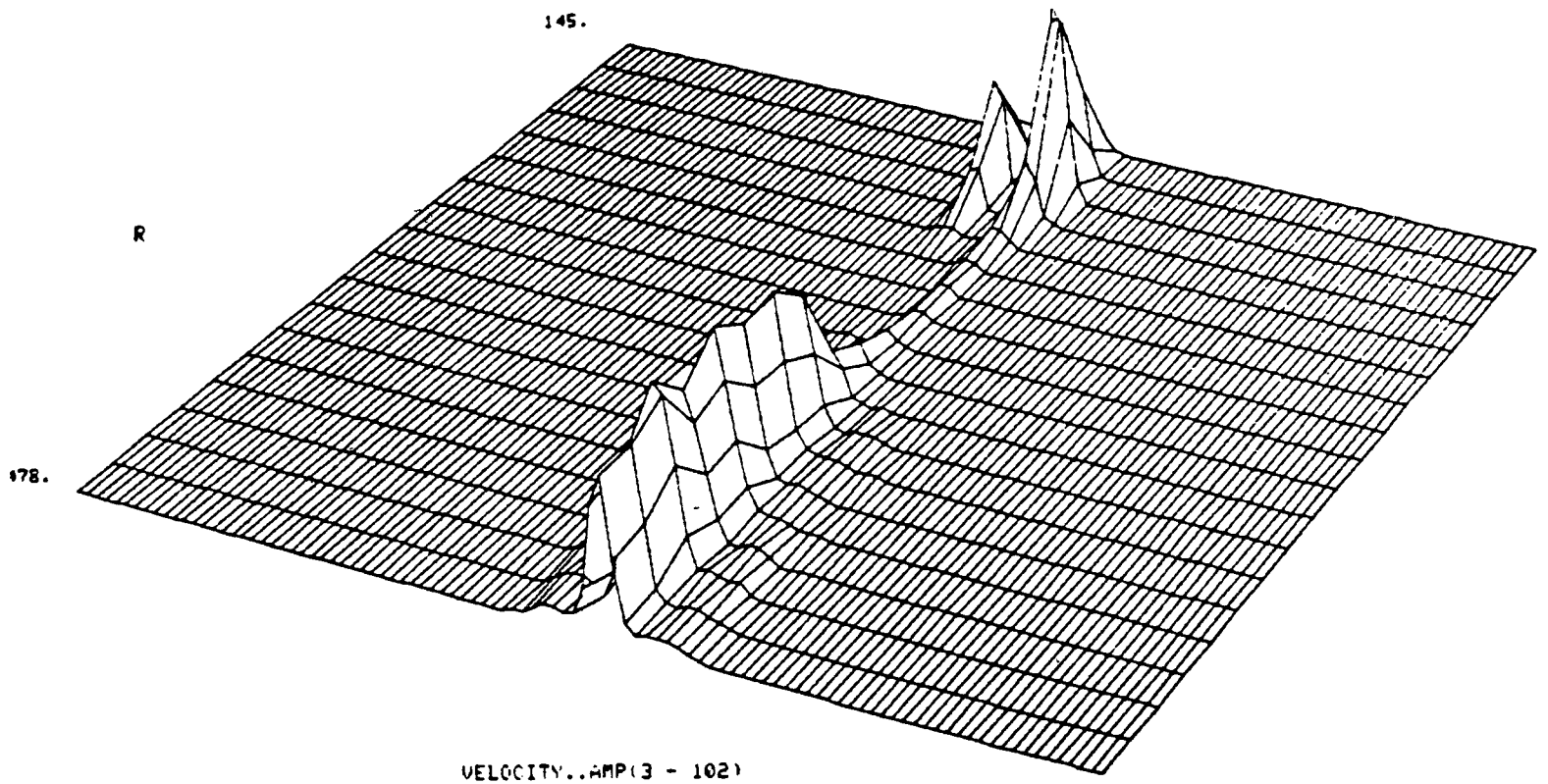

Figure 18. Intensity versus velocity and range.

VI. ENGINEERING DATA ANALYSIS AND PRESENTATION

The data processing algorithms from Section V were employed to operate on the high speed data collected from the dust devil test program. Using these algorithms, the data were prepared for presentation in formats that would easily be interpretable by persons totally unfamiliar with the operational peculiarity and detection characteristics of the Scanning Laser Doppler System. This operation, for the purposes of this report, is referred to as an engineering analysis of the data.

It is hoped that the data from the engineering analysis can be used by fluid dynamicists and meteorologists for developing a better understanding of the mechanisms by which these small scale tornado-like flows are generated, exist, and decay. Also, a study of the structure, strength, and flow patterns of the dust devil may lead to a better understanding of the larger scale tornado-like flow — the tornado.

A summary of the prevailing meteorological conditions is given in Section VI. A. The total data package from the engineering analysis is contained in References 21 and 22 and will not be presented in this report. Two examples of the analysis will be presented to demonstrate the SLDV system capabilities to remotely detect and collect valuable dust devil transport and velocity flow-field information under adverse environmental conditions (temperatures in excess of 38°C). The first example being a non-translated case in Section VI. B and the second, being translated, in Section VI. C.

A. Dust Devil Activity and Synoptic Features

1. Dust Devil Observations Period

Although the present dust devil field monitoring program covered a period of 11 days (i.e., August 10, 15-17, 19-20, and 22-26, 1975), only the meteorological conditions for the period of August 22-26 will be discussed. This 5 day period included the most significant dust devil data gathered. Particular attention has been given to this 5 day period from a meteorological viewpoint because the daily meteorological conditions were quite similar.

2. Meteorological versus Dust Devil Events (22-26 August 1975) — Air Temperature

Table 1 shows the hourly air temperature data as recorded on August 22-26, 1975, at the Sky Harbor International Airport at Phoenix. All data are shown for LST unless otherwise noted. Also, the maximum and minimum temperatures are provided as obtained from the Daily Weather Maps, Weekly Series, Environmental Data Service, NOAA, and US Department of Commerce.

No anomalies appear in these temperature data. Minimum temperatures are shown to occur at approximately 0500 to 0600 each day, whereas highest temperatures were from approximately noon until early evening. As is common, maximum dust devil activity occurred over the latter portion of the period of air temperature increase (i.e., between 1100 and 1500 LST). On-site maximum air temperatures were somewhat higher than those recorded at the Phoenix airport. The average maximum on-site temperature for the 5 day period was 40.6°C and occurred during the time of dust devil activity. One day a maximum of 46.7°C was recorded.

3. Wind Speed Data at Surface

Average near-surface wind speeds are shown on Figure 19 for the 5 day period as recorded at the Phoenix airport. These averages were obtained by using the five wind speed values for each hour of the day (i.e., five wind speeds were averaged for the 0100 LST observations, five for the 0200 LST observations, etc.). The time periods of maximum dust devil activity are indicated by the horizontally sequented lines on Figure 19 and are listed in Table 2.

It should be noted that dust devil events were observed during the period of low average winds. These low winds occurred prior to the late afternoon period when the average winds increased to approximately 5 m/s. From Section II.A it was noted that these small vortices do not occur so frequently or persist when surface winds exceed values of approximately 5 m/s. (See the discussion of winds aloft in the subsequent section on synoptic features for August 22-26, 1975.)

4. Wind Direction Data at Surface

The associated near-surface hourly wind data as observed at the Phoenix airport were used to obtain average wind direction changes as shown in Figure 20. The hourly wind directions for August 22-26 were plotted (data not shown herein), and the following statements can be made concerning wind directions in general:

TABLE 1. HOURLY AIR TEMPERATURE DATA RECORDED ON AUGUST 22-26, 1975, AT THE SKY HARBOR INTERNATIONAL AIRPORT AT PHOENIX

Date	22	23	24	25	26
Time (LST)	Temperature (°C)				
0100	47.2	47.2	48.3	48.9	47.8
0200	46.1	46.1	47.8	47.8	45.6
0300	46.1	45.6	45.6	47.2	43.9
0400	44.4	45.0	45.0	46.1	43.3
0500	43.3	45.0	44.4	46.1	42.2
0600	43.9	44.4	43.3	41.7	42.2
0700	44.4	45.6	45.0	43.3	43.3
0800	47.2	48.3	47.2	45.6	46.1
0900	50.0	51.1	50.0	48.9	48.9
1000	52.2	52.8	41.7	51.7	51.7
1100	53.9	54.4	53.3	53.3	53.9
1200	55.0	55.0	55.0	55.6	56.1
1300	55.6	56.1	56.7	56.7	57.2
1400	56.7	57.2	57.8	57.8	57.8
1500	56.7	58.3	58.3	57.8	58.3
1600	57.2	57.8	58.9	58.9	58.9
1700	57.8	58.3	58.3	58.3	58.3
1800	56.7	57.2	58.3	57.8	57.8
1900	56.1	56.7	56.7	56.7	55.0
2000	54.4	55.0	55.0	54.4	52.8
2100	53.9	53.3	53.3	52.8	52.2
2200	51.7	52.8	52.2	52.2	52.2
2300	51.7	52.2	52.2	50.6	51.7
2400	48.9	50.6	49.4	48.9	51.7
Daily Maximum	58.3	58.3	60.0	58.9	58.9
Daily Minimum	43.3	43.9	42.2	41.1	41.7

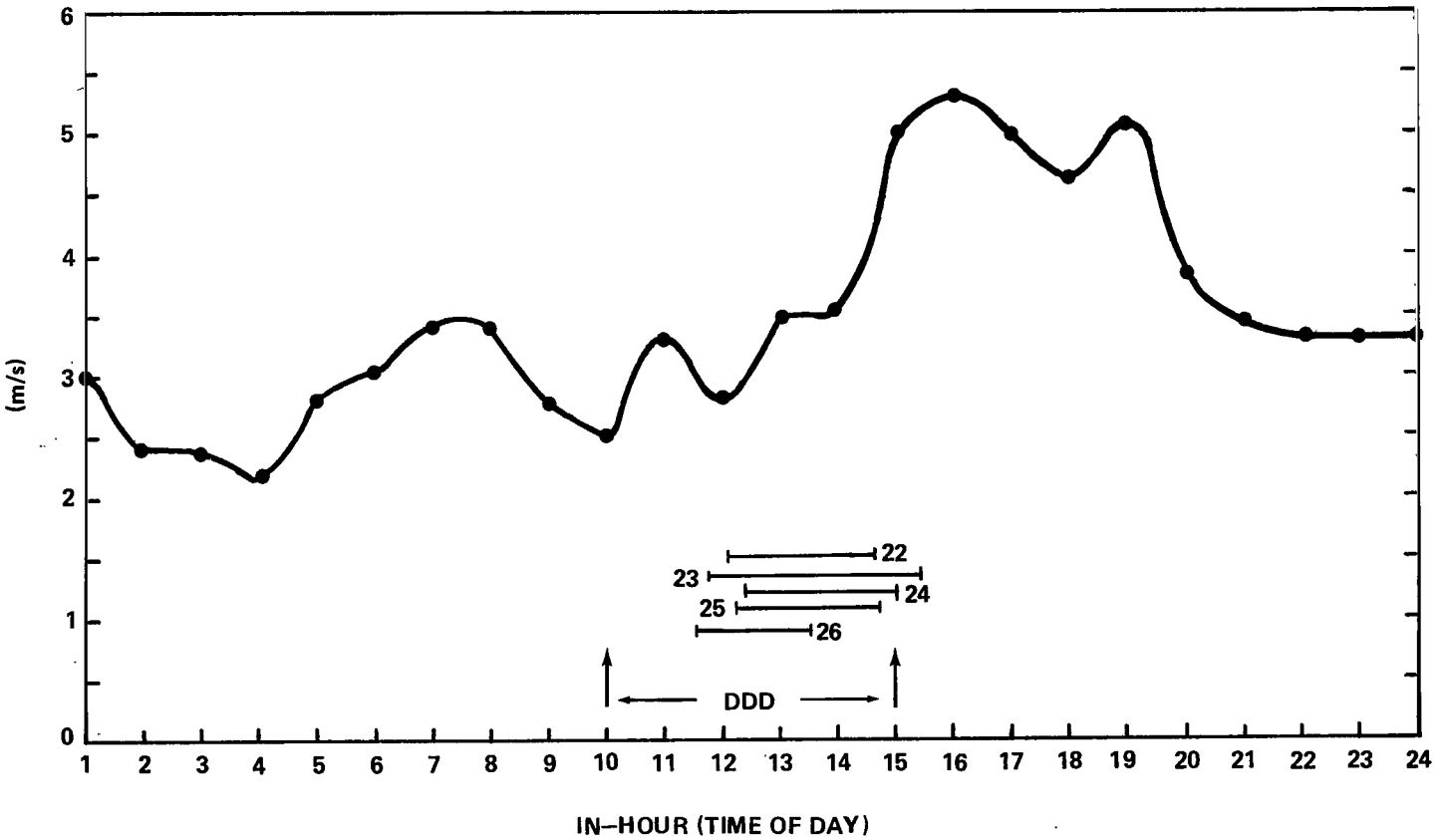

Figure 19. Averaged wind speed data for 5 day period.

TABLE 2. PERIODS OF MAXIMUM DUST DEVIL ACTIVITY

Date	Observed Dust Devil Activity (LST)	Approximate Number of Dust Devil Events	Soil Temperature (°C)
August 22	12:09 - 14:36	19	*
August 23	11:45 - 15:23	31	*
August 24	12:28 - 14:56	24	*
August 25	12:15 - 14:44	15	63.9**
August 26	11:32 - 13:33	11	66.7**

* Missing data

** Exact time of record unknown

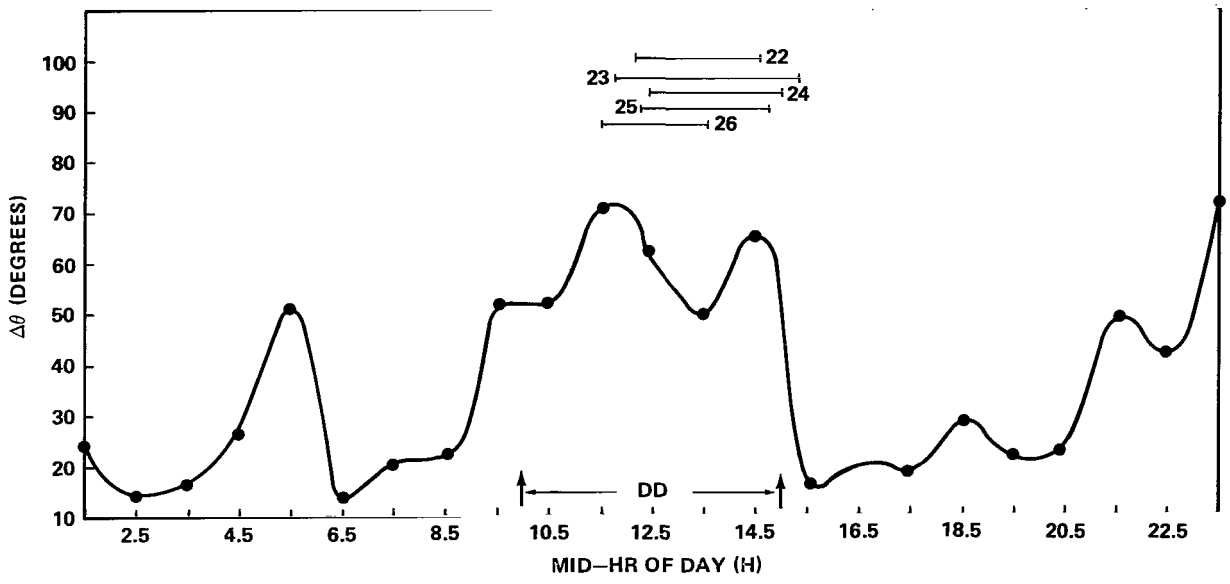

Figure 20. Average differences of wind speed data for 5-day period.

a. Winds were from the northeast-east-southeasterly direction from about midnight until early afternoon each day.

b. Wind directions took on a more northwest-westerly direction with greater persistence and higher wind speeds from about 1500 to about midnight each day.

c. The average wind direction change data shown in Figure 20 were obtained by calculating the wind direction changes between each consecutive hour for the 5 day period and then averaging the five differences between 0100 and 0200, between 0200 and 0300, etc.

It is interesting to note, as shown by observed dust devil activity lines 22, 23, 24, 25, and 26 (horizontal bars) in Figure 20, that the maximum dust devil activity occurred during the period of the day when the wind direction variability was the greatest from hour to hour. This indicates the following:

a. With greater wind direction variability, wind speeds are lower in magnitude.

b. Dust devils develop and persist during periods of low wind speeds and corresponding maximum wind direction variability.

Recall, too, that the ground and lower atmospheric boundary level air temperatures are highest during the period of maximum wind direction variability and relatively low wind speed.

5. Synoptic Features for Southern Arizona, August 22-26, 1975.

a. General Surface Conditions. The synoptic features that dominated southern Arizona during the August 22-26, 1975, dust devil field experiment were typical of those expected for that location and time of year. The thermal low (heat low) extended over southern California and southern Nevada down through southern Arizona, New Mexico, and south, engulfing northern Mexico. The atmospheric pressure gradient was very weak over this broad region. At Phoenix the average pressure converted to sea level was approximately 1.01×10^5 N/m^2 (1010 mb) with not more than a ± 200 N/m^2 (± 2 mb) change over the 5 day period. This thermal condition for Southwest United States, Phoenix included, causes convectional currents to be very pronounced.

Localized terrain, vegetation, and excessive surface heating were the major influences on localized air circulation. The lack of influx of moisture, from large-scale advective air mass motion, caused the Phoenix area to be

extremely dry and hot. The development of dust devils during this field experiment period supports the assumption that convective instability is the governing atmospheric feature for dust devil activity. The only frontal activity during the 5 day period occurred when a weak cyclonic wave moved into the Washington-Oregon region on August 22. The center of this low pressure system moved eastward, and by August 26 the low was over central Quebec in Eastern Canada. From this location, a weak cold front extended southwest through southern Michigan, central Illinois, and southwestward to the Texas Panhandle. This cyclonic system had little or no influence on the southern Arizona lower atmospheric conditions during the 5 day period of concern.

b. Upper Atmosphere. The upper atmospheric conditions showed a high pressure system extending over the Southern States of the U.S. and into Northern Mexico. On August 22, a trough with a closed low centered at the 5×10^4 N/m^2 (500 mb) level over British Columbia in Western Canada extended south over the western Pacific states. This trough, as associated with the weak frontal system at the surface, progressed eastward and by August 26 its center was over the Hudson Bay region of Canada. Circulation from this trough introduced little change to general wind velocities over the southern Arizona area during this 5 day period. Table 3 shows upper altitude winds observed at Tucson during the 5 day dust devil experiment.

TABLE 3. WIND ALOFT DATA FOR AUGUST 22-26, 1975, TUCSON INTERNATIONAL AIRPORT, ARIZONA

	22		23		24		25		26	
Altitude (km)	Direction (deg)	Speed (m/s)	Direction (deg)	Speed (m/s)	Direction (deg)	Speed (m/s)	Direction (deg)	Speed (m/s)	Direction (deg)	Speed (m/s)
1.5	130	3.08	090	5.1	310	5.1	319	7.2	335	5.1
3.0	230	3.08	085	3.6	345	6.2	295	6.2	226	2.1
4.5	208	15.4	205	11.3	346	3.6	260	1.5	060	1
6.0	224	14.4	195	3.6	240	1	282	7.3	240	10.3
7.5	222	16.5	218	9.3	240	9 3	270	9.8	240	7.7
9.0	221	22.6	247	18	236	7.7	247	12.9	252	10.8
12.0	223	25.7	239	30.3	274	11.8	268	22.6	260	19
15.0	238	16.5	245	18.5	267	9.3	285	13.9	282	15.9

c. Cloud Conditions. The following cloud conditions were observed at Phoenix, Arizona, August 22-26, 1975.

On August 22, cumulus and altocumulus clouds were reported generally northeast to southeast of Phoenix by 0600 LST. Towering cumulus were also seen in the easterly direction during this reporting period. Phoenix reported

scattered cloudiness with cloud heights at 2.8 km over the area by late afternoon; however, no major cumulus or cumulonimbus systems developed in the immediate area on August 22.

Cloudiness reported for Phoenix on August 23 was quite similar to that which had developed on August 22. In the early afternoon, dust devils were reported in the area east of Phoenix during the period when surface winds were listed as light and variable.

On August 24, the sky coverage for Phoenix was listed as clear. A few cumulus and altocumulus clouds were reported in the northeast-to-easterly direction but certainly not as many as had developed on the preceding 2 days. A few cumulus were reported south of Phoenix in the very late afternoon.

On August 25, a few cumulus clouds were reported to have developed in a direction east to southwest of Phoenix. No dust devils were reported.

On August 26, altocumulus castellanus clouds with virga were reported in the early morning northeast of the Phoenix area. By noon and through the late afternoon and evening period, heavy cumulus and cumulonimbus formations developed northeast to south of the Phoenix area. Some clouds were reported most of the day for the area. No major dust devil activity was recorded.

d. Precipitation. No precipitation was recorded at the Phoenix airport during the period of August 22 through 26. Traces to approximately 0.25 cm of rain were measured at weather stations in northern Arizona and northern and central New Mexico on August 22-24, but these areas were virtually without rainfall on August 25 and 26.

e. General Comments. It is not unusual to have the previously described synoptic conditions occur for the Phoenix area during the latter part of August. The cloudiness which existed generally northeast to south of the station was associated with the normal influx of moisture in the upper levels, from the Gulf of Mexico, causing buildup of cumulus and thunderstorm-type cloud activity in the afternoon and evening of each day. This condition, especially common over mountains where orographic lifting takes place, causes available moisture to condense and develop into well-established cumulus and cumulonimbus formations. This is the common cloud and weather situation for the Southwestern portion of the U.S. (i.e., Arizona, New Mexico, southern Colorado, Texas, etc.) during July, August, and September.

B. Analysis of Run 5, Day 235

Data from Run 5 were recorded from 12:08:51 p.m. to 12:10:53 p.m. on August 23, 1975. During this 2 min run, the scan plane was described by a 0.2 Hz azimuth scan from 6° to 48° and a 2.1 Hz range scan from 96 m to 300 m. Elevation slices were taken at 5°, 10°, and 20°. Only the first 50 s of this run provided useful velocity and transport data which were apparently due to the fact that the dust devil moved out of the scan region. The following plots (Fig. 21) of velocity versus azimuth are taken from the first 20 scan frames at an elevation of 5°. As can be seen from Figure 21, scan 1, the dust devil was initially detected at approximately 12°. Although it is not readily apparent, both sides of the dust devil are evident in this scan; due to the finger density, the peak velocity portion of the dust devil located near 16° was missed. This is illustrated in Figure 21, scan 2. Further verification is obtained by noting the location and movement of the dust devil in the successive scans. In scans 3, 4, 5, and 6, it is apparent that a second dust devil was picked up at approximately 38°; however, it was not of sufficient strength and duration to allow meaningful analysis. In scans 9 through 13 another dust devil appears to be evident at 45°; again, however, analysis is difficult. The existence of these two small dust devils was corroborated in the visual sightings. The possible existence of a complex dust devil, involving two or more rotating structures, seems to be indicated by the multiple peaks occurring in several of the scans, namely scans 3, 5, 7, 8, 12, 13, and 16. In particular, scan 16 shows three very distinct peaks over an 8° to 10° angle. While no mention is made of a complex structure in the data logs, it is known that such phenomena do exist. The analysis of such a complex structure is impossible because the system lacks the capability to sense velocity direction. However, the incorporation of a frequency translator into the system, as was done for Run 9, Day 238, greatly enhances the ability to resolve such a structure into the contributions due to the individual dust devils. The data shown in the next section demonstrate the ease of pinpointing individual dust devil centers through the use of a translator.

The angular transport for the main dust devil occurring in this run is shown in Figure 22. The angular position was determined approximately by the mean angular distances between the two predominant velocity peaks. The average transport of this particular dust devil was approximately 0.5°/s. The angular core width shown in Figure 23 fluctuated from 4° to 8°. This is described by the angular width between the two velocity peaks. It does not necessarily imply a true width because the dust devil was also moving in range; however, the approximate range given in Figure 24 indicates that the dust devil width remained at roughly 15 m for the duration of the run. The peak

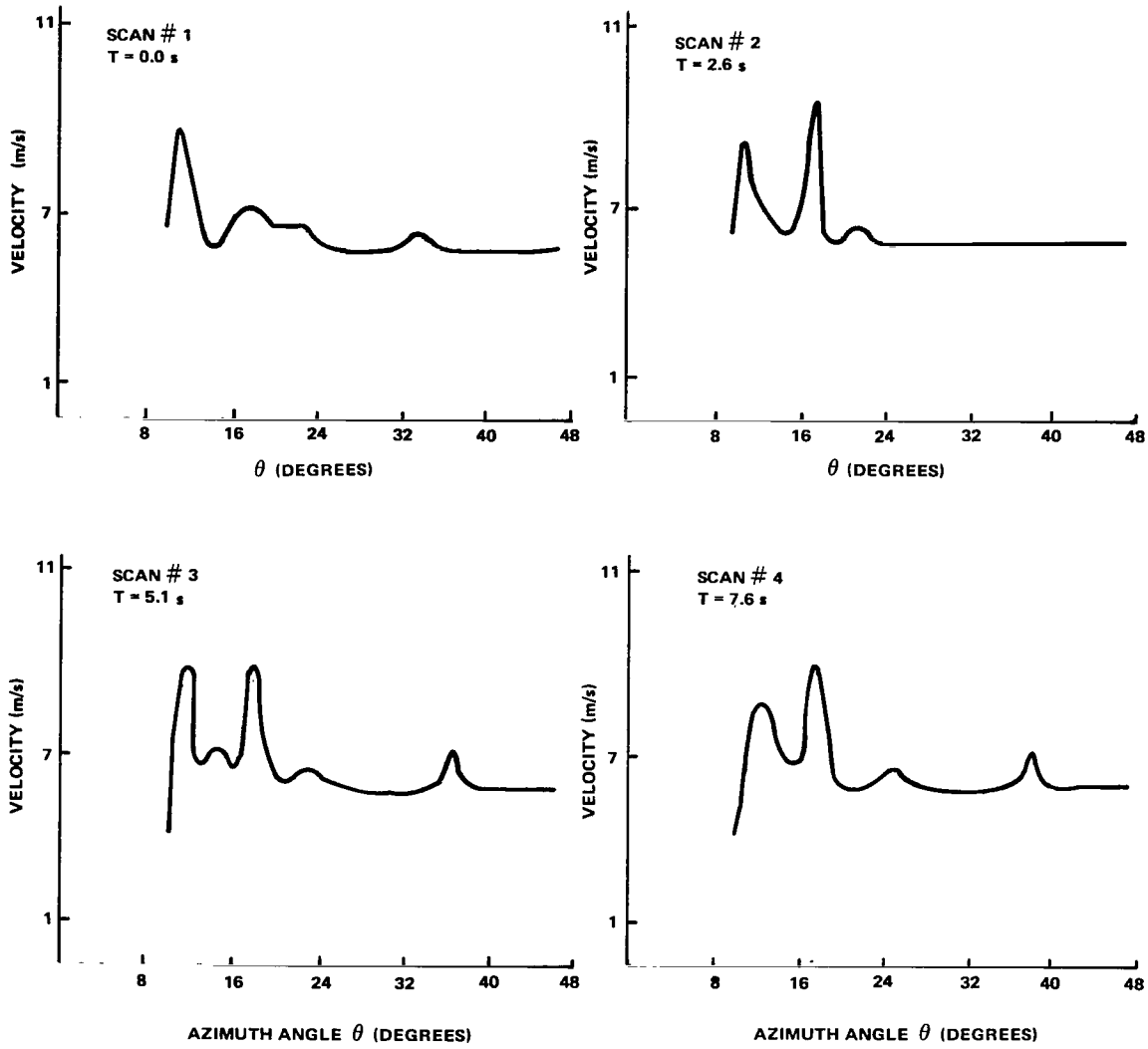

DAY 235 RUN 5 ELEVATION = 5°

Figure 21. Velocity versus azimuth.

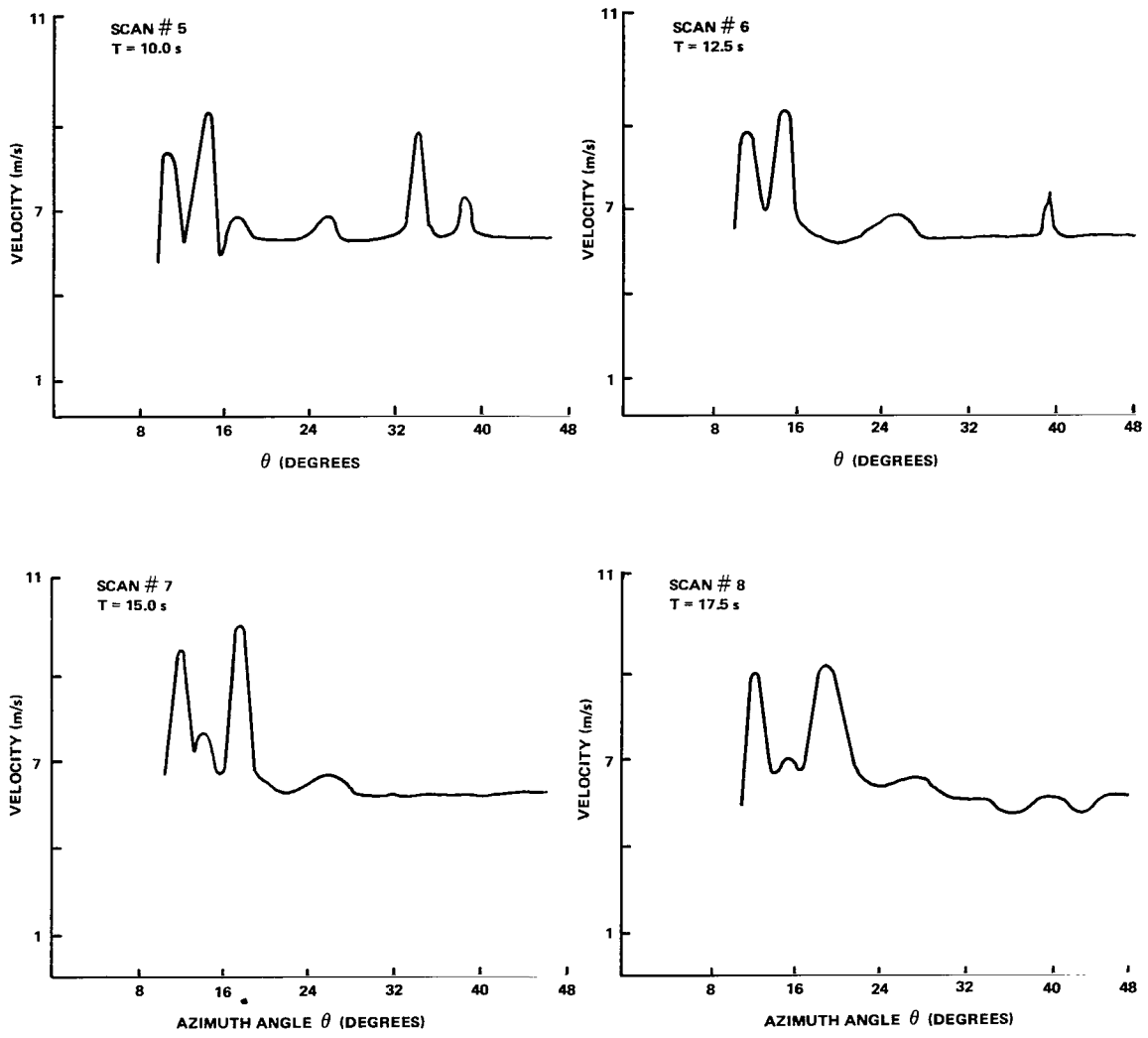

DAY 235 RUN 5 ELEVATION = 5°

Figure 21. (Continued)

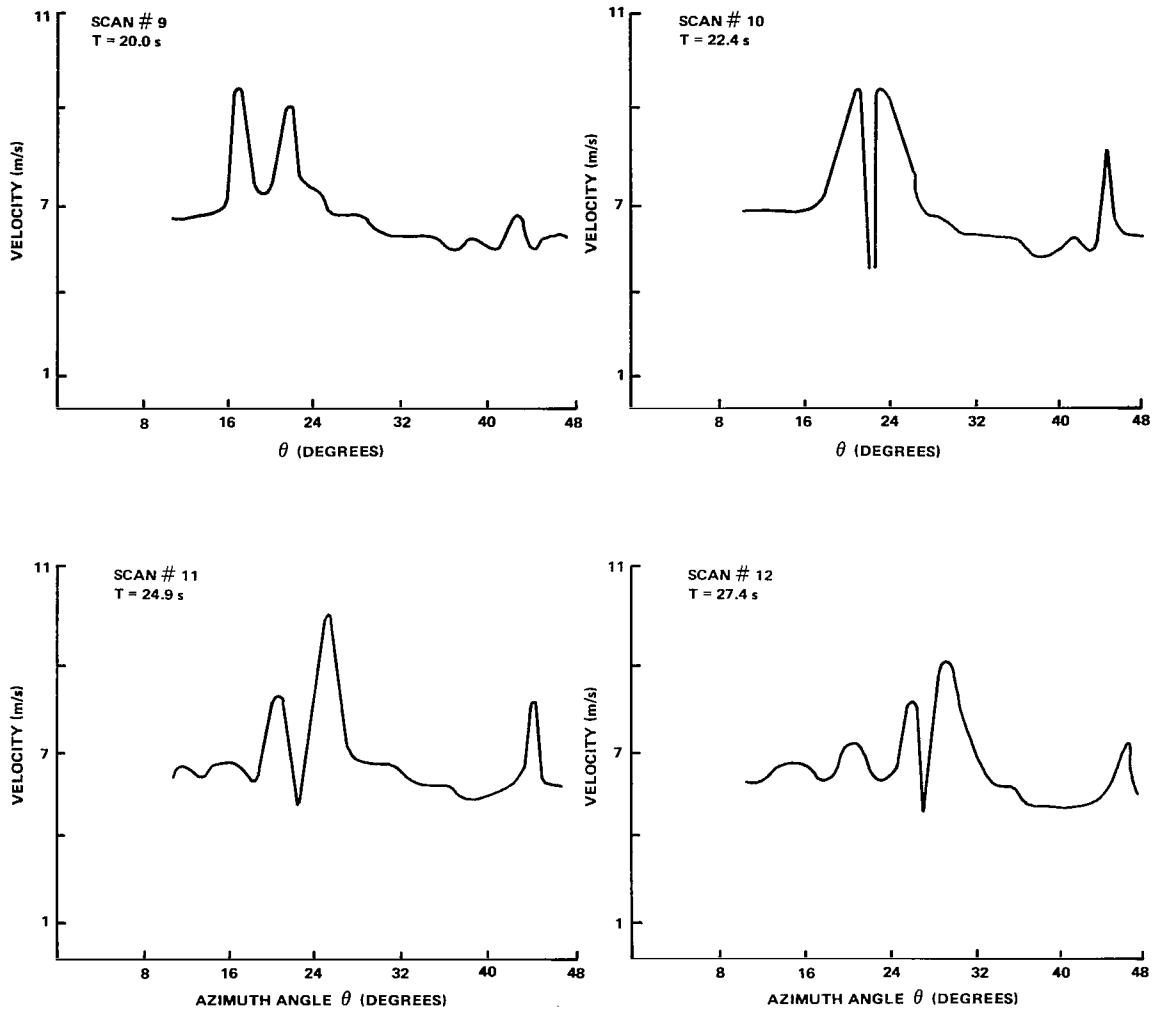

DAY 235 RUN 5 ELEVATION = 5°

Figure 21. (Continued)

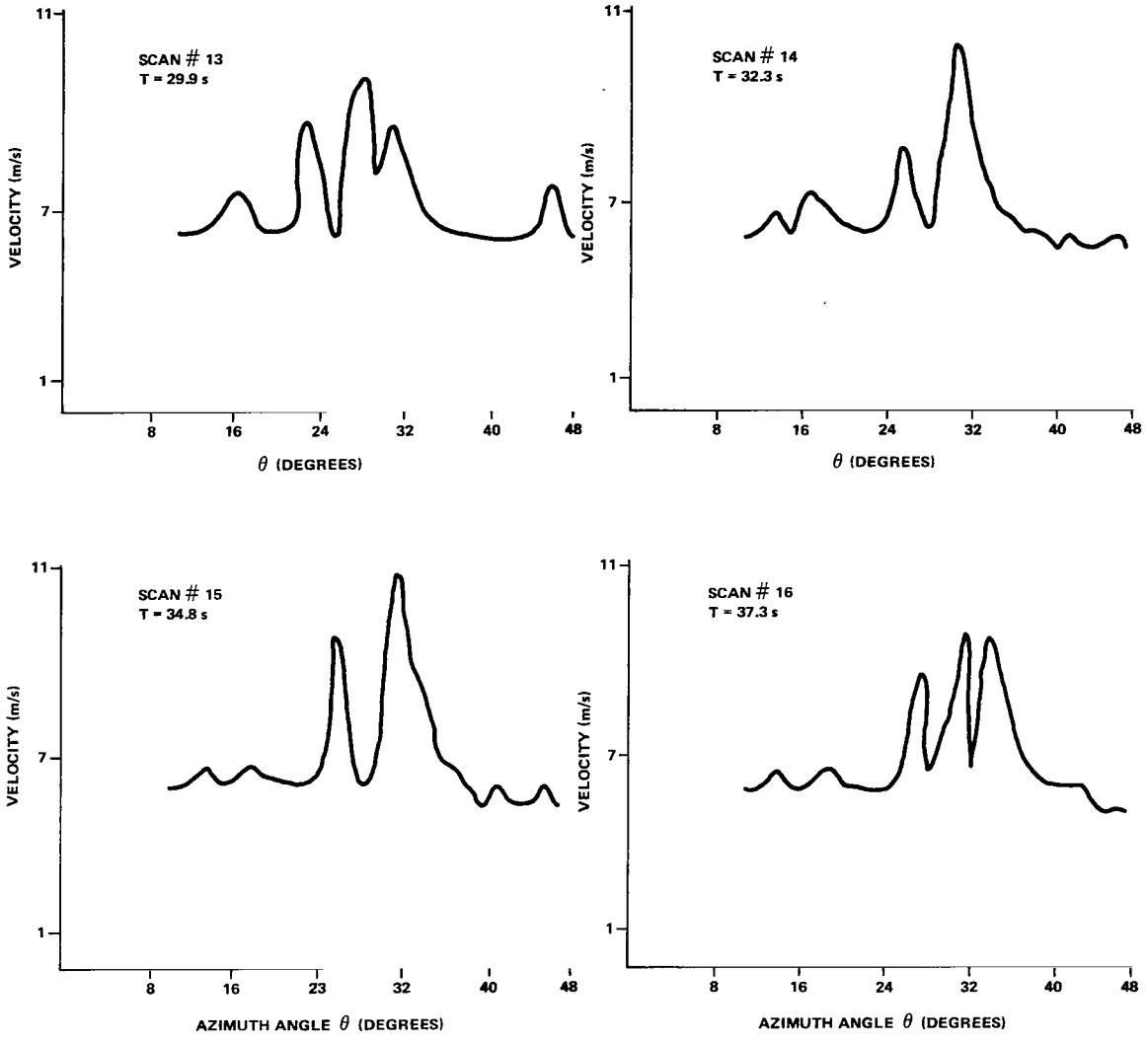

Figure 21. (Continued)

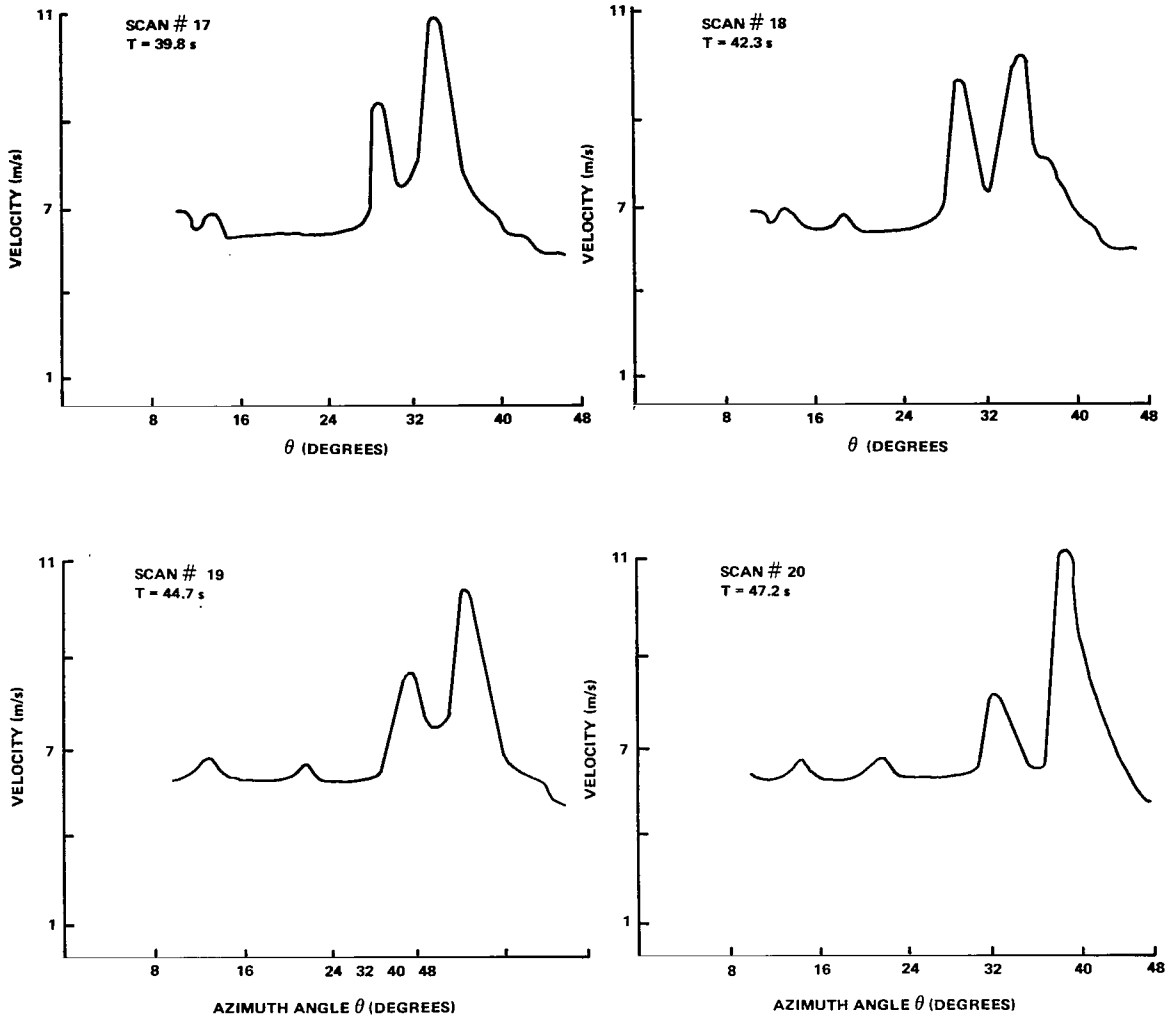

DAY 235 RUN 5 ELEVATION = 5°

Figure 21. (Concluded)

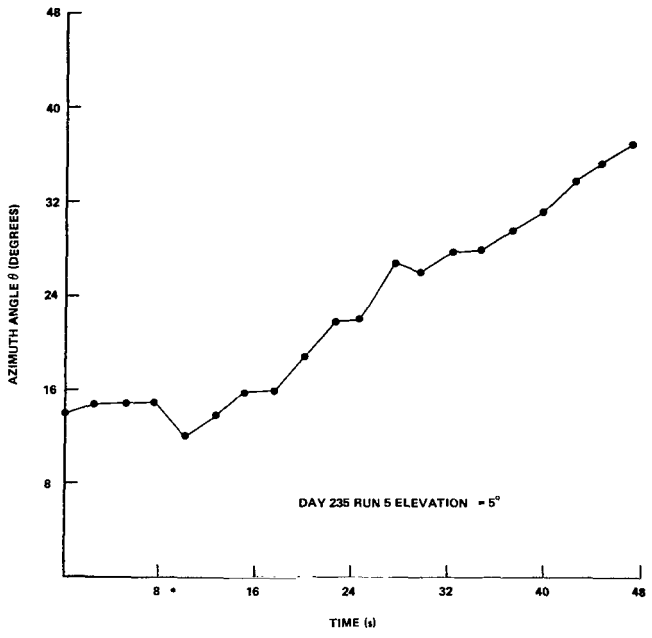

Figure 22. Dust devil angular transport.

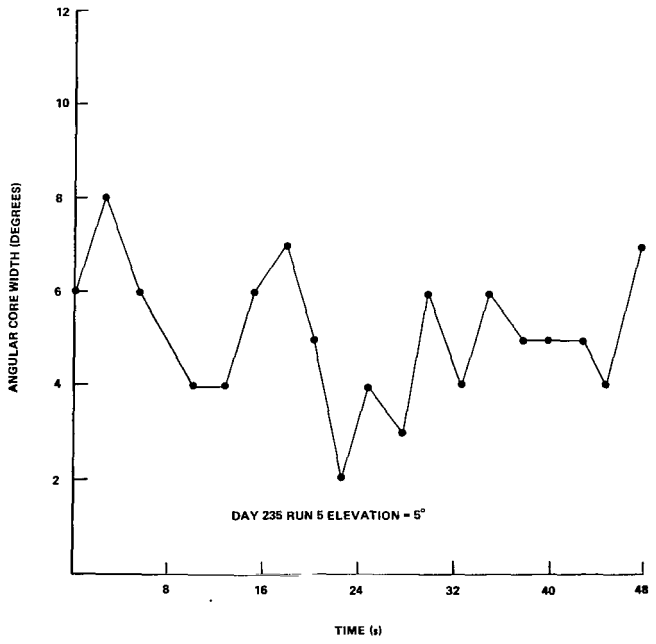

Figure 23. Angular core width time history.

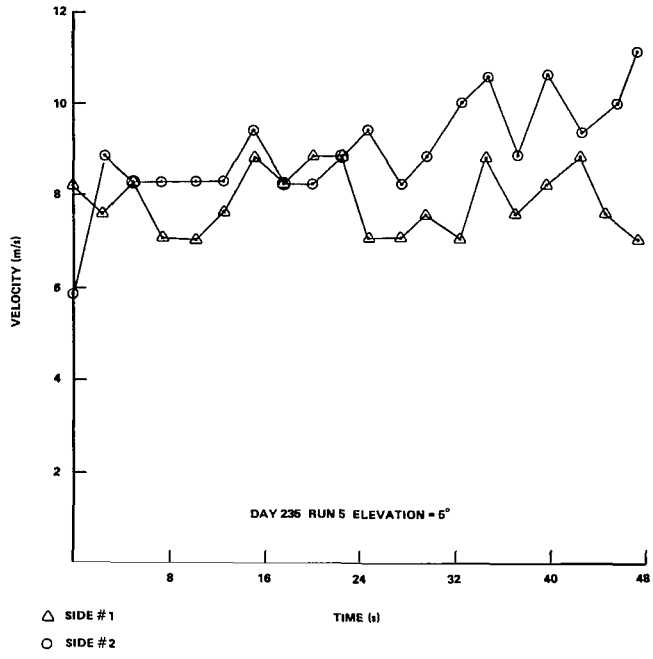

Figure 24. Peak velocity time history.

velocity time history shown in Figure 24 indicates the variations in the velocities of the two sides of the dust devil with time. The difference between these two velocities will be equal to approximately twice the wind velocity present, one side being positively biased by the wind, the other negatively. The average difference would appear to be on the order of 1 to 3 m/s corresponding to a wind velocity of from 0.5 to 1.5 m/s. This is within the range of the observed winds at the test site.

Backscatter intensity profile plots are shown in Figure 25 on a scan-by-scan basis, the plots being normalized to the highest backscattered return in a given scan with 99 being the highest value and zero being the lowest. These plots will provide an indication of the regions of highest signal return, that of the dust devil. Because of scale problems, the entire scan plane is indicated in the plots of the first two scans; however, it is still possible to note the area of highest return occurring near the bottom of the scan. Only the contributions due to the dust devil are shown by scan 3. It may be noticed that because of the inherent range resolution of the system together with the tremendous signal received from the dust devil, the determination of an exact target range is extremely difficult. The contributions of the smaller dust devils mentioned previously can be seen in various scans; however, it is again not possible to provide a meaningful analysis. A more detailed discussion of the intensity plots will be found in the section dealing with Day 238, Run 9.

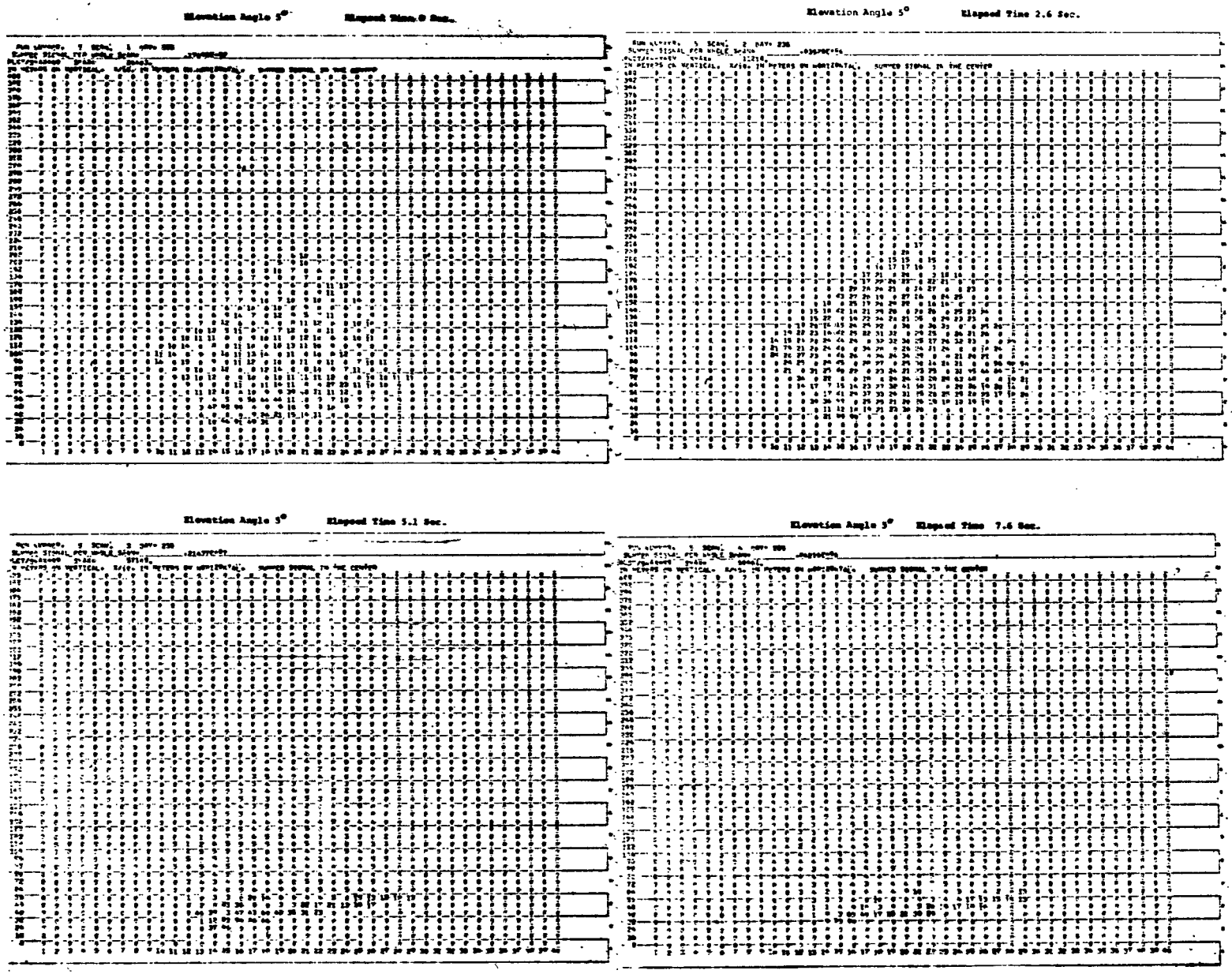

Figure 25. Dust devil backscatter intensity profile.

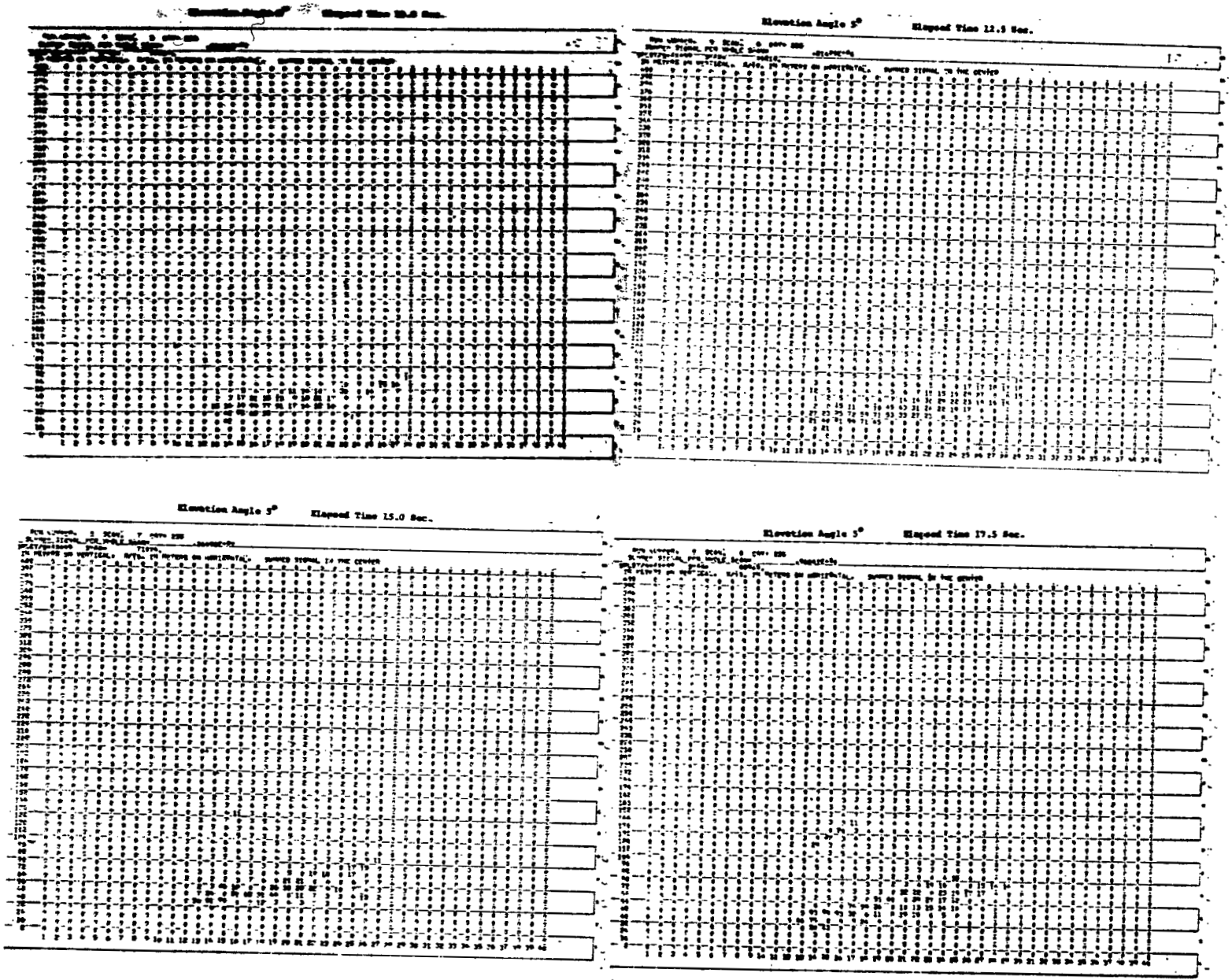

Figure 25. (Continued)

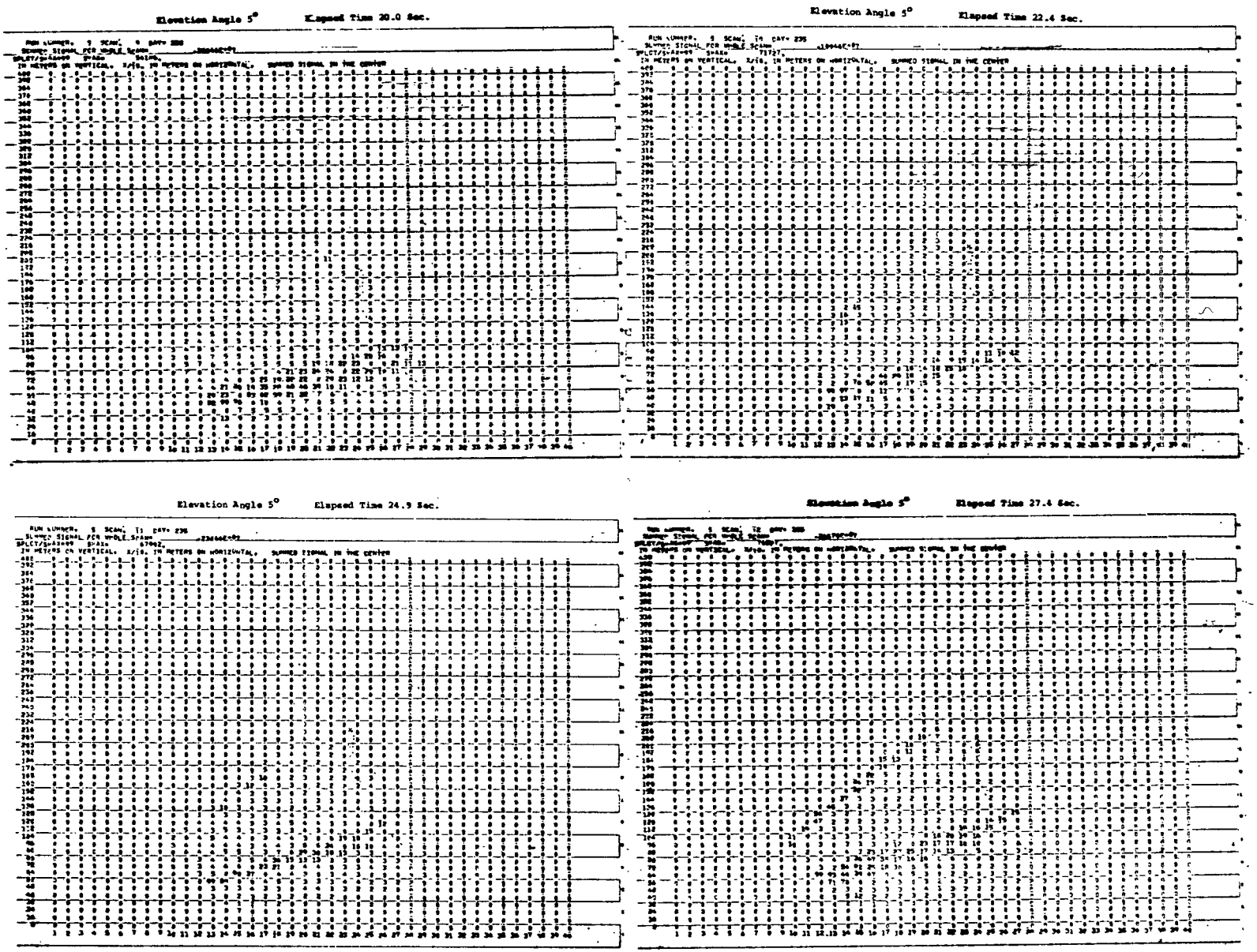

Figure 25. (Continued)

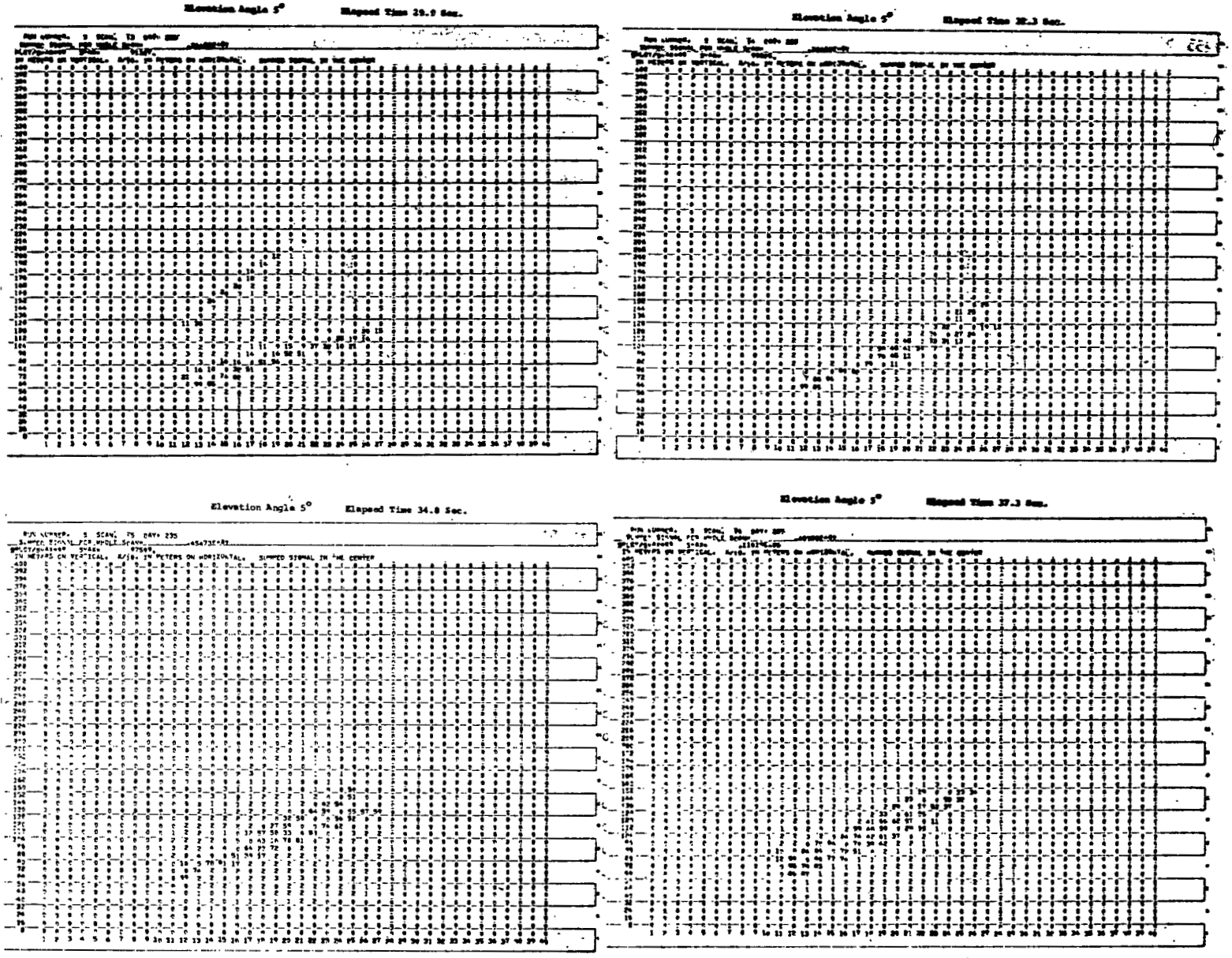

Figure 25. (Continued)

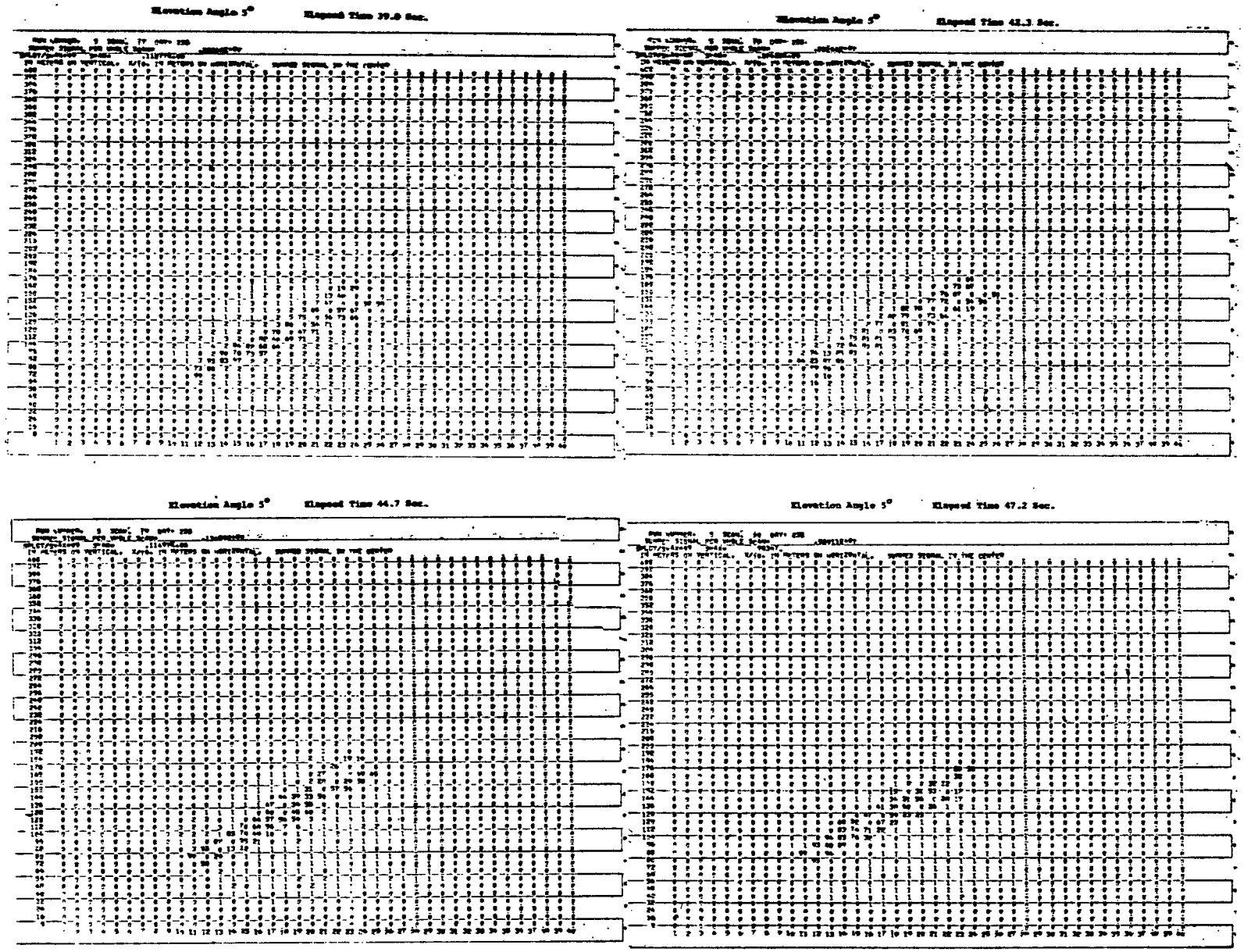

Figure 25. (Concluded)

The peak integrated signal plot shown in Figure 26 indicates the increase in signal return with time. While the fluctuations are possibly due to artificial entrainment of sand, the general increase in signal level together with the increase in peak velocity shown in Figure 24 shows a dust devil increasing in strength.

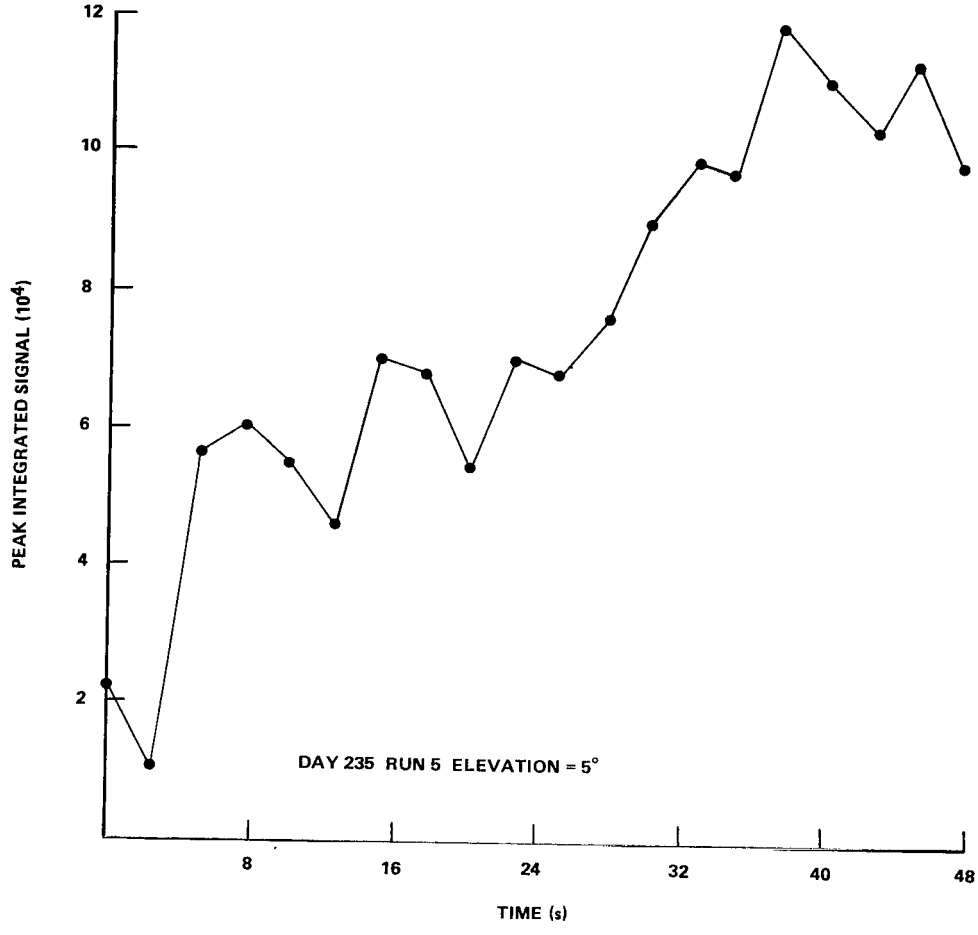

Figure 26. Dust devil peak integrated signal time history.

The peak signal transport shown in Figure 27 is drawn from the peak signals occurring in the individual backscatter plots. As mentioned previously, the range indication of the system is not of good quality, and this plot is not intended to serve as an absolute location, but rather as a trend in the dust devil movement. As can be seen from the plot, the dust devil traveled approximately 100 m in a northwesternly direction during the 47.2 s run. This corresponds to a rate of travel of approximately 2.1 m/s.

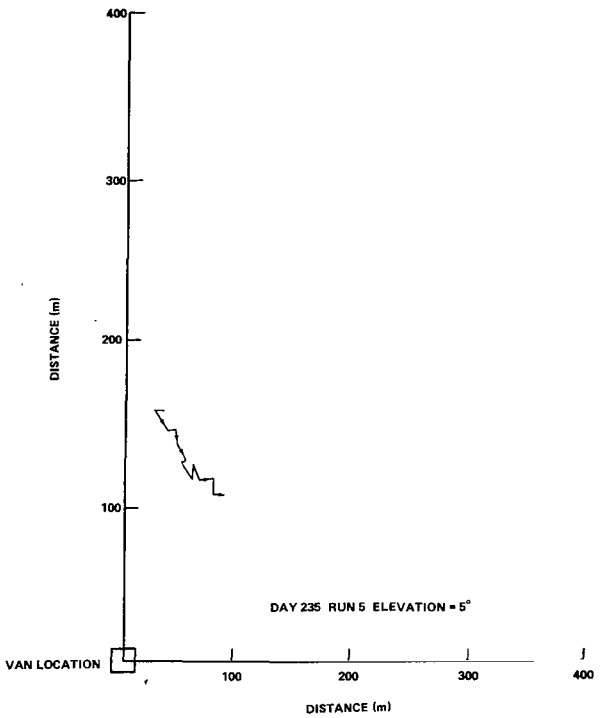

Figure 27. Dust devil peak signal transport.

C. Analysis of Run 9, Day 238

Data from Run 9 were recorded from 13:20:45 to 13:22:04 on August 26, 1975. During this 1 min, 14 s run, the scan plane was described by a 0.1 Hz azimuth scan from 6° to 66° and a 3.1 Hz range scan from 96 m to 450 m. Two elevation slices were taken, one at 5° and one at 10°. Only the 5° elevation scan produced useful data comprising 58 s and 13 scans.

As was previously mentioned, analysis of the data collected on Day 238 emphasizes the desirability and, in many cases, the necessity of having a translation capability in the SLDV. The ability to resolve the velocity sense increases the capability to determine very precisely the angular location of a vortex. This is extremely important in complex flow fields as was the case in the Day 235, Run 5. The plots, shown in Figure 28 indicate the relationship between detected

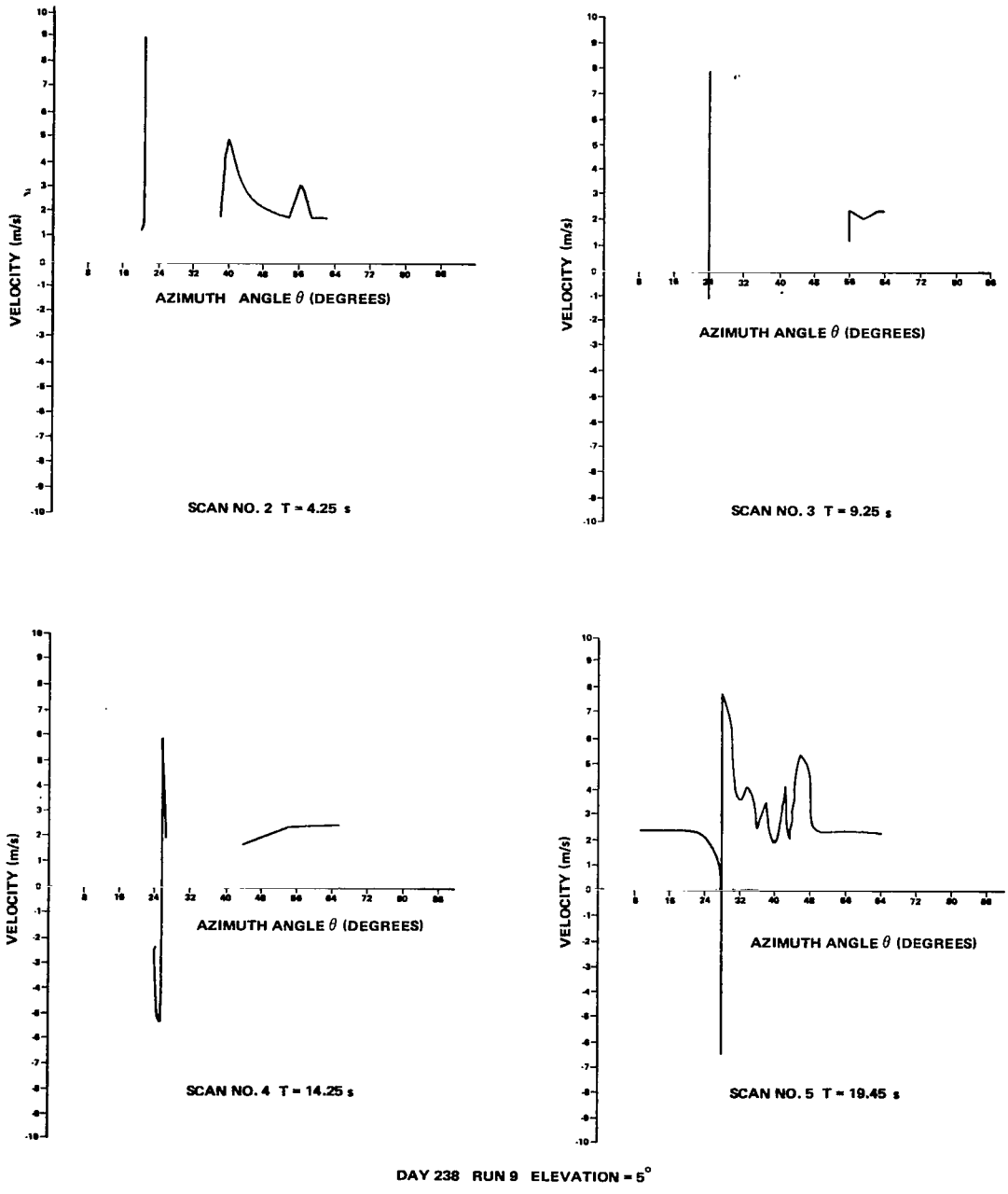

Figure 28. Velocity versus azimuth.

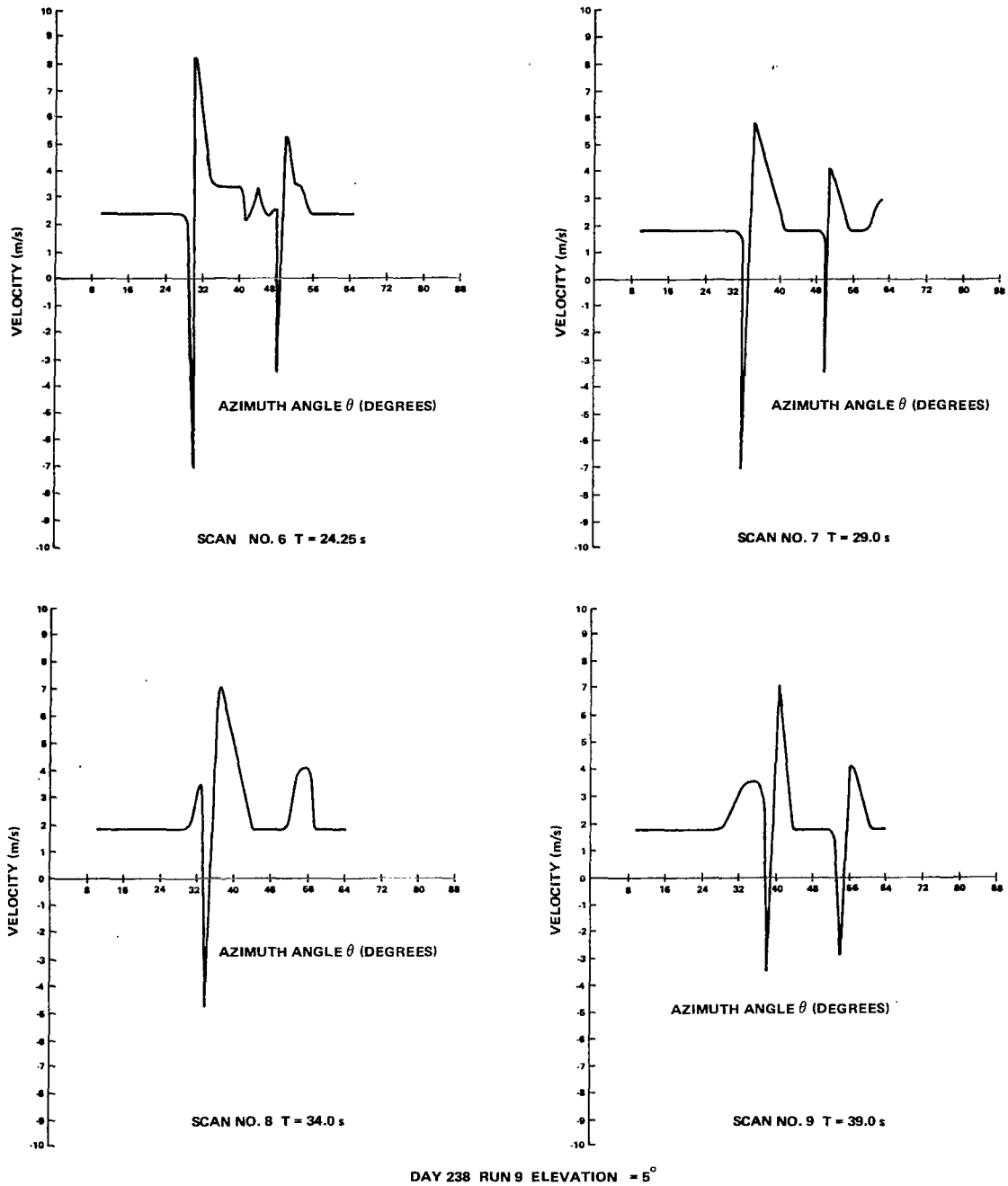

Figure 28. (Continued)

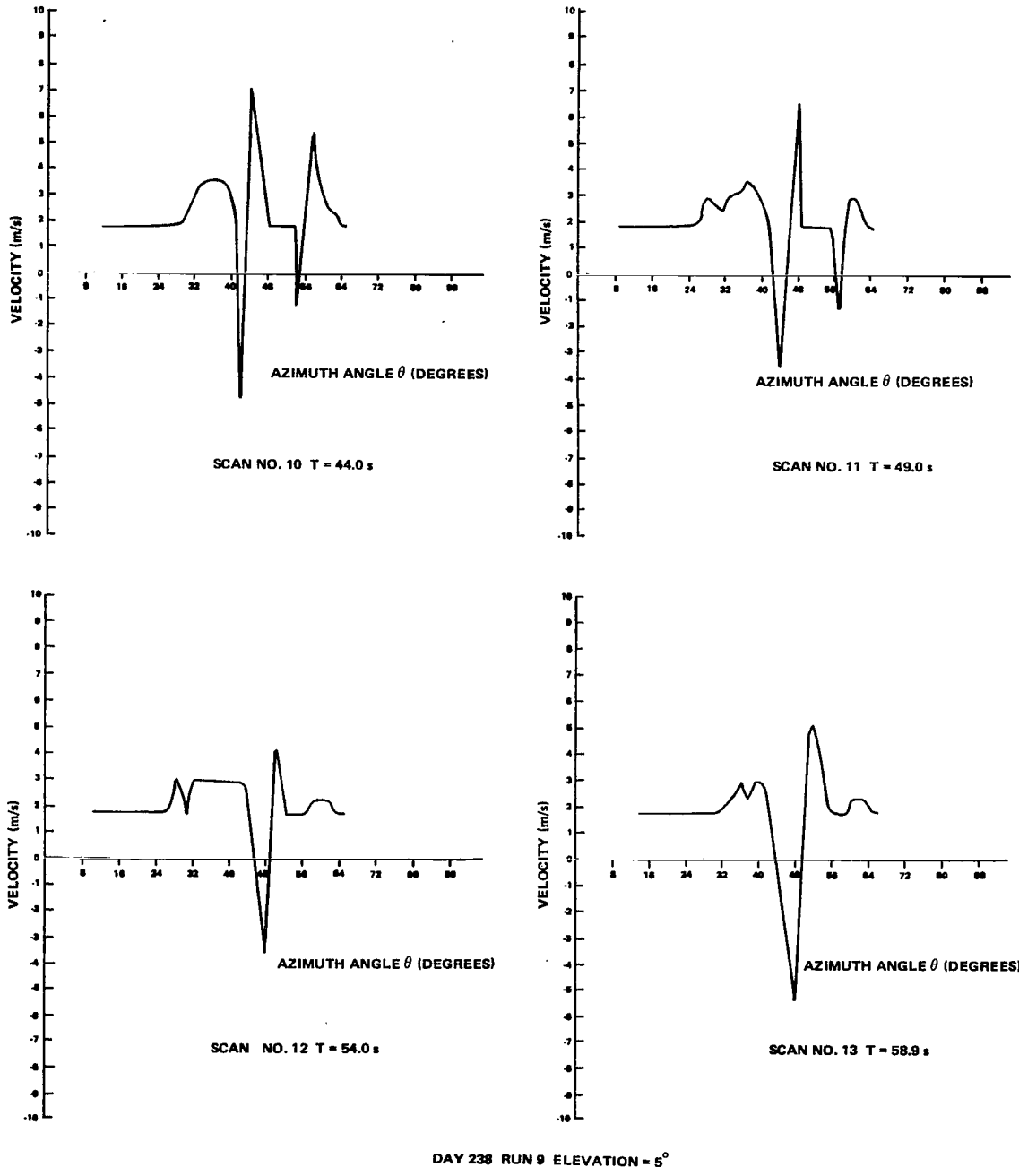

Figure 28. (Concluded)

velocity and azimuth angle at approximately 5 s intervals. The first plot in Figure 28 indicates a dust devil occurring at approximately 19°. Because of the separation between fingers of the scan (approximately 20), the negative portion of the dust devil was not detected. The negative portion begins to become evident in the second scan and by the third scan both sides of the dust devil have been detected. By the fifth scan, the dust devil has moved to approximately 28°, and it is evident that something is beginning to develop at approximately 46°. On the next scan it is obvious that a second dust devil has been formed within the scan plane. Both dust devils are evident until scan 12 when the second dust devil has moved beyond the scan plane. The first dust devil continues until the end of the data tape. It is obvious from these plots that both dust devils are anticyclonic. A plot of the angular transport of these two dust devils is shown in Figure 29 indicating a transport of 0.69°/s and 0.64°/s, respectively. The angular core width in this case is determined by the distance between the positive and negative peaks of the dust devil. A plot of the core width as a function of time is shown in Figure 30. It will be noted that both dust devils indicate a general broadening with time. This agrees generally with many observations; however, it was noted that in some cases an extremely tight core was formed immediately prior to the breakup of the dust devil. The plots shown in Figures 31 and 32 are of the peak velocities associated with each side of the dust devil. Since the wind during this run was generally below the threshold of 1.7 m/s, the maximum difference expected between the two peaks would be on the order of 3 m/s. While the second dust devil appears to have approximately the range of difference, the first dust devil has much wider separation in the early stages, reinforcing the supposition that the first several scans missed one side of the dust devil.

Intensity profile plots of this run are shown in Figure 33. A complete understanding of these plots can be obtained by comparing them with the angular velocity profile plots. Noise accompanying the lower turnaround point of the secondary mirror makes the data out to 140 m useless; however, for this particular run both dust devils appear to be beyond this range. In the first scan of Figure 33, aside from the turnaround noise, it can be seen that there were two areas within the scan that had significant backscatter intensities. The first area occurs at approximately 20° which coincides with the dust devil seen in the velocity plots. The second area occurs near 50° as can be seen from the velocity plots. There is no appreciable velocity associated with this region; this is due to the dust from the earthmover present in the field during these tests. This gives a very intense signal return but there is no Doppler velocity associated with it other than the ambient wind velocity. By scan 5, the earthmover has moved out of the scan, and by the next scan the second dust devil is seen. By scan 10, both dust devils are still shown, and the earthmover has reentered the scan plane on the opposite of the field.

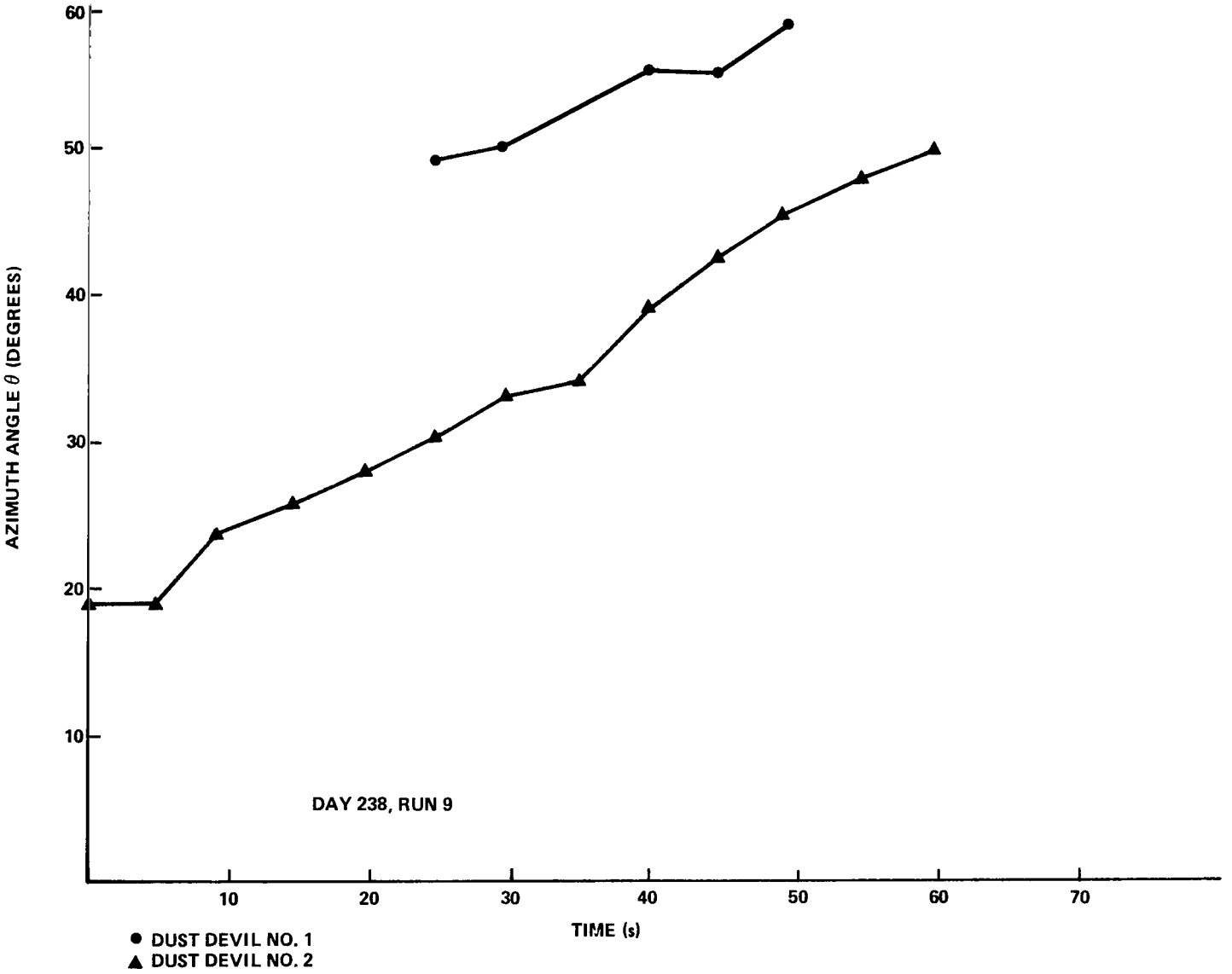

Figure 29. Dust devil angular transport.

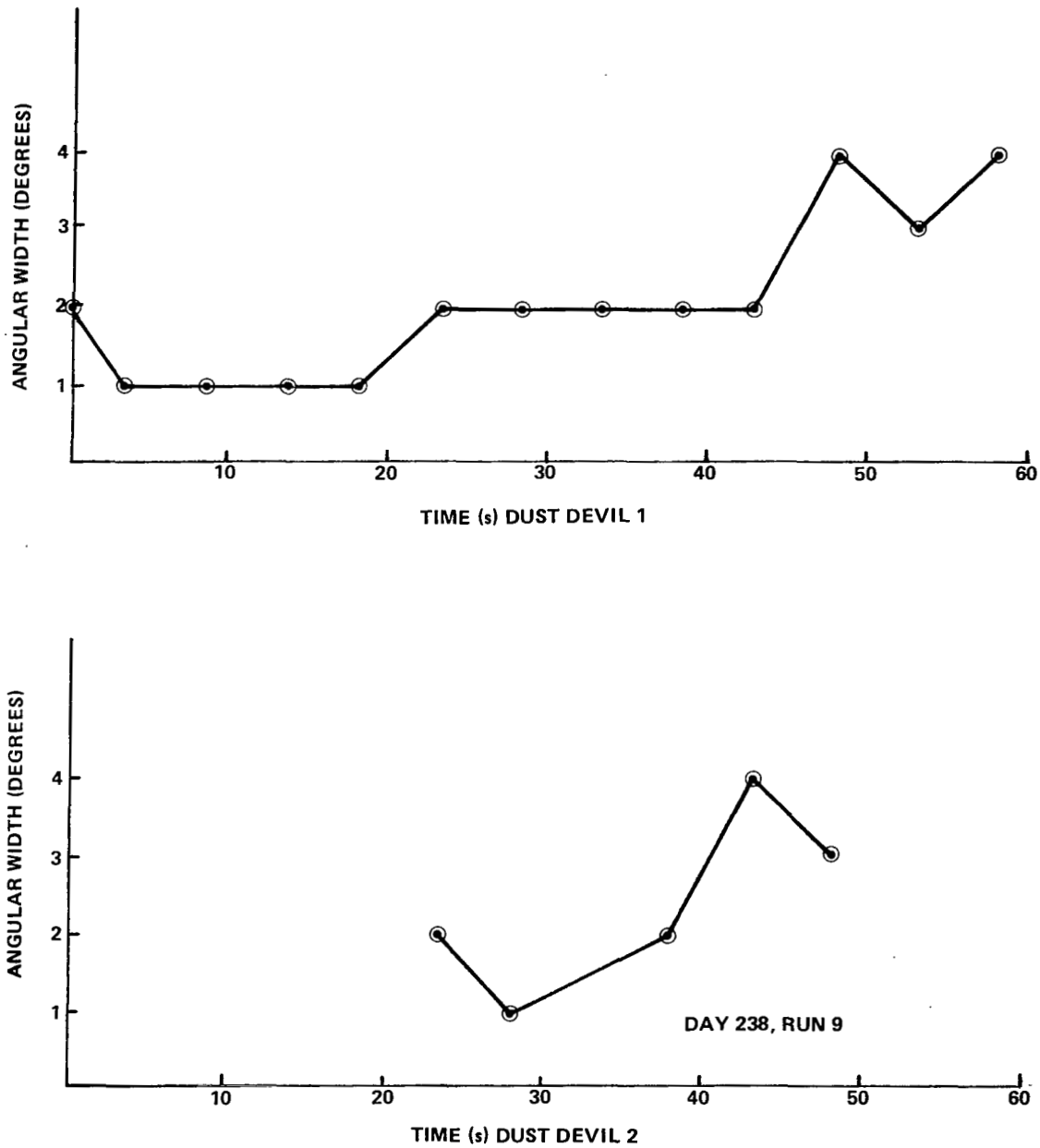

Figure 30. Dust devil core width time history.

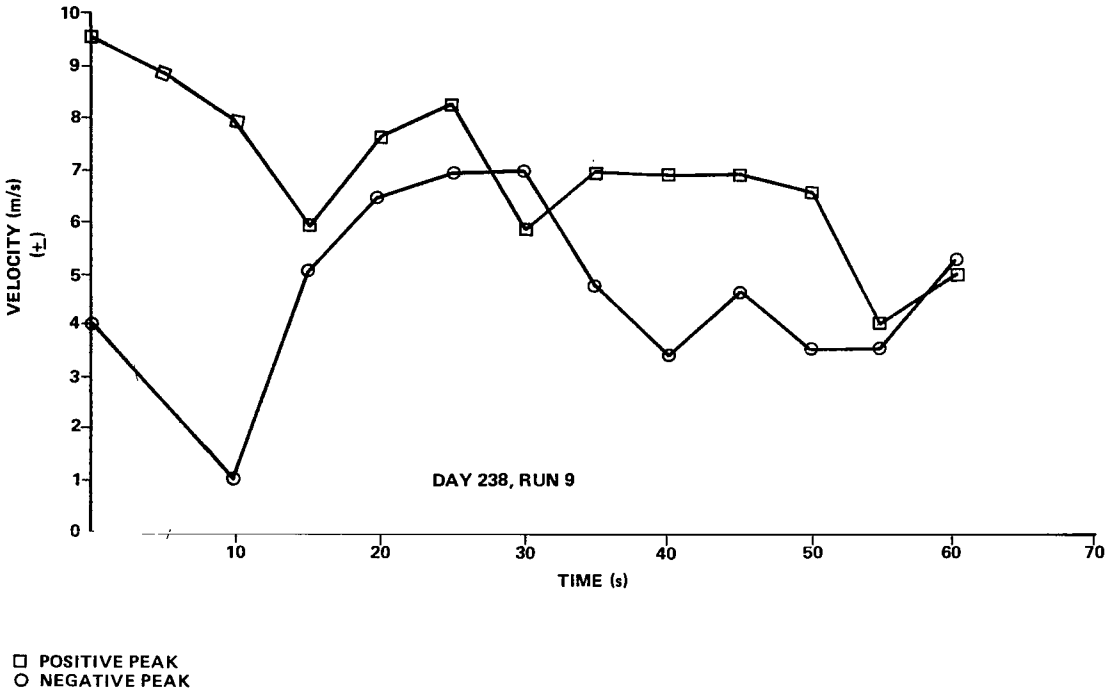

Figure 31. Velocity time history dust devil no. 1.

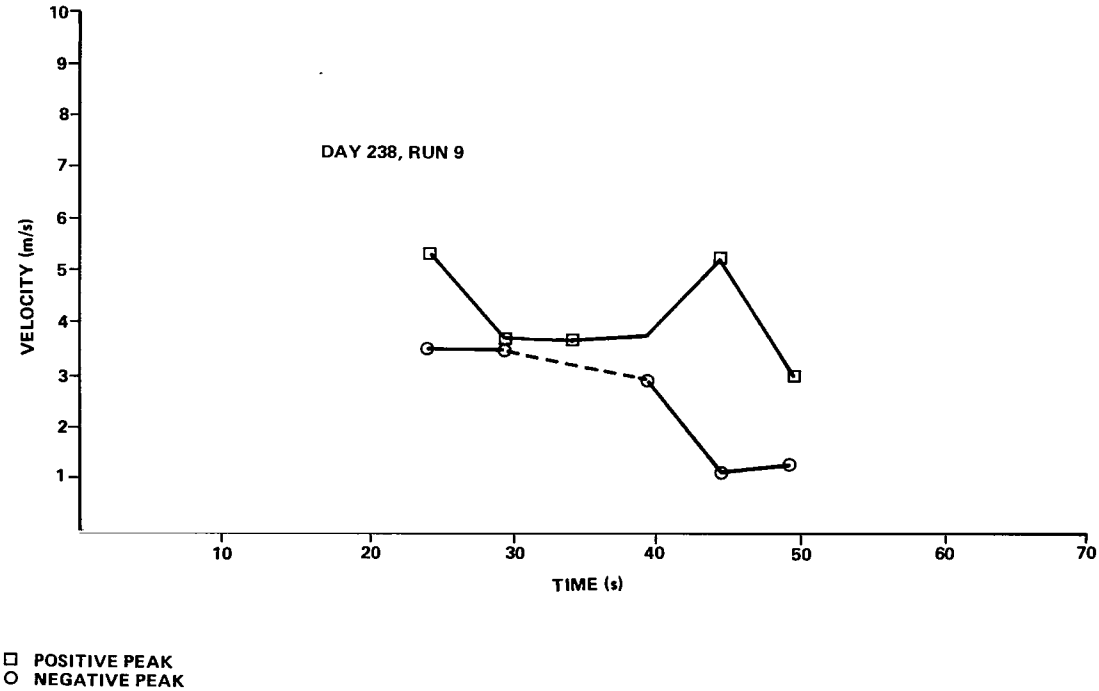

Figure 32. Velocity time history dust devil no. 2.

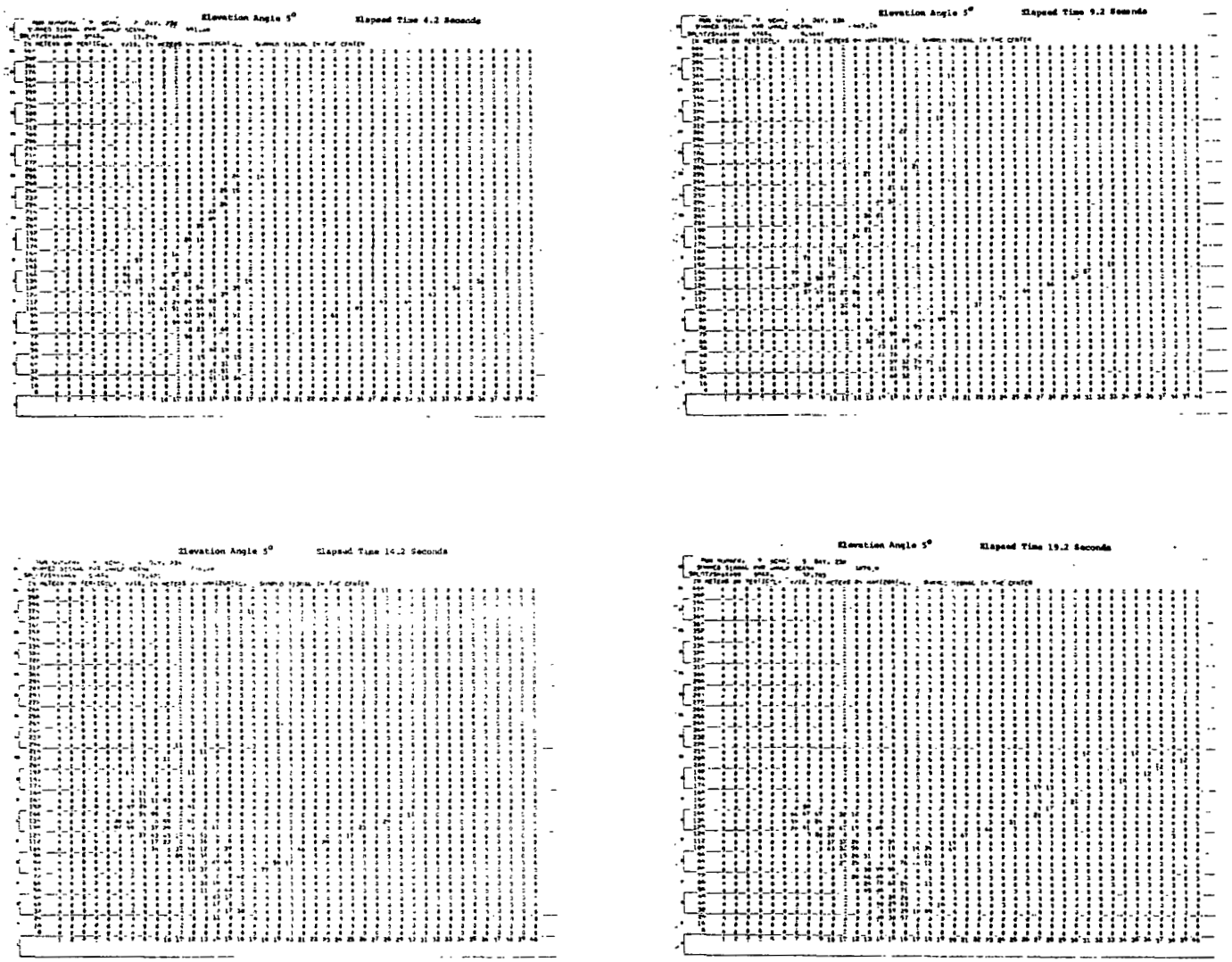

Figure 33. Dust devil backscatter intensity profile.

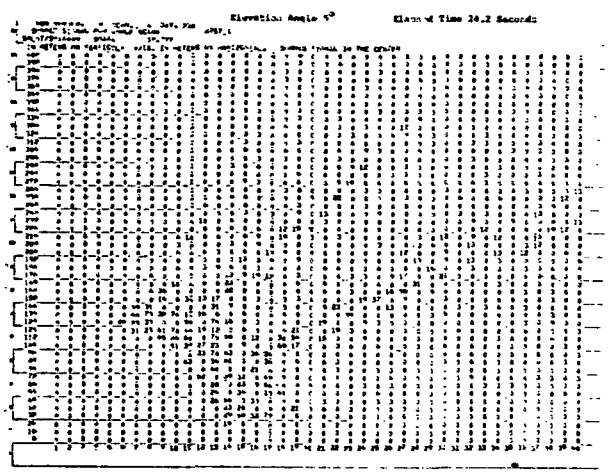

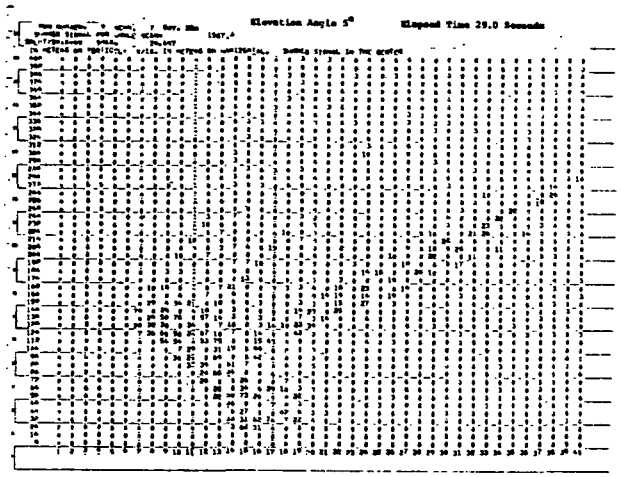

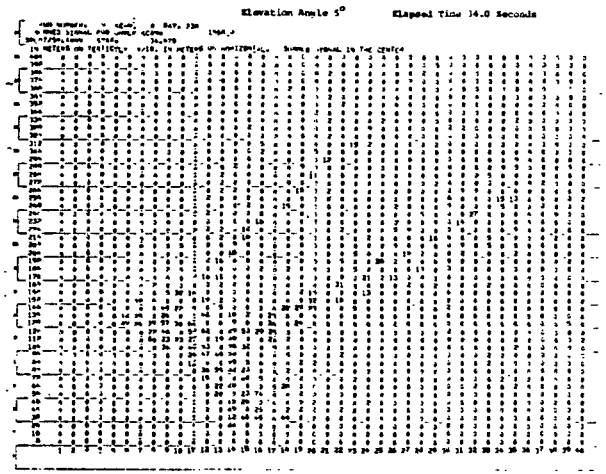

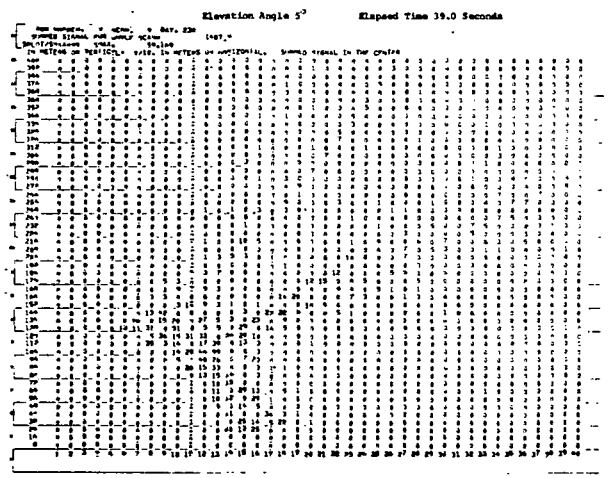

Figure 33. (Continued)

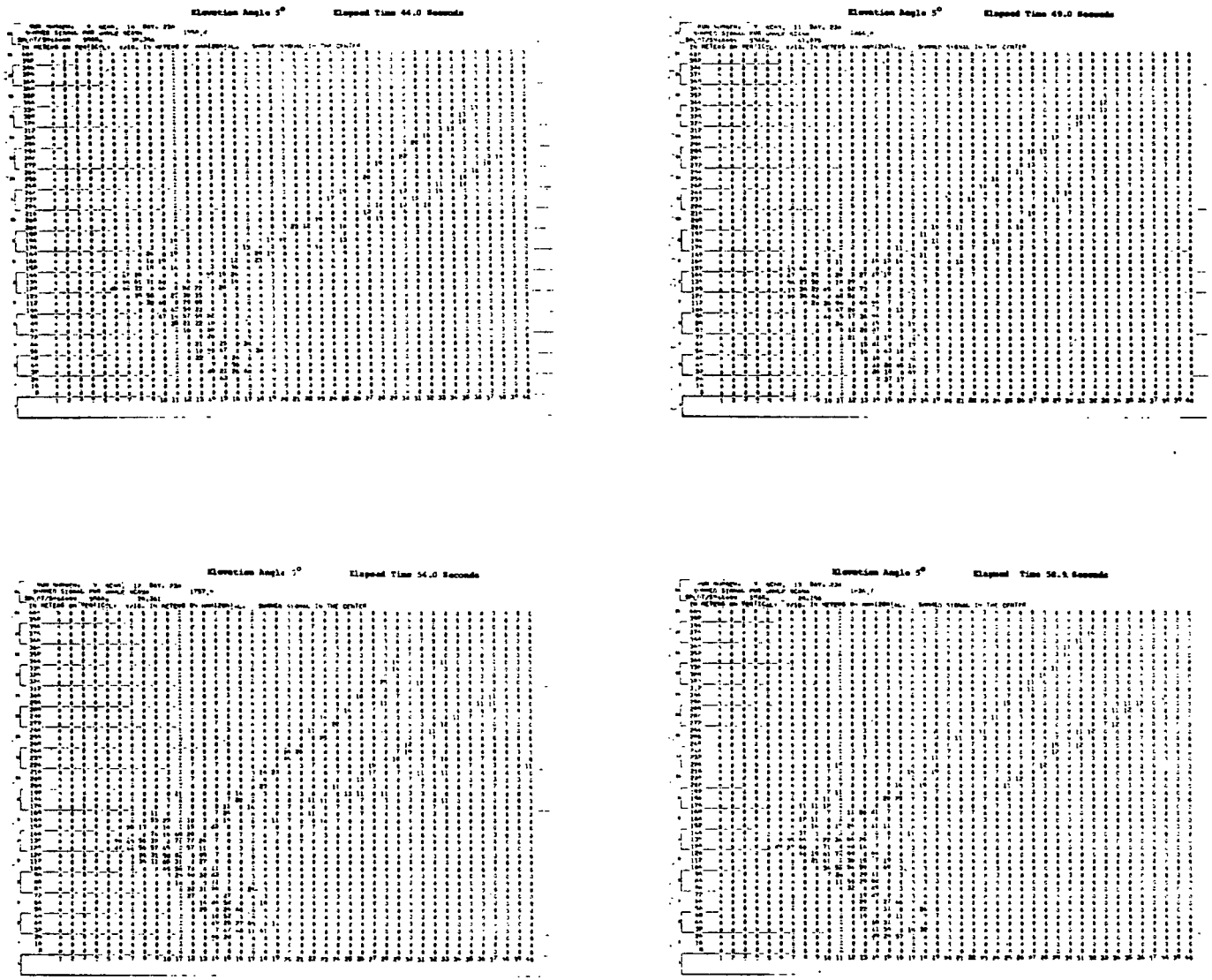

Figure 33. (Concluded)

A plot of the peak intensities of each dust devil with time is shown in Figure 34. It will be noticed that the intensity of the first dust devil fluctuates significantly with time while the second dust devil remains at a fairly constant level, slightly decreasing with time. This is due to the fact that dust was being artificially induced in the first dust devil for photographic purposes. This was an erratic process as is evident by the fluctuations. This plot and the peak velocity plot indicate that, unlike the previously analyzed dust devil, there was no significant growth of the dust devil during the run and in fact it appears that there was a general decrease in strength. The plot of the transport of the dust devils as determined by their peak signals is shown in Figure 35. As was previously mentioned, the range information is the most difficult to extract, and again this plot is intended to show only the general movement. In this particular case, it can be seen that both dust devils are moving in a southeasterly direction at approximately 1 m/s.

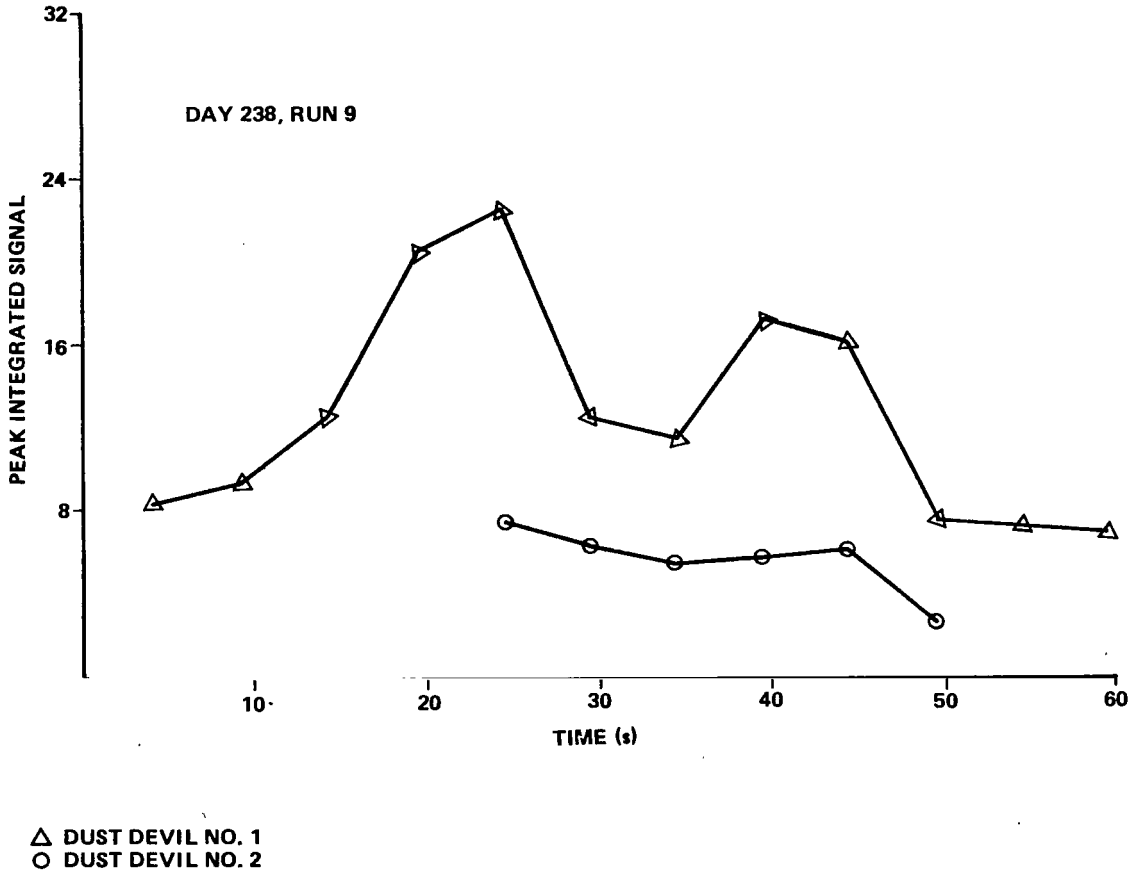

Figure 34. Peak integrated signals versus time.

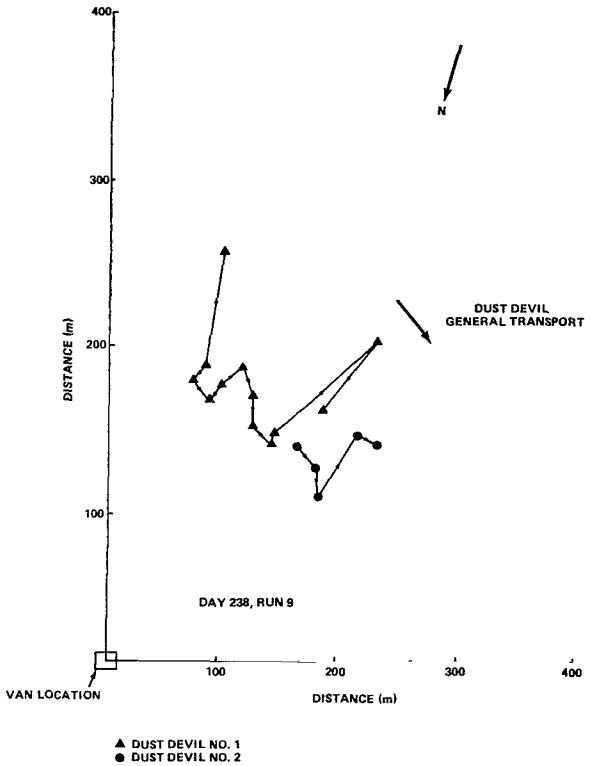

Figure 35. Dust devil peak signal transport.

VII. CONCLUDING REMARKS

As is shown in Section II, there have been a variety of test programs pertaining to the study of dust devils. While a substantial amount of data has been collected on the dust devil, no detailed velocity data have been collected that do not perturb the dust devil flow field. A laser Doppler system provides a unique opportunity to remotely determine the velocity structure of a dust devil without disturbing the flow field.

Several observations may be made concerning the dust devils observed and measured during this test program. As has been found by previous investigators, cyclonic and anticyclonic dust devils appeared to occur without preference, even within relatively short time periods. On August 26, 1975, four cyclonic and two anticyclonic dust devils were observed during the test period. Peak velocities of the order of 10 m/s were found to be common with circulation

strength calculations on the order of a few hundred m^2/s. In the data analysis, it was frequently noted that multiple peaks were exhibited in the velocity spectra. While these may be attributed to nonuniform density within the dust devil, it is suggested that in many cases the multiple peaks were due to a dust devil system which consisted of smaller dust devils rotating about a larger one. These complex systems have been observed by previous investigators [12]. The backscatter coefficients for dust devils were very high as expected by visible observations. S/N ratios were comparable to those obtained from the calibration target which was a sandpaper cover disk. Exact S/N ratio measurements could not be determined because the noise floor was below the quantitization level, which resulted from the extremely high signal return together with the limited dynamic range of the signal processor.

The information determined from the two cases discussed in Section VI.B and VI.C can be summarized as follows:

1. Width	Case 1 - 15 m	Case 2 - 7 m
2. Peak Velocity	Case 1 - 11 m/s	Case 2 - 9.5 m/s
3. Rate of Travel	Case 1 - 2.1 m/s	Case 2 - 1 m/s
4. Direction of Travel	Case 1 - North-West	Case 2 - South-East
5. Direction of Rotation	Case 1 - Anticyclonic	Case 2 - Anticyclonic

From the data presented in these sections it is concluded that while the angular resolution of the SLDV system is quite good, the range resolution could be much improved. With the use of two systems it would be possible to perform triangulation to pinpoint the location of the dust devil and thereby improve the quality of transport information.

The feasibility of measuring dust devil velocity flow fields using the SLDV has been successfully demonstrated. The combination of the information gained from this test and that gained by the survey of previous tests leads to a description of a test program which would improve the knowledge of dust devil generation, life time, and decay by an order of magnitude. This test program, as envisioned, would include a concentrated effort by a variety of sensor systems including the following:

1. Two SLDV systems to obtain velocity profiles, axial flow rates, and transport characteristics as well as ambient wind conditions.

2. Temperature sensors for multilevel including surface temperature measurements.

3. Pressure sensors.

4. Electric field meters.

5. Instrumental glider penetrations.

6. Local balloon releases.

7. Extensive use of the existing meteorological network.

While no program of this type is presently being planned, the outcome of such a test would undoubtedly lead to a better understanding of the dust devil phenomena, and possibly of an entire class of storms of this nature, including tornados and hurricanes.

REFERENCES

1. Brooks, H. B.: Rotation of Dust Devils. J. of Meteorology, Vol. 17, February 1960, pp. 84-86.

2. Malone, Thomas F., ed.: Compendium of Meteorology. American Meteorological Society, Boston, Massachusetts, 1951.

3. Ryan, J. A., and Carroll, J. J.: Dust Devil Wind Velocities: Mature State. J. of Geophys. Res., Vol. 75, No. 3, January 20, 1970, pp. 531-541.

4. Ryan, J. A.: Relation of Dust Devil Frequency and Diameter to Atmospheric Temperature. J. of Geophys. Res., Vol. 77, No. 36, December 20, 1972, pp. 7133-7137.

5. Fitzjarrald, D. E.: A Field Investigation of Dust Devils. J. of Applied Meteorology, Vol. 12, August 1973, pp. 808-813.

6. Fortner, L. E., Jr., and Ihara, Tatsuo: The Day of the Fuhjin, 1 March 1963. J. Met. Soc. Japan, Vol. 42, No. 4, 1964, pp. 269-272.

7. Sinclair, Peter C.: On the Rotation of Dust Devils. Bulletin American Meteorological Soc., Vol. 46, No. 7, July 1965, pp. 388-391.

8. Lamberth, Roy L.: On the Measurement of Dust Devil Parameters. Bulletin American Meteorological Soc., Vol. 47, No. 7, July 1966, pp. 522-526.

9. Kaimal, J. C., and Businger, J. A.: Case Studies of a Convective Plume and a Dust Devil. J. Applied Meteorology, Vol. 9, August 1970, pp. 612-620.

10. Geiger, Rudolf: The Climate Near the Ground. Translated from fourth German ed. of Das Klima der Bodennahen Luftschicht. Harvard University Press, Cambridge, Massachusetts, 1965.

11. Porch, W. M.: Fast-Response Light Scattering Measurements of Aerosol Suspension in a Desert Area. Atmospheric Environment, Vol. 8, 1974, pp. 897-904.

REFERENCES (Concluded)

12. Idso, Sherwood B.: Whirlwinds, Density Currents, and Topographic Disturbances: A Meteorological Melange of Intriguing Interactions. Weatherwise, April 1975, pp. 61-65.

13. Idso, Sherwood B.: Arizona Weather Watchers: Past and Present. Weatherwise, April 1975, pp. 56-60.

14. Idso, Sherwood B.: Observations of Dust Devils over Water. Bulletin American Meteorology Soc., Vol. 56, No. 3, March 1975, pp. 376.

15. Freier, G. D.: The Electric Field of a Large Dust Devil. J. of Geophys. Res., Vol. 65, No. 10, October 1960, p. 3504.

16. Crozier, W. D.: Dust Devil Properties. J. of Geophys. Res., Vol. 75, No. 24, August 20, 1970, pp. 4583-4585.

17. McGinnigle, J. B.: A Note on Observed Dust-Whirl Damage at Nicosia, Cyprus. Meteorological Magazine, Vol. 99, 1970, pp. 118-122.

18. Barcilon, Albert, and Frazin, Philip G.: Dust Devil Formation. Geophys. Fluid Dynamics, Vol. 4, 1972, pp. 147-158.

19. Maxworthy, T.: A Vorticity Source for Large-Scale Dust Devils and Other Comments on Naturally Occurring Columnar Vortices. J. of the Atmospheric Sciences, Vol. 30, November 1973, pp. 1717-1722.

20. Huffaker, Robert M.; Jeffreys, Harold B.; Weaver, Edwin A.; Bilbro, James W., et al.: Development of a Laser Doppler System for the Detection, Tracking, and Measurement of Aircraft Wake Vortices. NASA TMX-66868, FAA-RD-74-213, March 1975.

21. Ashmore, B. R., Kimura, A., and Skieth, R. W.: Data Processing and Display of Laser Doppler Experimental Results. University of Arkansas Final Report, NASA-Marshall Space Flight Center, Contract No. NAS8-31771, September 1976.

22. Sonneschein, C., DiMarzio, C., Clippinger, D., and Toomey, D.: Aviation Safety Research and Technology/Hazard Avoidance and Elimination Interim Report, NASA-Marshall Space Flight Center, Raytheon Company, Contract NAS8-30795, March 1976.

NASA-Langley, 1977

"The aeronautical and space activities of the United States shall be conducted so as to contribute . . . to the expansion of human knowledge of phenomena in the atmosphere and space. The Administration shall provide for the widest practicable and appropriate dissemination of information concerning its activities and the results thereof."

—NATIONAL AERONAUTICS AND SPACE ACT OF 1958

NASA SCIENTIFIC AND TECHNICAL PUBLICATIONS

TECHNICAL REPORTS: Scientific and technical information considered important, complete, and a lasting contribution to existing knowledge.

TECHNICAL NOTES: Information less broad in scope but nevertheless of importance as a contribution to existing knowledge.

TECHNICAL MEMORANDUMS: Information receiving limited distribution because of preliminary data, security classification, or other reasons. Also includes conference proceedings with either limited or unlimited distribution.

CONTRACTOR REPORTS: Scientific and technical information generated under a NASA contract or grant and considered an important contribution to existing knowledge.

TECHNICAL TRANSLATIONS: Information published in a foreign language considered to merit NASA distribution in English.

SPECIAL PUBLICATIONS: Information derived from or of value to NASA activities. Publications include final reports of major projects, monographs, data compilations, handbooks, sourcebooks, and special bibliographies.

TECHNOLOGY UTILIZATION PUBLICATIONS: Information on technology used by NASA that may be of particular interest in commercial and other non-aerospace applications. Publications include Tech Briefs, Technology Utilization Reports and Technology Surveys.

Details on the availability of these publications may be obtained from:

SCIENTIFIC AND TECHNICAL INFORMATION OFFICE

NATIONAL AERONAUTICS AND SPACE ADMINISTRATION

Washington, D.C. 20546